

**' SPATIAL AND ANGULAR CORRELATION FUNCTIONS
IN COSMOLOGY'**

BY

CHRISTOS DOMENIKIOTIS

Thesis

submitted to the

University of Glasgow

for the degree of

M.Sc.

**Department of Physics and Astronomy
University of Glasgow
Glasgow G12 8QQ
U.K.**

© Christos Domenikiotis 1992

ProQuest Number: 13831523

All rights reserved

INFORMATION TO ALL USERS

The quality of this reproduction is dependent upon the quality of the copy submitted.

In the unlikely event that the author did not send a complete manuscript and there are missing pages, these will be noted. Also, if material had to be removed, a note will indicate the deletion.



ProQuest 13831523

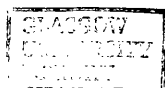
Published by ProQuest LLC (2019). Copyright of the Dissertation is held by the Author.

All rights reserved.

This work is protected against unauthorized copying under Title 17, United States Code
Microform Edition © ProQuest LLC.

ProQuest LLC.
789 East Eisenhower Parkway
P.O. Box 1346
Ann Arbor, MI 48106 – 1346

Thesis
9435
Copy 1



to my parents

'It is the great task of the natural sciences and of natural philosophy to paint a coherent and understandable picture of the Universe. All science is cosmology, and all civilizations of which we have knowledge have tried to understand the world in which we live, including ourselves, and our own knowledge, as part of the world.'

Karl R. Popper

Quantum Theory and the Schism in Physics, 1982, Unwin Hyman Ltd

SUMMARY

The purpose of this thesis is to study the role of the spatial and angular correlation functions for galaxies and clusters of galaxies. We discuss the various approaches to the problem of describing the statistical distribution of galaxies and discuss the connection between Peebles' and Limber's approach. The former describes the distribution as a point process, the latter considers the density distribution as a random function or process.

The density distribution that corresponds to a particular spatial correlation function can be generated by use of spectral analysis. We discuss some of the problems involved in generating the density distribution in this way, and use this description to derive the relationship between the angular and the spatial correlation function for particular forms of the latter. Selection effects are introduced first by simply truncating all galaxies beyond a certain distance, and secondly by introducing the Schechter luminosity function and excluding galaxies whose apparent magnitude is above some threshold value.

We briefly review the fractal description of galaxy distributions, and relate this to the description in terms of spatial correlation functions.

PREFACE

The study of the large-scale structure of the Universe has become an interesting area of research over the last decades. Observational and Physical Cosmology complement each other, leading to the better understanding of the nature of the Universe. The homogeneity and isotropy, on large scales, is an accepted fact (confirmed by the homogeneity and isotropy of the CMBR). It is also well known that on smaller scales (<150 Mpc) the Universe is very inhomogeneous, consisting of stars, galaxies, clusters and superclusters.

Many characteristics have been inferred from the data, provided by the great number of surveys, revealing the presence of filaments, voids etc. But in order to extract more information for the properties of the Universe, we need to apply quantitative tests (e.g. virial theorem etc.) which (i) give information on its dynamical properties (e.g. masses of galaxies & clusters, mean density of matter in the voids etc.) and (ii) offer a criterion for the selection of models for the formation and evolution of the Universe.

The study of the structure formation in the Universe can be approached by assuming that the density perturbations (at some linear stages) are a random Gaussian field. Since the early stages of modern Cosmology, attempts have been made to describe statistically, the structures in the Universe. One of the statistical methods used to measure, mainly, the irregularities in the space distribution, is the correlation function (spatial and angular). The spatial correlation function can be connected with the power spectrum of the density fluctuations, through Fourier analysis. Statistical methods, combined with more information gathered in

the future from the 2^D map of the CMBR, will give us a deeper understanding of the density oscillations at high redshifts ($\sim 10^3$)

The distribution of galaxies can usefully be described in the language of stochastic process, and in this thesis we show how the statistical measures of inhomogeneities in the large scale structure can be placed in the framework of this theory.

In the first chapter we outline how the cosmological ideas have progressed, starting with some ancient beliefs about cosmogony. We state the problems arising from the so called standard model and describe the initial conditions with the subsequent evolution of clustering in the linear and nonlinear regime. We then discuss the problem of the subluminal, but gravitationally influential, dark matter. A discussion of the literature and simulations follow the references to the large scale structure observed today.

Chapter 2 is devoted to the presentation of the theory concerning the stochastic processes and spectral analysis. They both constitute the basis for the development of theory in the following two chapters, as an application for the study of the large-scale matter distribution. We illustrate the above theory, in particular, the construction of realizations of random functions in 1^D to highlight problems that arise in 3^D

In the third chapter we show how we can apply the spatial and angular correlation functions, to measure the nature of the distribution of objects. Four forms of two-point autocorrelation functions are studied. We explain the problem arising from the use of the common form, of the power law, for the generation of continuous functions and suggest a different form, to overcome this difficulty (the problem was illustrated by the 1^D approach in the previous chapter). The remaining sections are concerned with the 3^D

approach. In the last section we examine the small angle approximation, deriving the angular correlation function from the spatial correlation function without the intervention of the simulation.

In the beginning of the forth chapter, some definitions of the luminosity function are given and we discuss the morphology-density relationship. The universality of this relation, although somewhat puzzling, is generally accepted as a fact and confirmed by the comparison between the redshift surveys and data on clusters. The general luminosity function as introduced by Schechter (1976) is mainly used. It is obvious that the sampling effects come into the upper limit of the integrals over all ranges of magnitude, determining a cut-off in the probability distribution of the galaxies. The consequence of this, is included in the programme and the resultant angular correlation function is obtained.

Finally we discuss our results and give two appendices with proof of the power spectrum of the suggested spatial correlation function and the programme utilised for the simulation.

The work in this thesis was carried out while the author was a research student in the Department of Physics and Astronomy, Glasgow University and it would not have been possible to be completed without the contributions of people who helped me, directly or indirectly. Firstly, I thank my parents for their continued support, without which none of this would have been conceivable; my supervisor, John F.L. Simmons, who, with his advice and guidance, gave purpose to my work and also proved he can 'cook' science as he does bean casserole; Martin for general discussions and I hope that, even if he continues to forget to switch off the computers and loses everything (from my pens to his

wallet), he will not lose his way back to Glasgow; Alan Thompson, my greatest ally when it came to computer systems and I wish him the best of luck in his new role as a father; Daphne, who, although she 'refused' to keep me in constant supply of pencils, I will never forget her essential generous supply of coffee and biscuits. Also I must not forget Carole for her moral support and encouragement, especially in the final stages; all the guys with whom I have shared room 412 and Murray and Richard for haunting the department with me on many nights (as yet, uninvestigated by Professor A.E. Roy).

CONTENTS

	page
SUMMARY	i
PREFACE	ii
CHAPTER 1: INTRODUCTION	1
1.1 From Myths to Reality	1
1.2 The Dawn of Modern Cosmology	3
1.3 Initial Fluctuations	9
1.4 Evolution of Clustering	11
1.4.1 Linear	11
1.4.2 Nonlinear	13
1.5 Dark Matter	16
1.6 Large-scale Structures in the Universe	18
1.7 Literature	22
1.8 Simulations	23
CHAPTER 2: STOCHASTIC PROCESSES	31
2.1 Random Processes	31
2.1.1 Definitions	31
2.1.2 Stationarity	33
2.1.3 First & Second Moments	33
2.1.4 Continuity	34
2.1.5 Correlation Length	36
2.2 Matter Density as Random Function	37
2.3 Spectral Analysis	38
CHAPTER 3: CORRELATION FUNCTIONS	53
3.1 Spatial Correlation Function (s.c.f.)	53
3.2 Observed S.C.F.	56
3.3 Spectrum of Power Law	58

3.4	Other Correlation Functions and Their Spectra	59
3.5	Alternative S.C.F.	61
3.6	Angular Correlation Function (a.c.f.)	61
3.6.1	Estimated from the Generated Distribution of Galaxies	61
3.6.2	Analytic Expression for the A.C.F. and Small Angle Approximation	63
3.7	A.C.F. Estimation	64
3.8	Fractals	66
3.8.1	Definitions & Properties	66
3.8.2	Global Density	68
3.8.3	Cut-off	69
3.8.4	Fractal S.C.F.	69
CHAPTER 4: LUMINOSITY FUNCTION		88
4.1	Definitions	88
4.1.1	Morphology-density Relationship	88
4.1.2	Schechter's Luminosity Function	91
4.1.3	Change of Variables	93
4.2	Selection Effects	95
CHAPTER 5: DISCUSSION		102
APPENDICES A		108
	B	113
REFERENCES		137

CHAPTER 1**INTRODUCTION**

In this chapter we give a brief historical review of cosmology. We examine several questions which are central to the cosmology today. We mention the outstanding problems to be confronted and we state the resulting structures from the first 3-dimensional surveys. We describe how the initial perturbations grew in the early stages of the Universe's evolution. We give some statistical methods used in cosmology and explain why the correlation functions appear to be more complete in both the quantitative analysis of clustering and reconstruction of the density field in the simulations.

1.1 From myths to reality

What we call mythology consists of stories that reveal a search for the meaning of the world either philosophically or scientifically; as the myths in the ancient world were a simplification of a complex science. We should not forget that astronomy was one of the first sciences developed by the people of that era, thousands of years ago. O'Brien & Major (1982) write: 'we can analyse myths in many different ways to discover their insight. But scholars today tend to use one or more of basic approaches. Fundamentalists believe that creation myths are historical accounts

of the origins of things; moral fictionists believe the myths provide useful lessons for living; structuralists have pointed out the universal patterns of thought which myths contain; and symbolists believe the myths contain truth which is symbolic rather than historical'.

Everything, in the most ancient cosmologies, was one in the beginning. Then a god, like Marduk for instance in Mesopotamia, created the Earth, the planets and humans. After a long conflict, Marduk conquers the old god Tiamat and the status of order begins. Once more we can see the fight between chaos and order, which is common in many creation stories. Generally the gods and goddesses are forces that give form to pre-existing matter. In 712 A.D., the 'Chronicles of Japan' describe the beginning in the first chapter 'Hajimari'. The heavens and the earth were one. The sky was a mass of huge clouds which began to swirl and grow. A terrible rain started and lasted for a long time. When it stopped the heavens and the earth separated.

In Vedic Cosmology (India), Varuna separated and established heaven and Earth. Dyaus was the son of Heaven and Earth, born in the atmosphere, thereby combining in himself the threefold structure of the Universe, dependent upon the universal cosmic order Rta (Brandon, 1963).

In Theogony, Hesiod gives the cosmogony through the genealogies of the gods. The birth of new generations means the evolution of the world toward an ordered and more civilized one. Different explanations of the origin of the world had been given by Sophocles, Aeschylus and Aristophanes. But particularly interesting is that the Greek thinkers, for the first time, attempted to break away from the mythological approach to origins and propose

various 'physical' cosmogonies (O'Brien & Major 1982). Thus Thales, Heraclitus and Empedocles tried to give scientific explanation, in the sixth century B.C.

1.2 The Dawn of the Modern Cosmology

In the centuries following the early ages, the interests of the astronomers (and/or philosophers) were directed to the study of the planetary motions. Scientists like Claudius Ptolemy (second century A.D.), Nicholas Copernicus (fifteenth century), Tycho Brache, Johannes Kepler, Galileo Galilei etc. pioneered in the foundation of the principles in Astronomy. The applications of Newton's law (published in 'Principia' in 1687) in the Solar System, showed that the physical phenomena can be described under the assumption of an Euclidean space in every scale.

Everybody, before our century, believed that the Universe is infinite and static. From these assumptions some problems found a solution but some did not. For example Newton, using the gravitational theory argued that the Universe could be infinite and static without the stars falling in the same point, once the gravitational forces between the stars are balanced by the force of stars on the other side. Although a 'reasonable' explanation has been given to the above problem, nobody managed to solve the Olber's paradox (in an infinite and static Universe, for uniformly distributed stars, the total flux of their light should be infinite, making the 'night, day' on Earth).

A turning point for cosmology was the proposition by Einstein of the theory of relativity. Firstly, in 1905, Einstein published the special theory of relativity which connects the

observations of events, made by observers who are in uniform relative motion. In this theory there are two basic postulates: (i) all the inertial frames are equivalent when we carry out experiments in them and (ii) the velocity of light is constant, in all the inertial frames. About ten years later he developed the general theory of relativity, which is a generalization of the Newtonian gravitation. Affected by the conceptions of his era for the static Universe, Einstein regulated his equation, adding the term Λ , called the cosmological constant.

Cosmological principle: Before the twentieth century, the concept of cosmologists was, that the Universe is full of matter with constant density and is distributed uniformly over all scales. The first exemptions were made on small scales, where Newtonian mechanics predicted gravitational instability.

The assumption of the cosmological principal means that the Universe is homogeneous and isotropic (H&I). By homogeneity we mean that every observer in the Universe can see exactly the same picture of the Universe as a function of time. Isotropy indicates that the Universe, for an observer, looks like the same in all directions.

Hubble's law: The first systematic attempt to measure the distance of the stars was made, in 19th century, by Bessel, Henderson and Struve. A catalogue of 100 stars prepared with the distance estimated by their parallax. The same period Secchi and Draper prepared catalogues of stars and Huggins estimated the first recession velocity of Sirius by it's Doppler redshift.

It was just at the beginning of our century that astronomers realized that the Milky Way does not comprise the whole Universe. For the first time, Kant suggested that the 'nebulae'

were outside our galaxy. The controversy as to whether the 'nebulae' were inside or outside the Milky Way continued, until 1924 when Edwin P. Hubble, using the period-luminosity relation of the Cepheids, determined the distance of nearby galaxies. The next step was to use giant stars. He assumed that they have the same absolute luminosity and finding the apparent luminosity, he worked out the distance. In that way he measured distances out to 10,000,000 ly. Then he applied the same method, but for the absolute luminosity of galaxies and extended this limiting to 240,000,000 ly. In addition to this study, he classified them, mainly, as ellipticals, spirals, barred spirals and irregular. The result of his work (established in 1929) was the velocity-distance relation, $v=Hr$ (where v is the velocity and r the distance), known as 'Hubble's law', indicating the expansion of the Universe. His work is summarized in 'The Realm of the Nebulae' in 1936.

'Big Bang' & CMBR: An important inference from the Hubble's law is that, about 20 billions years ago the galaxies were much closer than today and the matter density of the Universe much larger. This is the standard (or Big Bang) model for the origin of the Universe. In the 1940's, Gamow and his colleagues Alpher and Hermann, trying to explain the existence of elements, we observe today in the Universe (fig. 1.1), assumed that this should be more than a million degrees at an early time. The predicted echo of that epoch was detected by Arno Penzias and Robert Wilson (1965). When they were working on the telecommunication systems at the Bell Laboratories, they found a signal coming from all directions in the sky, in the microwave band of the spectrum. The CMBR provides evidence for H&I of the universe on large scales (>100 Mpc), supporting the standard model, and it's study will play a

significant role in the better understanding of the origin of structures in the Universe.

Inflation: The standard model leads to three important, experimentally testable predictions (e.g. Guth and Steinhart, 1991): (i) Hubble's law, (ii) the microwave background radiation and (iii) the abundances of the elements. However, it fails to explain: (i) why the Universe appears to be uniform over distances that are large compared with the horizon distance at recombination (the so called horizon problem), (ii) the spectrum of inhomogeneities which requires the initial state of matter to be non uniform (smoothness problem), (iii) the small (compared with the number predicted by the standard model) number of isolated north or south magnetic poles (magnetic monopoles), predicted by the GUTs (monopole problem) and (iv) according to the Big Bang model the density, pressure and temperature would have been infinite in the beginning, $t=0$ (singularity problem); this problem can probably be solved by models in quantum physics.

In the last decade a theory came up which seem to explain most of the above problems arising from the standard model. It is called inflation and was proposed by A. Guth (1981). In order to understand better the inflation, we state the fundamental idea on which is based. As we know, according to different equilibrium states of the molecules, we have three phases of the water: liquid, solid and gaseous. When the temperature drops, latent heat is released. In the Universe, in the beginning there is symmetry between nuclear and electromagnetic forces. Then the temperature drops (to 10^{27} Kelvins) and the energy is not large enough to maintain the symmetry. So a new status is established. The new situation is based on the overwhelming of the electromagnetic force.

At this period the light travel distance grew exponentially large and the length, for say a centimetre, extended out to a distance of hundreds of billions of light-years (fig. 1.2 from Guth et al. (1989,1991)). The inflation occurred after the first 10^{-35} s. According to Borner (1988), inflation is the assumption that the expansion factor $R(t)$ of a Friedmann-Lemaitre cosmological model grows exponentially during a brief time interval in the very early universe.

Although quite a new theory, there are different versions, for which Borner (1988) wrote: one can say that the old inflation scenario is dead; the new scenario is old, and the chaotic inflation scenario is in a good order. According to the chaotic inflationary scenario, the inflationary Universe life exists only in the 'bubble' in which we have large size, spatial flatness and high isotropy. Other regions either have not inflated or they are not long-lived enough to stable life (Barrow & Tipler, 1986).

What makes the inflationary scenario especially interesting is the fact that it can link together a number of properties of the Universe, each of which plays a key role in creating a cosmic environment (small-scale inhomogeneity, high degree of isotropy and proximity to critical density).

Recently it has been proposed that the phase transition may have occurred tens of millions of years after the Big Bang, when the temperature was about 100^0K . This is between the era of microwave background radiation and the galaxy formation.

Friedmann model: The separation between two events, for H&I Universe is expressed by the Robertson-Walker metric

$$ds^2 = dt^2 - \frac{R^2(t)}{c^2} \left[\frac{dr^2}{1 - kr^2} + r^2(d\theta^2 + \sin^2 \theta d\phi^2) \right]$$

Alexandre Friedmann, in 1922, gave three classes of solutions to the Einstein field equations under the conditions of Weyl postulate (that the galaxies are moving along paths without interacting each other) and the cosmological principal. Assuming that the distribution of matter can be described by a perfect fluid with density, ρ , pressure, p , and $\Lambda=0$, the Friedmann equation expresses the evolution of matter as

$$\left(\frac{\dot{R}}{R}\right)^2 = \frac{8\pi G\rho(t)}{3} - \frac{kc^2}{R^2} \quad \text{and} \quad \frac{d}{dt}(\rho R^3) + \frac{p}{c^2} \frac{d}{dt}(R^3) = 0 \quad (1.1)$$

where R is the scale factor and k the curvature. The pressure, p , and the density, ρ , can be written as the sum of components, specifying the contribution from the mass and radiation, as follow: $p=p_m+p_r$ and $\rho=\rho_r+\rho_m$ (where m and r indicate mass and radiation). We call radiation-dominated era the epoch in which $\rho_r>\rho_m$ and matter-dominated era the epoch for $\rho_m>\rho_r$. At present, matter content is dominant ($\rho_m\gg\rho_r$), but matter pressure is negligible ($p_m\ll p_r$).

The Hubble's constant, H , we can say expresses the scale change rate and can be written as $H=\dot{R}/R$ with units $\text{km s}^{-1} \text{Mpc}^{-1}$ and so the equation (1.1) determines the evolution of Hubble parameter. $\tau=1/H$, for expanding Universe in the standard model, is an upper limit to the age of the Universe ($\sim 2\times 10^{10}$ years for a value $H=50 \text{ km s}^{-1} \text{Mpc}^{-1}$). According to the initial value of H the age estimated to $\sim 4.7\times 10^9$ years, is contradictory to the geological theories for the age of the Solar system.

1.3 Initial Fluctuations

There are two key cosmological epochs of radiation and matter domination regimes: the epoch of equal matter and radiation pressure and the recombination. In the first state, radiation was coupled to the matter. Recombination occurs when the radiation temperature drops to $\cong 3000\text{-}4000^0\text{ K}$ and the protons and electrons combine to form hydrogen. At this point, the radiation no longer be scattered effectively by the matter and we say the radiation and matter decoupled. Any inhomogeneity in the matter distribution at this time would give rise to anisotropies in the microwave background radiation, characterized by small variations in the temperature with direction.

According to the Friedmann solutions if the present mean density of the Universe is ρ_0 then the density parameter (density/critical density) is

$$\Omega_0 = 8\pi G\rho_0 / 3H_0^2 \quad (1.2)$$

If $\Omega_0 > 1$ the Universe will eventually collapse, while $\Omega_0 \leq 1$ implies expansion will continue for ever. The last case can give two models : (i) $\Omega_0 = 1$ (Einstein-de Sitter case), and (ii) the open one $\Omega_0 < 1$

In the Universe small irregularities in the distribution of matter would tend to grow because the gravitational attraction of a particular lump would overcome the cosmological expansion in the region near it. At the same time as gravity causes clustering, it also causes low-density voids to expand and to pile up matter around their edges. The negative amplitude density areas, which are the progenitors of the voids, decrease as the positive density peaks increase (Hoffman & Shaham, 1983)

The initial density fluctuations, generally, can be divided in two categories (Gott, 1977):

(i) isothermal in which the fluctuations do not conserve entropy per baryon. They represent baryon fluctuations in a uniform photon bath. In this case, the matter density increases in some regions, but the background radiation field remains uniform. This kind of perturbation grows only after decoupling because the intense radiation field prevents the electrons from moving much. From these fluctuations we can have the smallest disturbances at size of globular cluster.

(ii) adiabatic; here the perturbations vary together in time and space like sound waves. After decoupling the matter component of the disturbances grow slowly giving mass concentrations comparable to a cluster of galaxies. These perturbations exactly conserve the entropy per baryon and are like sound waves with equal photon and baryon fluctuations. They enter the horizon at an amplitude of 10^{-4} and do not grow prior the recombination. According to Silk (1974) we can not find adiabatic fluctuations on scales smaller than a characteristic mass because they are damped by photon viscosity. According to Zeldovich (1972) the perturbations can be studied better when they first come within the horizon and so show us how different parts of the Universe are connected.

The Ω problem: If Ω were not, initially, close to 1 then any deviation from unity would have grown rapidly giving values to Ω out of the range 0.1 and 0.2. If the assumption, that the mass density has been equal to the critical density one second after the Big Bang is true, then the question arises is why the Universe started off so close to this value. Statistical measures used to extract

information from iso-temperature contours of microwave background radiation which will help to understand better the initial conditions (Sazhin, 1985)

1.4 Evolution of Clustering

1.4.1 Linear

As we described in previous section, at redshift $z \sim 1.400$ the radiation decoupled from the matter and as the first atomic hydrogen formed, the radiation was freely moving through it. This is assumed to be the starting point for the evolution of clustering. At this epoch the density distribution of the Universe was almost homogeneous. The fluctuation, $\frac{\delta\rho}{\rho}$, was very small (10^{-4}) and its evolution can be described by linear theory.

If the perturbations are isothermal, then the radiation is distributed uniformly ($\delta\rho_r=0$). In the case of adiabatic perturbation the radiation and matter oscillate together, like acoustic waves, with fluctuations connected by the equation

$$\frac{\delta\rho_r}{\rho_r} = \frac{4}{3} \frac{\delta\rho_m}{\rho_m}$$

The perturbations tend to be damped by photon diffusion (Peebles, 1980). In order for an irregularity to avoid the dissipation need to have a mass, called characteristic mass, which ranges from galaxies to clusters of galaxies, for adiabatic perturbations and globular star clusters for isothermal.

The equation (1.1) can be

$$\left. \begin{aligned} -\frac{kc^2}{R_0^2} &= H_0^2 - \frac{8\pi G\rho(t_0)}{3} \\ H_0^2 &= \Omega_0^{-1} \frac{8\pi G\rho(t_0)}{3} \end{aligned} \right\} \Rightarrow -kc^2 = [\Omega_0^{-1} - 1] \frac{8\pi G\rho(t_0)}{3} R_0^2 \quad (1.3)$$

The subscript 0 refers to the present epoch. Solving the eq. (1.1) in terms of kc^2/R^2 , substituting the eq. (1.3) and knowing that $\rho(t)R^3 = \rho(t_0)R_0^3 = \text{constant}$ we get

$$\left(\frac{\dot{R}}{R}\right)^2 = \frac{8\pi G\rho(t)}{3} \left[[\Omega_0^{-1} - 1] \frac{R}{R_0} + 1 \right] = \frac{8\pi G\rho(t)}{3}$$

since today $R_0 \gg R$. Solving this differential equation we find

$$R(t) = (6G\rho(t_0)R_0^3)^{\frac{1}{3}} t^{\frac{2}{3}} = R_0 (6G\rho(t_0))^{\frac{1}{3}} t^{\frac{2}{3}} \Rightarrow R(t) \propto t^{2/3} \quad (1.4)$$

If we consider that the matter flows as an ideal fluid and neglect the pressure gradients the 'linear perturbation equation' is (e.g. Fall (1979), Peebles (1980)):

$$\frac{d^2\delta}{dt^2} + \frac{2}{R}\dot{R}\frac{d\delta}{dt} = 4\pi G\rho\delta \quad (1.5)$$

Using the (1.4) and assuming that one solution is $\delta_1 \propto t^n$, we find the general solution of the linear homogeneous differential equation (1.5), δ , to be: $\delta(t) = C t^{2/3}$, for large t .

As we can see the initial fluctuations of baryonic matter expands linearly. The density perturbations grow proportional to the scale factor $\delta\rho/\rho \propto R$. The density fluctuations increase because of the gravitational instability till the moment the perturbations become big enough to form the first structures.

1.4.2 Nonlinear

The epoch in which the first objects formed marks the end of the linear evolution. According to the Big Bang model, galaxies are described as the gravitational collapse of large enough density fluctuations. The amplitude of the perturbations to become gravitational bound and collapse out of the expanding Universe is dependent on the mean mass density of the Universe. If Ω is close to unity (large) small perturbations can collapse. Lifshitz (1946) studying the evolution of the contrast $\delta\rho/\rho$, showed that the growth of perturbations is slow because the background density decreases. Kolb & Turner (1990) showed that the perturbations, containing $10^{12} M_{\odot}$, would be of the scale 1.9 Mpc if they had not been separated from the general expansion in the non-linear stage. The problem with the Big Bang model is that the initial fluctuations spectrum is something that should be regarded as initial condition because the amplitude of the fluctuations have no explanation. In the inflationary model, the Universe inflated in such a scales as is not possible to be damped out and becomes decoupling with $\Omega=1$.

Jeans Length: Here we pose the fundamental idea on which the formation of the irregularities is based. Say we have a medium (with density ρ_m) perturbing slightly. The areas which are denser than others tend to condense under the gravitational attraction. The growth of the density increases the pressure. Jeans found that the minimum length, L_J , of the region in which the gravity overwhelms the pressure is (e.g. Rowan-Robinson, 1977): $L_J = v_s (G\rho_m)^{-1/2}$, ($(G\rho)^{-1/2}$ is the time it takes the perturbation to collapse under gravity) where v_s is the velocity of sound, taking (i) $v_s \sim c / \sqrt{3}$ in the radiation dominated era and (ii) $v_s = (5KT / 3m_p)^{1/2}$ (m_p is the mean density of the particles in the material medium) after

recombination. The Jeans Mass is defined as $M_J \propto \rho L_J^3$, with (i) $10^{15} M_\odot$ before recombination (clusters of galaxies) and (ii) $\sim 10^6 M_\odot$ after recombination (globular star clusters).

The first structures to form from adiabatic perturbations are 10^{13} - $10^{15} M_\odot$ which then fragmented into galaxies. Their rotational motion caused shock waves. The perturbations larger than those above, cancelled out once the amplitude was less than unity (Doroshkevich et al., 1974). All the structures, we observe today in large scales, came from gravitational clustering. The smaller mass scales were either absent initially or were erased (e.g. adiabatic fluctuations damped by viscosity on mass scales smaller than $M = 10^{12} \Omega^{-5/4} h^{-5/2} M_\odot$) (Fall, 1979)

Some models for structure formation: The beginning of the nonlinear stage called intermittency, is characterized by the appearance of pancakes, filaments, compact clusters etc. Here are some models trying to explain how these structures formed.

In the early 1970s, the Soviet cosmologist Zeldovich (1970) suggested a model to explain the distribution of galaxies on large scales. The comparison with a 'pancake' gives a picture of the idea. The matter is initially distributed over enormous sheets which fragment to form galaxies and clusters of galaxies. Computer simulations based on these ideas produce a three dimensional web-like structure in which most galaxies are strung out along thin, thread-like structure of the threads which are the locations of the intersections of the original sheets.

Based on this model, another Soviet researcher, Einasto (1980), first argued that large voids in the distribution of galaxies must be common. In general few filaments of a web would lie in thin slice through it. But what we can see, from the new surveys is,

connected networks and not separated clumps as we would take 'slicing' the Zeldovich's model. So the 'pancake' model probably proved to need more 'sauce' in order to correspond to the reality.

Another model which uses adiabatic fluctuations in an $\Omega_0 < 1$ cosmology, is given by Doroshkevich, Sunyaen & Zeldovich (1974). Here we first have the protoclusters with mass $10^{14} M_0$. When these formations collapse the shock fronts give rise to dense pancakes of matter that could fragment into galaxies via the usual Jeans instability. Production of bound protoclusters of $10^{14} M_0$ requires $(\delta\rho/\rho) > 10^{-2}$

Peebles (1974) suggested the case which is nearly the opposite process to the one above. That means that the galaxies form first and clusters of galaxies form later. Previously, in 1968, Peebles & Dicke proposed (recalling the studies of James Jeans in 1902), that globular clusters, corresponding to the Jeans mass at recombination, were the first objects formed in the Universe and that galaxies are aggregates of such primordial objects. This happens because regions of higher density than the average, and because of the gravitational attraction, are moving towards the centre. This picture implies an isothermal density fluctuation spectrum that extends down to the scales of the Jeans mass at recombination. Peebles cites as evidence for this picture the fact that covariance function of galaxies has a power law form with no intrinsic scales.

Ostriker et al. (1981) suggested that explosions occurred when the Universe was less than a billion years old and drove the hydrogen into thin shells which fragmented to form galaxies. In the beginning a generation of extremely massive stars formed and went supernova. The shock (spherical) waves from the explosions swept

up and compressed ordinary matter. These shells then fragmented and the fragments collapsed to form galaxies. The largest structures we see could be the results of a merging of several adjacent shells. Much less interactive elementary particles left behind, 'filling' the voids with dark matter. The objection in this theory is that these enormous explosions would have an effect which should be detected in the microwave radiation background.

1.5 Dark Matter

In 1936, when Zwicky applied Newton's law for the Coma cluster, he found that the cluster's mass is 10 times larger than the mass of stars in the member galaxies. This 'dark matter problem' has puzzled astronomers since then.

Recently astronomers realized that there has not been time for gravity to pull together the matter to make the structures, we can observe. Consequently, a suggestion came up to cover this difficulty: the dark matter. That is to say, a large fraction of matter in the Universe is invisible. The fraction ρ/ρ_{cr} is believed to be one today, although only 0.1 comes from the data. This balance is very crucial for the evolution of the Universe. Slightly greater than 1, gives a closed Universe, going forward for Big Crunch. For less than 1, we have infinite expanding Universe.

Evidence for the existence of dark matter has also been provided by the rotation curves of galaxies, which tell us how much mass exist within the orbit (from equation $V^2(R)=GM(R)/R$ where $M(R)$ is the mass in a sphere of radius R , and V the rotational velocity) . But this speed seems to be constant after a certain

distance or decreasing slightly. That means there must be a dark halo with more mass than what we can see.

Generally speaking, we can say there are two possible explanations for the dark matter. It is either baryonic or non-baryonic material.

The first moments, after the Big Bang, the Universe was a thermonuclear reactor. The first light elements were hydrogen with admixtures of deuterium (hydrogen-2), helium-3, helium-4 and lithium-7.

A part of the unseen matter (~ 5%) could be baryonic material, like giant planets, dwarf stars, black holes, hot gas between galaxies (it must be hot enough to leave no absorption lines in the light travelling through it and not so hot to emit x-rays), and new galaxies (huge mass of gas with no stars).

The low density of the baryon density reveals, that the Universe cannot be closed due to the normal matter. The only way to explain the 80%, is through existence of nonbaryonic matter.

The theories, trying to explain the most abundant matter, are divided into two categories:

- (i) hot dark matter (HDM)
- (ii) cold dark matter (CDM)

HDM consists mainly of neutrinos (25 electron volts), moving near the speed of light since just before the galaxy formation. They are not affected by the gravity. In 1981, Carlos Frenk, Mark Davies and Simon White, in Berkeley, simulated the evolution of the galaxies, using mathematical models for a neutrino-dominated Universe. But the HDM model did not work because it did not produce small objects (on cosmological scales) like galaxies fast enough and made galaxies too big. After three years George

Efstathiou joined the team and the CDM era began. This model includes 'exotic' particles (\sim several billion electron volts) which move slowly at the epoch of galaxy formation and they are affected by the gravity, clumping together on small galaxy-size scales. Candidates for these particles are axions, photinos and gravitinos, but they are simply hypothetical. This model seems to be contradicted by the Q-DOT survey (e.g. Efstathiou et al. (1990), Kaiser et al. (1991)) (since structures appeared on much larger scales than the theory predicted) and although the galaxy-galaxy spatial correlation function is similar with those estimated by the surveys, the cluster-cluster spatial correlation function is lower (Bond, 1988). What now is possible is either to adjust the CDM or to look for a new model.

The models, implied by different composition of the dark matter, have the basic problem that the seeds which made the structures, do not grow fast enough to give the structures we observe today. This problem prompted the suggestion that a late phase transition occurred after the microwave background radiation decoupled from the matter. With this model we overcome the problems arise from both the HDM and CDM.

1.6 Large-scale Structures in the Universe

Over the last forty years powerful telescopes have enabled the construction of catalogues of positions of galaxies on the sky. Abell (1958) published a catalogue of 2712 rich clusters, Zwicky et al. (1961-68) catalogued 30,000 galaxies and clusters of galaxies in the Northern Hemisphere, and J. Maddox et al. (1988) produced a map of about 2,000,000 galaxies in the Southern Hemisphere

The last years, the new maps are made in redshift space. This combination of celestial coordinates and redshift, reveals patterns in the distribution of galaxies. At the moment, although the area covered is very small, the uncertainties of the Hubble parameter can be neglected because the 'points on the map' are independent of the radial distance. Since 1981 many cosmologists, e.g. Huchra et al. (1990), Eder et al. (1989), Kirshner et al. (1987), Da Costa et al. (1989), Strauss et al. (1990), Gott et al. (1989), Maddox et al. (1990) (APM galaxy survey), Dressler (1988)(900 galaxy survey) etc., designed and studied 3-dimensional surveys looking for large structures. Many catalogues are analysed automatically by electronic devices of institutes like ROE, RGO etc. The new instruments, like CCDs, make the telescopes 50 times more efficient than those in Hubble's era and new instruments are planned to carry out redshift surveys (i.e. 100-inch telescope of Astrophysical Research Consortium of Universities, see also Giovanelli and Haynes (1991) with references therein).

The new maps (as in figures (1.3) & (1.4)) indicate that the general pattern in the distribution of galaxies could be like bubbles or sponges. The galaxies are located in thin surfaces, surrounding holes; the voids. These structures appear to be common in the large-scale distribution of galaxies. Another feature seen in the redshift survey is the Great Wall. It is extended up to ~ 150 by ~ 60 Mpc and is ~ 4 Mpc thick.

In 1983, IRAS satellite was put in orbit. Although the main purpose was to make the first extra-terrestrial infra-red map of our galaxy, it found many very faint galaxies, that had never been catalogued before. Apart from the many other low mass, low luminosity galaxies discovered, suggesting that the intergalactic

voids may be populated by massive, slowly evolving objects, a whole class of galaxies, like Malin 1, seem to be undetected in the surveys, because, although they are luminous, this light is spread over an enormous area, making their disks invisible on the photographs. All these galaxies, hidden by the conventional surveys, might form stars sporadically and very slowly, as implied by the low surface brightness of their disks.

The new observations confirmed, as well, that there is a large accumulation of galaxies more than 150 million l-y away, called Great Attractor. It was found in 1988 (Lynden-Bell et al., 1988) by a group of astronomers, known as 'seven samurai'. They showed that many elliptical galaxies of our neighbourhood are streaming towards the same point in the sky, with velocities higher than predicted by the expansion of the Universe.

The next decades are going to reveal more details for the large-scale structure of the Universe, dark matter and the relationship with the light-emitting matter. The existing telescopes will take advantage of the new technology. The fiber-fed spectrographs will help the measurements of redshift of, at least, hundred galaxies at the same time.

Statistical measure of the structures: The first large scale surveys, during fifties (and even the two dimensional by Shapley (1930, 1933, 1934)) showed that the galaxies are not distributed randomly. They clump together forming groups and clusters of galaxies. The first attempt to approximate the mean number density of galaxies in clusters was made by Carpenter (1938) who derived the form $n(r) \propto r^{-\gamma}$ from the surveys (where r is the radius of the cluster and $n(r)$ the number of galaxies). A value 1.7 was given for γ , by De Vaucouleurs (1960, 1971).

The measure of the irregularities has always been an interesting and attractive way to extract information of the physical systems. Different methods has been used for the comparison between sample systems and the assessment of the agreement between models and data. For example

- multiplicity function: Let n indicate multiplicity and $m(n)$ the fraction of galaxies in a system between n and $n+dn$, of multiplicity $f(n)$. The multiplicity function is defined, in the interval

$$(0,1), \text{ as } M(n) = \sum_{i=1}^n m(i)$$

- nearest neighbour distribution: This function is defined with similar way as the multiplicity function. In this case the nearest neighbour distribution $f(r)$ expresses the fraction of galaxies which exist in the interval $(r,r+dr)$ from each galaxy of the sample.

- percolation analysis: This method is mainly used in Physics, but it was introduced in Cosmology by Shandarin (1983). It has been applied and developed by many cosmologists (e.g. Bhavsar et al. (1983), Einasto et al. (1984))

The problem with the first two methods is that the angular data is not obvious that it is connected with the spatial distribution (Peebles, 1980). The weakness of the percolation method is that the percolation parameter B ($B=(4/3)\pi r^3 n_0$, where n_0 the mean number of particles in a sphere of radius r) depends upon the mean density of particles in the volume we study (Einasto, 1990)

The most popular and frequently used, quantitative analysis includes the correlation function (c.f.). Although the third (or more) order c.f. is more accurate to describe the clustering properties, the two point c.f. seem to be handy and adequate. The power law form c.f., $A r^{-\gamma}$, used mainly today, was established by

Peebles in the beginning of 70's. With the new surveys, new structures has been revealed and other methods (e.g. void probability function introduced by White (1979)) has been created but the c.f. remains a powerful tool to understand better the structure of the Universe. The structures, we observe today, arose from random Gaussian field of small density perturbations and the incomplete information, we have today from the CMBR temperature distribution, does not permit us to conclude with confidence about the initial state of the Universe after decoupling. But using correlation theory and Fourier analysis we can connect the linear density fluctuations with the observed structures.

1.7 Literature

In order to specify the area of our interest we could name it as 'statistical cosmology'. One might object to the definition on the basis that some of the methods were used for others studies, like the distribution of stars in our galaxy. However, cosmology, today (the last seventy years), is well separated from other parts of Astronomy; the studies and methods follow their own path.

Unfortunately, although cosmology has become a popular subject, there is a lack of literature covering the statistical methods. Initially students, new to cosmology, experience difficulties in accessing the information they need. The main source is papers which, often, are very specific and require specialised knowledge of that topic, unavailable in a 'condensed' form elsewhere.

The only suitable book is written by Peebles (1980) who is an enthusiastic researcher of the correlation function. The book is mainly based on papers published about 15 years before the

publication of the book. The 'hub' of his work consists of seven papers which are: (i) Peebles (1973), (ii) Hauser & Peebles (1973), (iii) Peebles & Hauser (1974), (iv) Peebles (1974), (v) Peebles & Groth (1975), (vi) Peebles (1975), (vii) Groth & Peebles (1977). Of course many others, such as Michael Fall (1979), Shandarin & Zeldovich (1989) and Einasto (1990) have contributed significantly. The first use of statistics to study the process of galaxy clustering in the Universe was by Neymann & Scott (1952, 1955), Neymann et al. (1954, 1956).

The statistical methods that were developed in the sixties and seventies for the study of Abell and Zwicky catalogues and the fixed parameters (e.g. the slope of the spatial correlation function) have not changed much since. During the last decade more catalogues appeared adjusting the parameters slightly and verifying the existing laws on larger scales.

All the books concerning cosmology in the 80s are more interested in inflation and physical cosmology than the statistics. In my opinion more data and analysis is needed, before models are constructed. Nature is speaking to us, we must learn how to listen to her!

1.8 Simulations

The improved capability of the computers today, provides the facility to recreate situations which, otherwise, would very difficult to study. In areas of research, like cosmology, where the experimental verification is almost impossible, the simulations contribute significantly. For example in the 'double Poisson processes' we can generate N points according to the Poisson

distribution. These points constitute the centres for secondary clusters which are distributed normally with a mean μ and variance σ^2 . Changing the parameters N , μ and σ^2 , we can take a variety of structures. Then we can apply statistical methods (like pattern-recognition statistics) for the study of these patterns (Ripley, 1981). In addition to other simulation techniques used (study of evolution of overdensities), it is equally important to see how the voids would evolve using 'Voronoi Tessellation' model, as in the case of Matsuda et al. (1984) etc. and statistics of deduced patterns has been studied. In Voronoi Tessellation model we regard the voids as random points. Each point is inclosed by its own polygon which is closer to that point than any other nearby polygon. The periphery could expand outwards and the intersections are where the clusters are formed. This model seem to give spatial correlation function very similar to those derived by the observations (Yoshioka et al., 1989). A way to measure the connectedness of the filamentary structures is the 'minimal spanning tree' (MST) (Barrow et al., 1985) and the method has been applied to catalogues (e.g. Zwicky, CfA etc.) and simulated data (Bhavsar & Ling (1988), Martinez & Jones (1990), Martinez et al. (1990)). Other quantitative methods have also used (e.g. Einasto et al., 1983).

The simulations offer the advantage of testing models, starting with initial conditions and comparing the results with the observations. Generally the resulting structures are not identical to those observed. For instance in some simulations the contrast between high and low density regions is not large enough, the voids are too small and the remarkable observed coherent patterns in the galaxy distribution are not reproduced. The problems which usually arise, originate when some results could correspond to a

variety of initial conditions. Most numerical simulations are based on the assumption that the initial perturbations are Gaussian. The theoretical conclusion that structures in a density distribution arise at the nonlinear stages if the spectrum of the linear perturbations falls off steeply enough with decreasing wavelength is confirmed (Shandarin et al., 1989). The problem of initial conditions has been put very well by Hawking in 'New Physics' (1989): '... the laws of science would not fix what the state of the Universe was in the infinite past. In order to pick out one particular state of the Universe from among the set of all possible states that are allowed by the laws, one has to supplement the laws by boundary conditions which say what the state of the Universe was at an initial singularity or in the infinite past. ... the Universe could have started off in a completely arbitrary state.... but one can merely pick a reasonable set of boundary conditions, calculate what they predict for the present state of the Universe and see if they agree with observations'. One prominent effort in cosmology is the reconstruction of the primordial power spectrum using the two-point correlation function and Fourier analysis.

Generally the simulations are used for the dynamical study of the Universe. They are oriented to the evolution of the structures and the changes produced under the action of the gravity. They are used to compute the distribution of mass (e.g. Bertschinger & Gelb, (1991)) and then the regions, which exceed a predefined threshold of continuous underlying gaussian density field, form galaxies (the so called 'biased galaxy formation'). Work on the gaussian fields in one and three dimensions has been done by Kaiser (1984) etc.

Our simulation aims at the 'static' description of the structures. We set up a software in order to see the connection

between the spatial and angular correlation function. We are mainly oriented to the computation of the angular correlation function from a generated sample. The theory is based on the Fourier analysis and uses the spatial correlation function as a fundamental tool for the generation of random functions. We extended the programme in such a way as to provide the basis for a continuing examination involving of different factors, like for instance, the selection effects, the direct derivation of the angular correlation function (without generating a data), the simultaneous study of different forms of spatial correlation functions etc.

During the last years, we can see an increasingly number of models, attempting to explain the origin and structure of the observed Universe. Although many fundamental properties can be explained, no theory can fit 'exactly' the observations. Many problems remain to be solved the next years. In the near future, the concurrent of the observational techniques and the new theories in particle-physics, might give answer to many of the problems which the cosmology faces today.

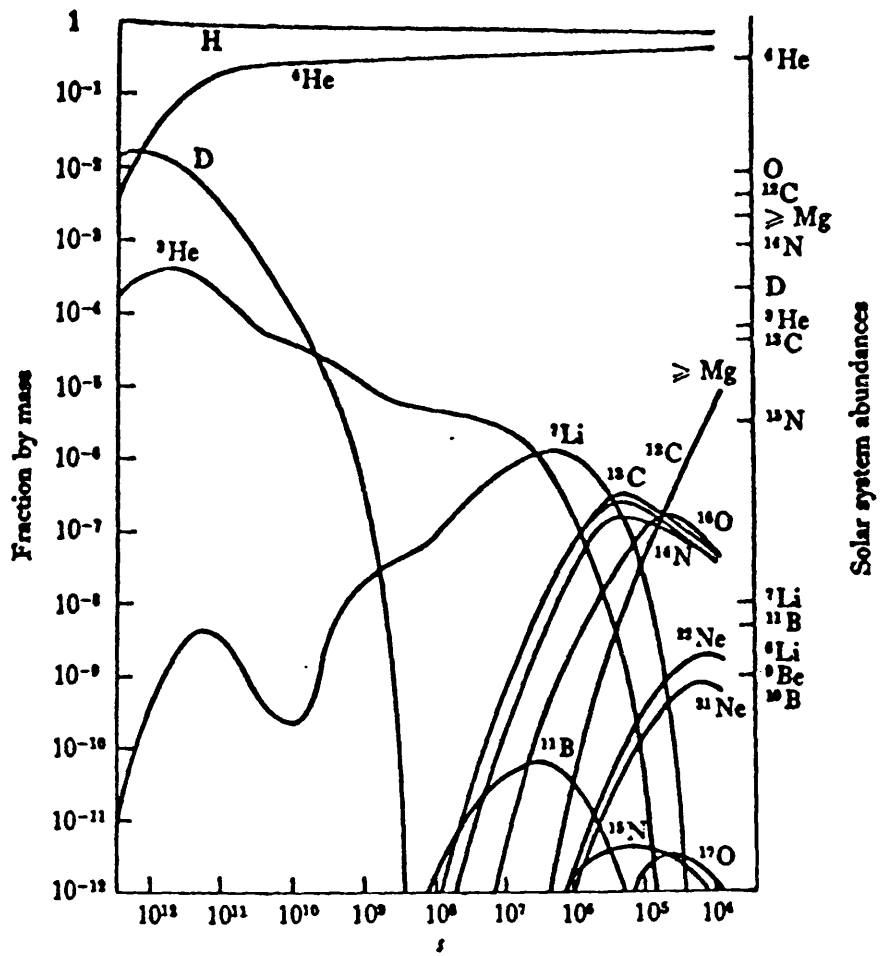


Fig. 1.1: Element production in the hot Big Bang (adopted by D. W. Sciama, 1975)

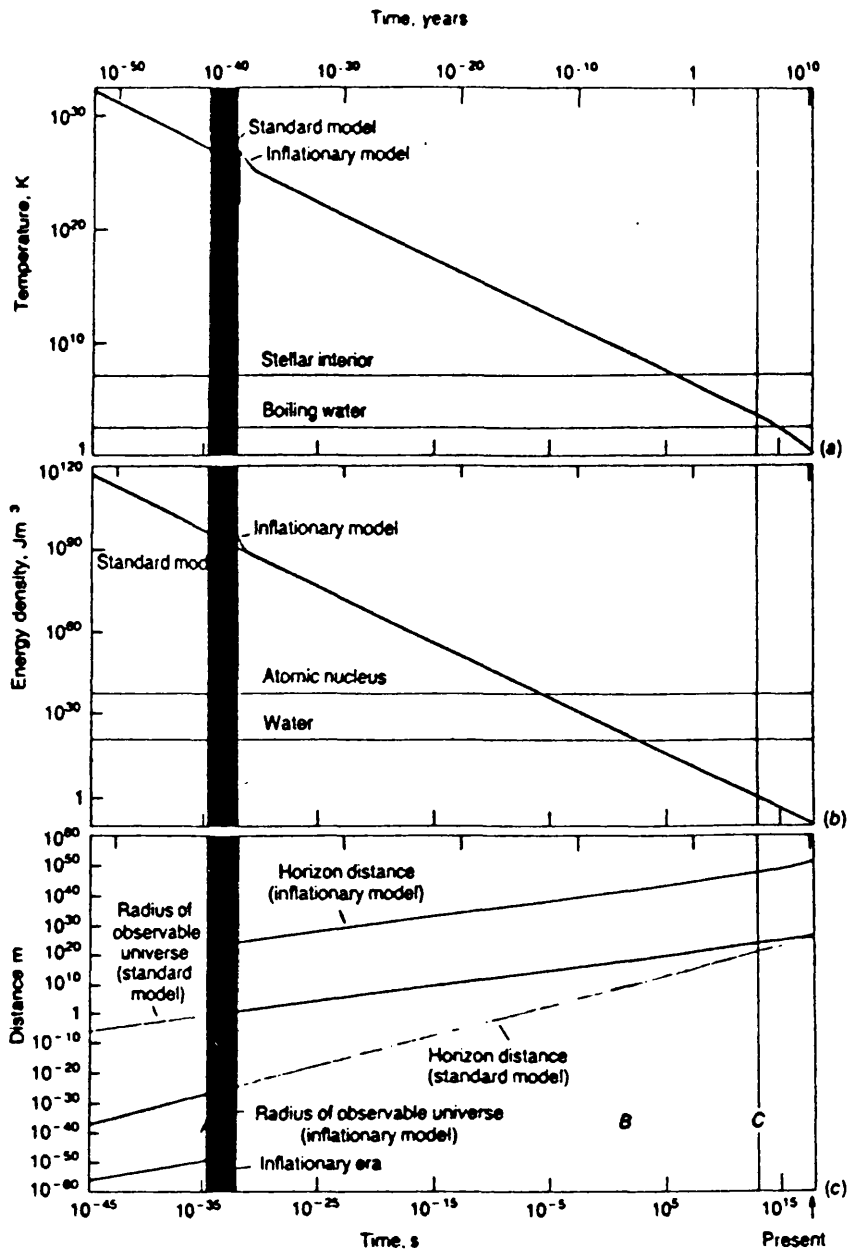


Fig. 1.2 Three parallel graphs comparing the inflationary model with the standard one for different parameters (temperature, energy density and distance). They are divided vertically by two bands indicating the period the inflation occurred (A) and the nucleosynthesis (B). The line C is standing for the time when the Universe became transparent to electromagnetic radiation. The two horizontal lines in (a) and (b) represents the corresponding values for the water and star.

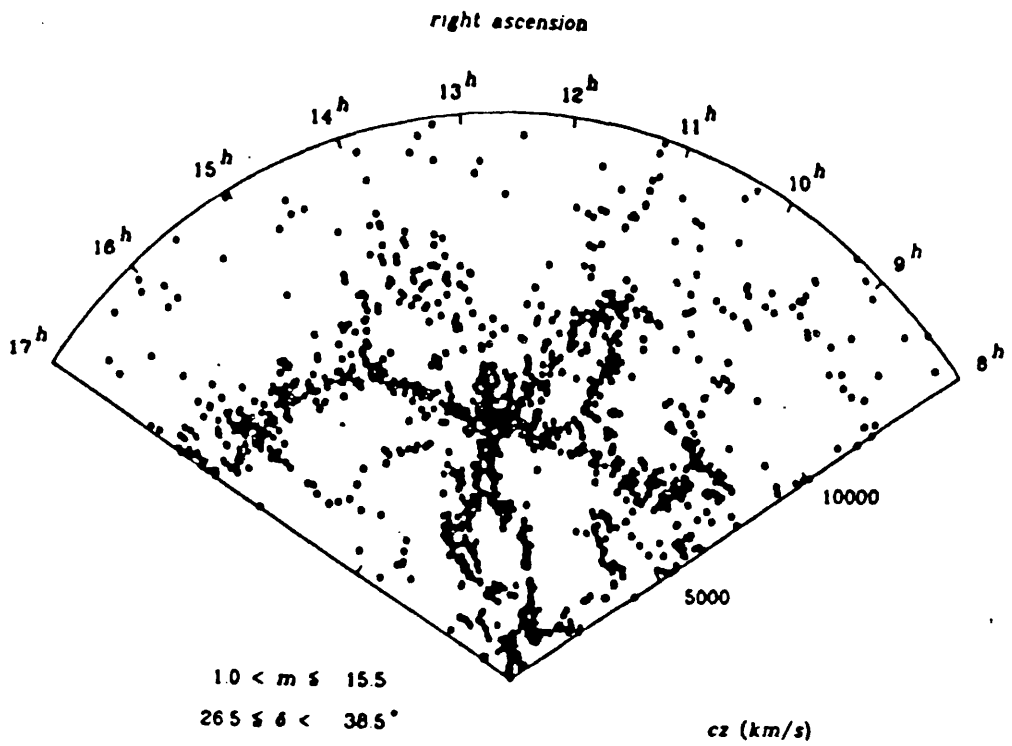


Fig. 1.3: Cone diagram for 1778 galaxies. It is obvious that the distribution of galaxies is inhomogeneous surrounding empty voids (Geller and Huchra, 1988)

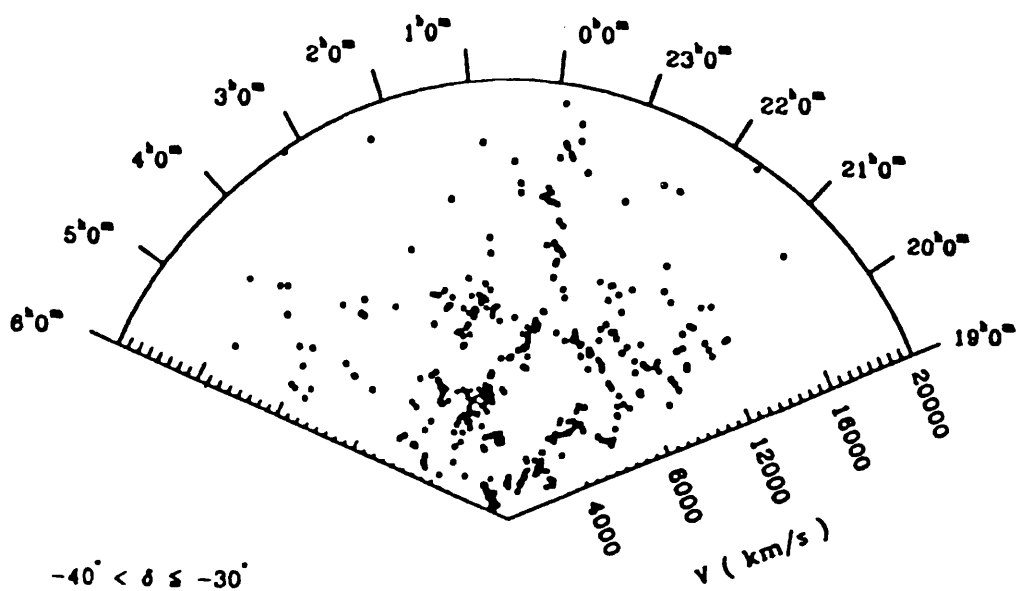


Fig. 1.4 : Distribution (in redshift space) of 480 galaxies from the Southern Sky Redshift Survey (Nicolaci Da Costa et al., 1989)

CHAPTER 2

STOCHASTIC PROCESSES

We shall assume that the matter distribution can be described as a realization of a stationary random function. In this chapter on random processes, we shall deal with problems of stationary random functions from a theoretical point of view. In section 2.1 we define what is meant by the random processes and introduce the notion of stationarity, and the correlation function. We are mainly interested in the first and second moments of the random functions. The theory based on the mean value and correlation function is called correlation theory. References for the first section, which give an extensive analysis and discussion, are Chatfield (1989), Papoulis (1965), Yaglom (1962), and Cox & Miller (1964).

2.1 Random Processes

2.1.1 Definitions

Consider a regular die with a different number on each of its six faces; If we toss the die repeatedly there are only six possible outcomes, called elementary events, which form a set Ω . To every element, ω , of this set we associate a real number $x(\omega)$. The relation between the two sets is called a real valued *random variable* (r.v.). x , is a real function whose domain is the space Ω and such that

(i) the set $\{x \leq x\}$ is an event (subset of the space Ω) for any real number x

$$(ii) P\{x = +\infty\} = P\{x = -\infty\} = 0$$

A complex r.v., c , is defined as

$$c = a + ib \quad (2.1)$$

where a and b are real random variables. If to every elementary event ω (with domain the set of all the experimental outcomes) there corresponds a function $x(t, \omega)$, defined on R , then we say that we have a *stochastic process*. When the domain of t is the real axis and t represents time, then the process is called *continuous-time stochastic process* or random function. When the domain is a set of integers, it is a *discrete-time process*. For every fixed value ω , we get one *realization* (or sample path). For a particular t we have a set of possible values (the states) corresponding to possible outcomes ω , called state space. Thus fixing t and regarding ω as a random outcome, $x(t)$ becomes r.v. The cumulative distribution of $x(t)$, $F(x; t)$, is given by

$$F(x; t) = P\{x(t) \leq x\}$$

The probability density function $f(x; t)$ is obtained differentiating with respect to x , i.e.

$$f(x, t) = \frac{\partial F(x, t)}{\partial x}$$

A complete description of the random process will be given by specifying the joint distribution of $\{x(t_1), x(t_2), \dots, x(t_n)\}$ for $n=1, 2, 3, \dots$ and real values of t_j , $j=1, \dots, n$. Thus we may describe the process by giving the set of functions

$$f_n(x_1, x_2, \dots, x_n; t_1, t_2, \dots, t_n)$$

A complex process can be defined similarly by

$$c(t) = a(t) + ib(t)$$

where $a(t)$ and $b(t)$ are real r.f. In this case the family of r.v. consists $2n$ values. The process $c^*(t)$ denotes the conjugate.

2.1.2 Stationarity

There are two kinds of stationarity: the first one is called strict and occurs when the joint probability density function of $x(t_1), x(t_2), \dots, x(t_n)$ is the same as the joint probability density function of $x(t_1+r), x(t_2+r), \dots, x(t_n+r)$ for all t_1, t_2, \dots, t_n, r ; the other one is called second-order (or weak) and requires constant mean and the covariance to depend only on the lag. Strict stationarity implies second-order stationarity for Gaussian processes (e.g. Chatfield, 1989). We shall assume that the random processes are weak sense stationary.

2.1.3 First & Second Moments

The mean is defined by

$$\langle x(t) \rangle = \int_{-\infty}^{+\infty} xf(x, t)dx$$

This is also called the first moment. If the process is stationary, $\langle x(t) \rangle$ is independent of t . We can define the second moment

$$R(t_1, t_2) = \langle x(t_1)x(t_2) \rangle = \int_{-\infty}^{+\infty} \int_{-\infty}^{+\infty} x_1 x_2 f(x_1, x_2; t_1, t_2) dx_1 dx_2 \quad (2.2)$$

For a stationary process $R(t_1, t_2) = R(|t_2 - t_1|)$. The autocovariance of $x(t)$ is the second central moment

$$\begin{aligned} C(r) &= \langle [x(t) - \langle x(t) \rangle][x(t+r) - \langle x(t) \rangle] \rangle \\ &= \langle x(t)x(t+r) \rangle - \langle x(t) \rangle^2 \end{aligned} \quad (2.3)$$

The ratio

$$\gamma(r) = \frac{C(r)}{C(0)} = \frac{C(r)}{\sigma^2}$$

where σ^2 is the variance, is called autocorrelation function with the properties

$$(i) \gamma(r) = \gamma(-r)$$

$$(ii) |\gamma(r)| \leq 1$$

(iii) a stochastic process has a unique autocorrelation function but the converse is not true.

For a complex stochastic process the autocorrelation function is defined as

$$R(r) = \langle x(t)x^*(t+r) \rangle$$

and the autocovariance as

$$C(r) = \langle [x(t) - \langle x(t) \rangle][x^*(t+r) - \langle x(t) \rangle] \rangle$$

with the property $C(-r) = C^*(r)$

2.1.4 Continuity

We say that a process $x(t)$ is continuous at t if $\lim_{\epsilon \rightarrow 0} x(t + \epsilon) = x(t)$ for almost all the outcomes or realisations and continuous in the *mean square sense* if

$$\lim_{r \rightarrow 0} \langle [x(t+r) - x(t)]^2 \rangle = 0 \quad (2.4)$$

Eq. (2.4) implies the continuity of the *mean* in which the expected value of $x(t)$ must be continuous:

$$\lim_{r \rightarrow 0} \langle x(t+r) - x(t) \rangle = 0 \quad (2.5)$$

The meaning of eq. (2.4) is that almost all the realizations $x(t)$ will be continuous at a particular point in an interval, but does not imply that will be continuous for every t . We can state this using the theorem which is very important when we discuss the problems arising from the definition of a particular form of autocorrelation function, because indicates that we can not generate a continuous process when the autocorrelation is not continuous in the origin.

Theorem: A stationary process $x(t)$ is mean square continuous if and only if its autocorrelation function $R(r)$ is continuous for $r \rightarrow 0$.

Proof: (\Leftarrow) Expanding the square (2.4), assuming the process is stationary and using eq. (2.2) we have

$$\lim_{r \rightarrow 0} \langle [x(t+r) - x(t)]^2 \rangle =$$

$$\lim_{r \rightarrow 0} \langle x^2(t+r) \rangle - 2 \langle x(t+r)x(t) \rangle + \langle x^2(t) \rangle =$$

$$\lim_{r \rightarrow 0} [R(0) - R(r)] = 0 \quad (2.6)$$

(\Rightarrow) $R(r) - R(0) = \langle x(t+r)x(t) \rangle - \langle x^2(t) \rangle$. We assume that the process is continuous in m.s.s which implies that $x(t+r) \rightarrow x(t)$ for $r \rightarrow 0$. So we have

$$\lim_{r \rightarrow 0} [R(r) - R(0)] = 0$$

2.1.5 Correlation Length

Till now we were talking about the r.v. x as a function of time, t . From now on we define it to represent a function over distance. The correlation length r_0 is the scale length over which $x(t)$ is correlated with $x(t+r_0)$. Let assume that a correlation function is expressed by decay law. That means the correlation at any distance x is directly proportional to the total average number of points at any separation. This is denoted as

$$-\frac{dR}{dx} \propto R$$

where the negative sign indicates that the R decreases as x increases. If we define the constant of proportionality $1/r_0$, the above expression is

$$-\frac{dR}{dx} = \frac{1}{r_0} R \quad (2.7)$$

For $R(0)=1$ and assuming that at distance x_0 the R takes the value R_0 we have,

$$R = e^{-\frac{x}{r_0}}$$

integrating the (2.7). We could also define the correlation length as the distance at which the s.c.f. falls to half of its value.

2.2 Matter Density as Random Functions

Random functions can also be defined over R^3 . We can regard the matter distribution in the Universe as a realization of a random function $\rho(\underline{x})$. We assume that the distribution of galaxies represent a 'stationary random process'. Taking $\rho(\underline{x})$ to be the number of galaxies per unit volume in a given direction and at a distance \underline{x} (Limber, 1953), we describe the distribution of objects by a continuous density function

$$\rho(\underline{x}) = \rho_0(1 + \delta(\underline{x})) \quad (2.8)$$

where ρ_0 is the average number density of galaxies and $\delta(\underline{x})$ the density fluctuation. The $\rho(\underline{x})$ is a function of the position. It is generated by a random (or stochastic) process and is one of an ensemble of random functions which might be generated by the process. The random process is assumed to be Gaussian (generally this is not necessary, but more convenient) which means that, for every n , $\underline{x}_1, \underline{x}_2, \dots, \underline{x}_n$, the joint probability distribution of

$$\delta(\underline{x}_1), \delta(\underline{x}_2), \dots, \delta(\underline{x}_n)$$

is an n -dimensional Gaussian or normal distribution. Such a Gaussian random process is completely determined by the ensemble averages $\langle \delta(\underline{x}) \rangle = \langle \{ \delta(\underline{x}_i) \} \rangle$ and by the covariances

$\langle (\delta(\underline{x}_i) - \langle \delta \rangle)(\delta(\underline{x}_j) - \langle \delta \rangle) \rangle$. As a matter of convenience in development we will assume that the averages $\langle \delta(\underline{x}_i) \rangle$ are zero. The covariance then reduce to $\langle \delta(\underline{x}_i) \delta(\underline{x}_j) \rangle$.

Usually in stochastic processes we study the statistics of an ensemble of different realizations. But in some cases (i.e. communications engineering) is more usual to work with a single time function of infinite extent instead of many realizations. There is a series of theorems concerning with the asymptotic behaviour of time averages in the framework of the ergodic theory. The mean value of the process $\mathbf{x}(t)$ for various realizations is called *ensemble-average* and gives the average over n states ($\frac{1}{n} \sum_i \mathbf{x}(t, \omega_i)$). When

we have one sample, then we can use the *time-average* given by

$\lim_{T \rightarrow \infty} \frac{1}{T} \int_{-T}^T \mathbf{x}(t, \omega) dt$. These definitions can, of course, be applied for functions of distance.

2.3 Spectral Analysis

Spectral analysis is an application of Fourier analysis for stochastic functions. On the one hand, in Fourier analysis, a function is approximated by a sum of sin and cos terms. On the other hand, spectral analysis is concerning mainly with the study of the spectral density function estimated by the ensemble of random functions. In our case spectral analysis is a very handy way to represent the density inhomogeneities in the Universe. In this section we shall see how this is possible.

Power Spectrum: The *power spectral density function* (or simply *spectrum*) is defined as the fourier transform of the autocorrelation function:

$$f(\underline{k}) = \int_{-\infty}^{\infty} \int_{-\infty}^{\infty} \int_{-\infty}^{\infty} R(\underline{r}) e^{-i\underline{k} \cdot \underline{r}} d^3 \underline{r} \quad (2.9a)$$

It can be shown that $f(\underline{k})$ characterizes the distribution of the density contrast, δ , in Fourier space. The inverse of (2.9a) is

$$R(\underline{k}) = \frac{1}{(2\pi)^3} \int_{-\infty}^{\infty} \int_{-\infty}^{\infty} \int_{-\infty}^{\infty} f(\underline{k}') e^{i\underline{k} \cdot \underline{k}'} d^3 \underline{k}' \quad (2.9b)$$

The spectrum gives the contribution of the frequencies to the variance in the range $(k, k+dk)$. When $k=0$ then the area underneath the curve $f(k)$ corresponds to the variance of the process. The power spectrum of a stochastic process is a real function and >0 .

1D Approach: Say we have a stationary process $\delta(x)$ with autocorrelation function $R(r)$. There are two cases

(i) if the stationary process, $\delta(x)$, is periodic then $R(r)$ is also periodic in $(0, L/2)$ and expanded in Fourier series

(ii) $R(r)$ is not periodic (which is actually the case we are interested in). We form the sum

$$\hat{\delta}(x) = \sum_{k=-\infty}^{\infty} \delta_k e^{-ikx} \quad (2.10)$$

If $R(r) \rightarrow 0$ as $|r| \rightarrow 0$ then

$$\lim_{L \rightarrow \infty} L \langle \delta_n \delta_m^* \rangle = \begin{cases} f(k) & n = m \\ 0 & n \neq m \end{cases} \quad (2.11)$$

and we can generate a realization, $\hat{\delta}(x)$ in the interval $(0, L/2)$ with the coefficients of the series (2.10) taking values given by

$$\delta_k = |\delta_k| e^{i\phi_k} \quad (2.12)$$

where $|\delta_k|$ is called Fourier Spectrum of δ_k and ϕ_k its phase angle, which we choose it to be drawn from a uniform distribution. The realization $\hat{\delta}(x)$ is a periodic function. It can be proved that if $\hat{\delta}(x)$ is mean square periodic, then its autocorrelation $\hat{R}(x)$ is periodic. But the original autocorrelation function $R(r)$ was not periodic. That is to say that the $\hat{\delta}(x)$ is only good approximation to realization of $\delta(x)$ with autocorrelation function $R(r)$ in the interval $(0, L/2)$.

From now on we shall assume (for convenience) that $\delta(x)$ is the $\hat{\delta}(x)$. Expanding the function $\delta(x)$ in Fourier series we have

$$\delta(x) = \sum_{k \geq 0} \delta_k e^{-ikx} = \sum_{k \geq 0} 2|\delta_k| \cos(kx - \phi_k) \quad (2.13)$$

This equation means, in practice, that every variation in the space is caused by variations with different frequencies and $|\delta_k|$ is their amplitude.

The different sets of graphs fig. 2.1-2.4 show realizations of the random processes obtained for four correlation functions, which are: $(r/r_0)^{-\gamma}$, $\exp(-(r/r_0)^2)$, $\exp(r/r_0)$, $(r+r_0/r_0)^{-\gamma}$ (fig. 2.5). Every graph indicates three realizations. The FT for the correlation functions are respectively

$$\frac{2r_0^\gamma \cos[\frac{\pi}{2}(1-\gamma)]}{L \Gamma(1-\gamma)^{1-\gamma}} 2\pi \quad (2.14)$$

$$\frac{2}{L} \frac{1}{r_0} \frac{1}{\frac{1}{r_0^2} + k^2} 2 \quad (2.15)$$

$$\frac{2}{L} \sqrt{\pi} r_0 e^{-\frac{1}{4} k^2 r_0^2} \quad (2.16)$$

$$\frac{2r_0^\gamma}{L} \frac{1 - \cos\left[\frac{\pi}{2}(1-\gamma)\right]}{e^{ak} \Gamma(1-\gamma)^{1-\gamma}} 2\pi \quad (2.17)$$

where r_0 is the correlation length and γ the exponent of the c.f. We took 50 frequencies corresponding to length $L=20$. The minimum length is taken to be 0.4.

In the first figure we can distinguish clearly the tendency of the process to discontinuous values as the cor. length increases. In this case, the realizations should be discontinuous because, according to the theorem in section 2.1.4, the correlation function $(r/r_0)^{-\gamma}$ is not continuous in the origin when $r \rightarrow 0$. This, we believe, has to do with high amplitudes coming from the coefficients of the Fourier series. Its spectrum is flat and does not depend upon the frequency k , but depend only upon the r_0 , resulting higher values for the amplitude of the process.

Spectral analysis in 3^D : The stochastic process $\delta(\underline{x})$ is expanded in Fourier series in 3^D as follow

$$\delta(\underline{r}) = \sum_{3^D \text{ k-space}} \delta_{\underline{k}} e^{-i\underline{k}\underline{r}} \quad (2.18)$$

where the Power spectrum $|\delta_{\underline{k}}|^2$ is the F.T. of the a.c.f. We can rewrite the above equation (2.18), choosing wavenumber values such that we limit the waves to propagate into half of the k -space only, in the form

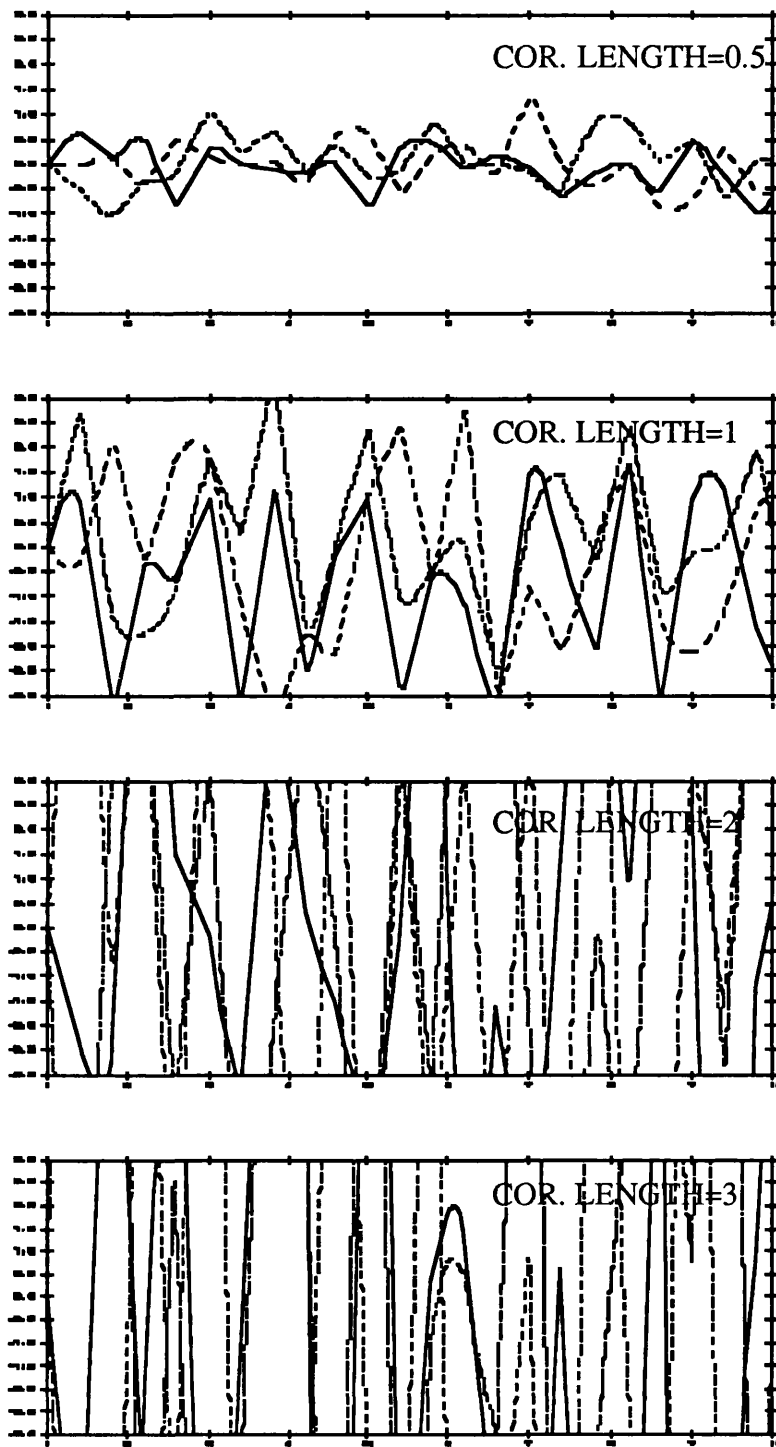


Fig. 2.1 : Realizations generated by the S.C.F. $(r / r_0)^{-\gamma}$
in 1D

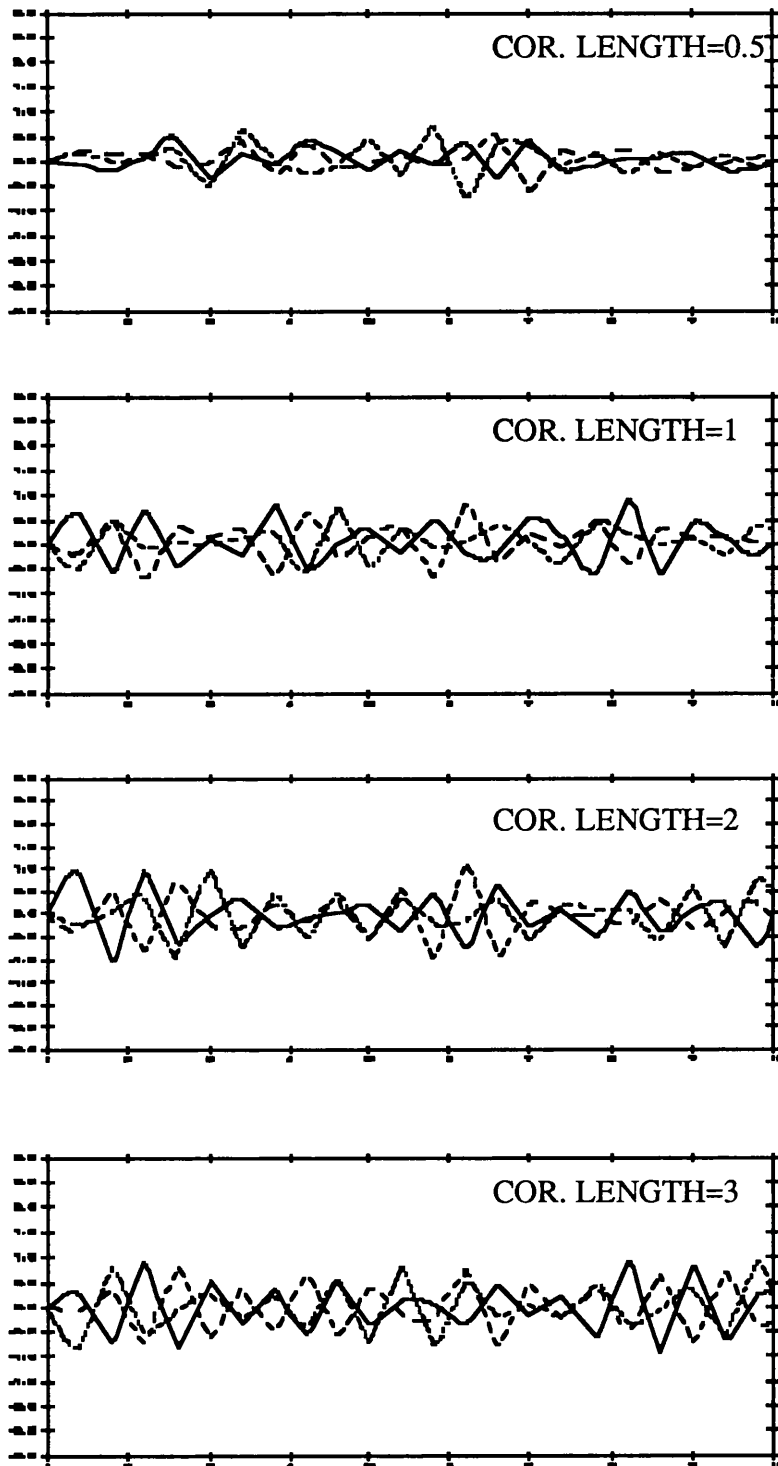


Fig. 2.2 : Realizations generated by the $\exp(-r/r_0)$ in 1d

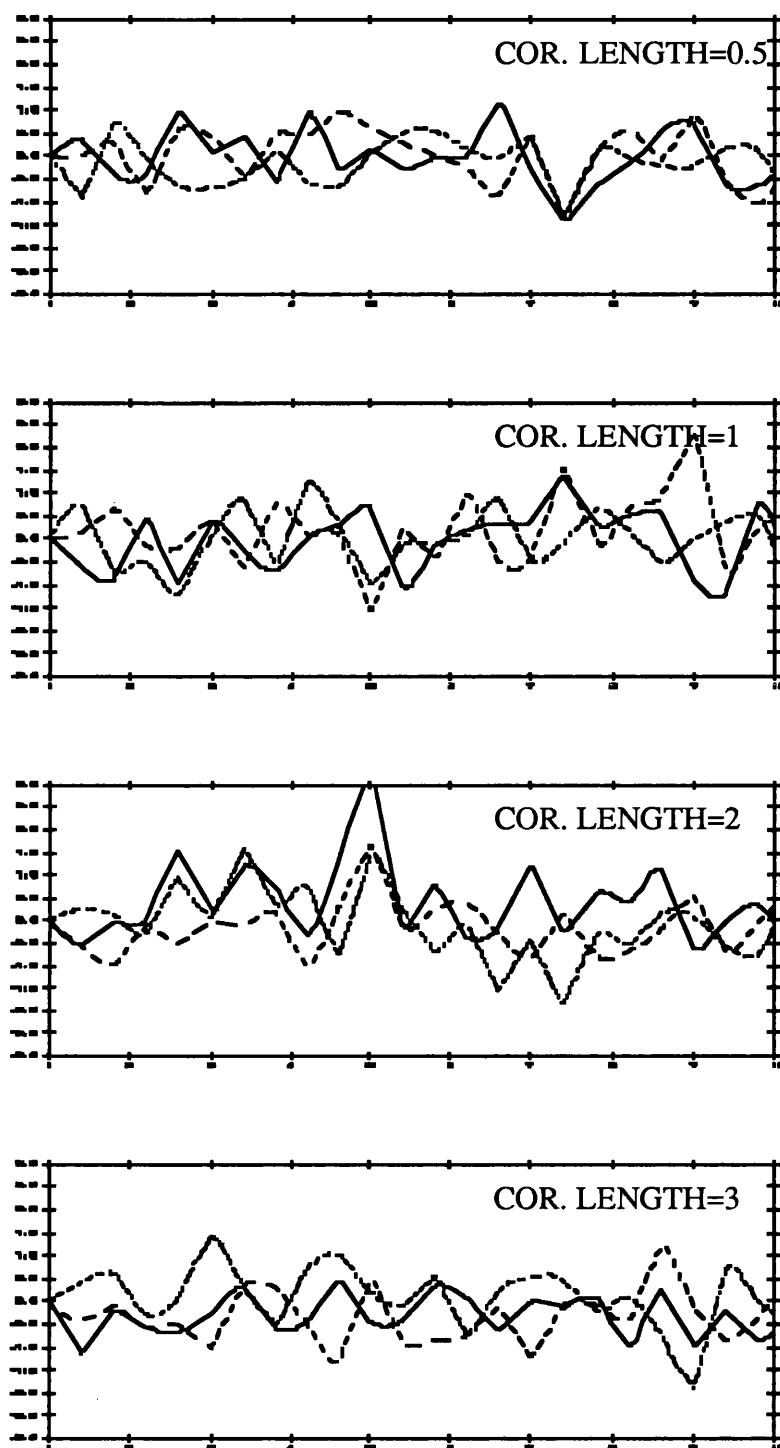


Fig. 2.3 : Realizations generated by the S.C.F. $\exp(-r/r_0^2)$ in 1d

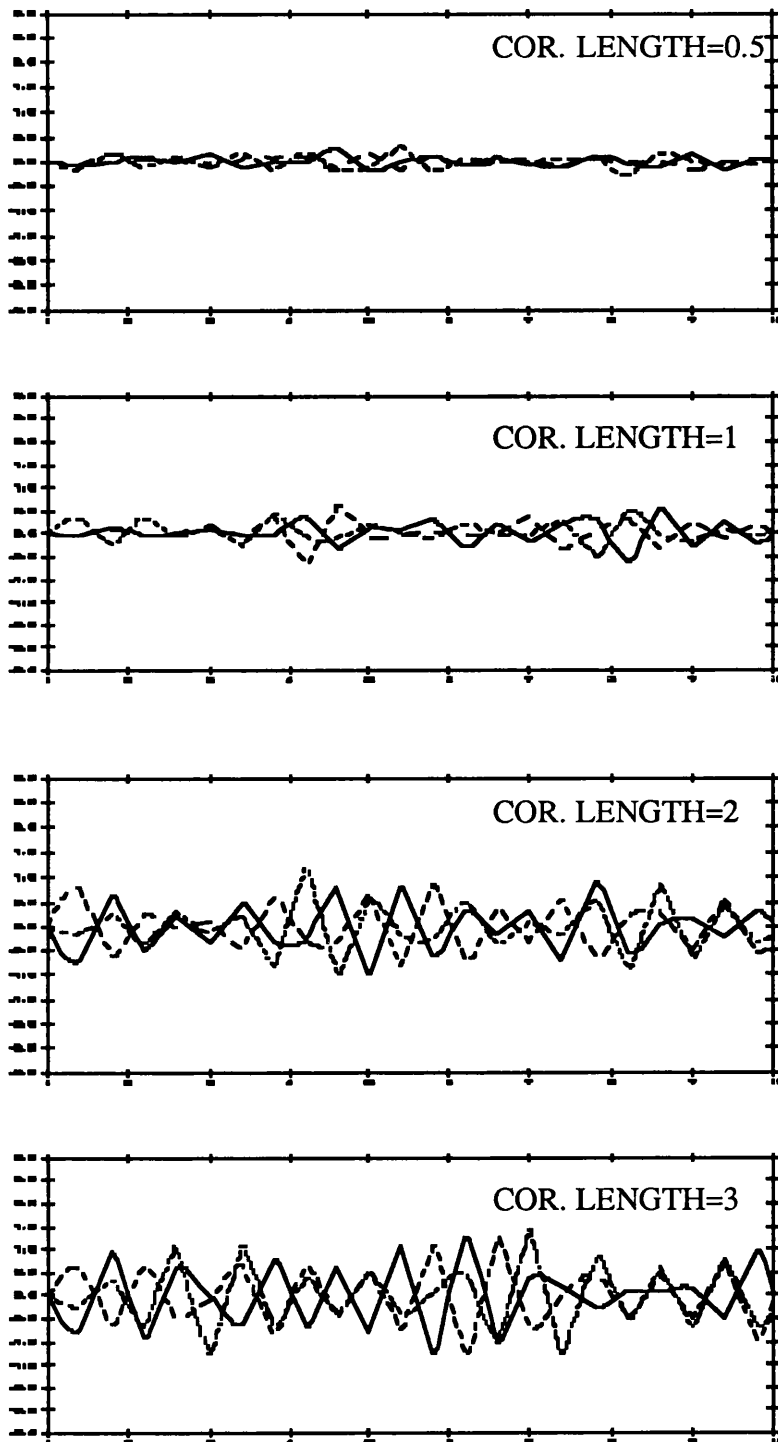


Fig. 2.4 : Realizations generated by the S.C.F. $(r + r_0) / r_0^{-\gamma}$
in 1d

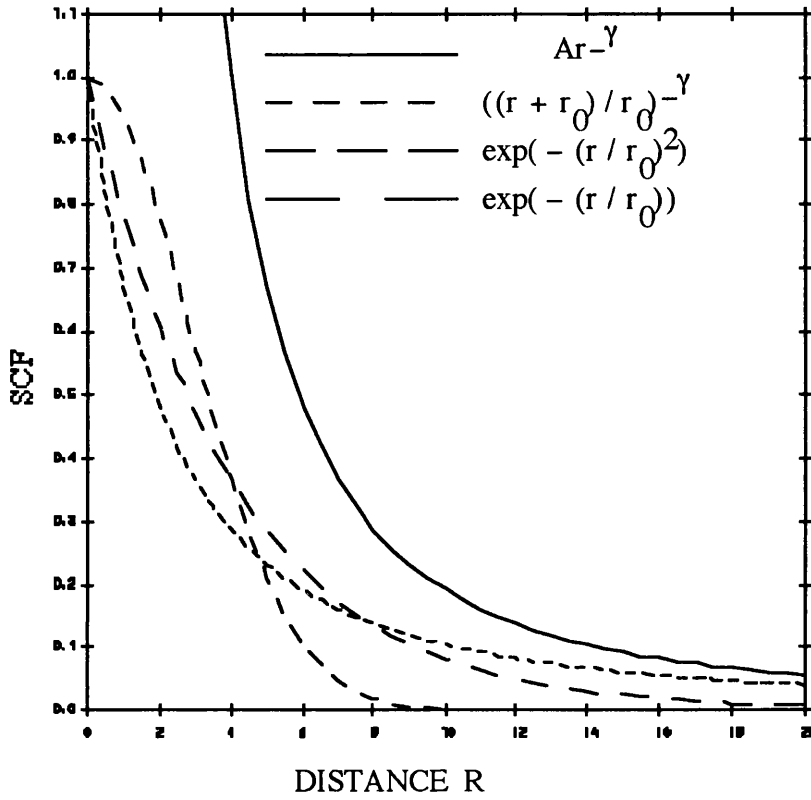


Fig. 2.5 : Different formulae for spatial correlation function

$$\delta(\underline{r}) = \sum_{k_x=0}^{\text{numfreq}} \sum_{k_y=-\text{numfreq}}^{\text{numfreq}} \sum_{k_z=-\text{numfreq}}^{\text{numfreq}} (\delta_{\underline{k}} e^{-i\underline{k}\cdot\underline{r}} + \delta_{\underline{k}}^* e^{-i\underline{k}\cdot\underline{r}})$$

and because $\delta_{-\underline{k}} = \delta_{\underline{k}}^*$ we have

$$\delta(\underline{r}) = \sum_{k_x=0}^{\text{numfreq}} \sum_{k_y=-\text{numfreq}}^{\text{numfreq}} \sum_{k_z=-\text{numfreq}}^{\text{numfreq}} 2 \operatorname{Re}(\delta_{\underline{k}} e^{-i\underline{k}\cdot\underline{r}})$$

Let $\delta_{\underline{k}} = |\delta_{\underline{k}}| e^{i\phi_{\underline{k}}}$, where $\phi_{\underline{k}}$ is a phase of mode \underline{k} having uniform random distribution between 0 and 2π . So

$$\delta(\underline{r}) = \sum_{k_x=0}^{\text{numfreq}} \sum_{k_y=-\text{numfreq}}^{\text{numfreq}} \sum_{k_z=-\text{numfreq}}^{\text{numfreq}} 2|\delta_{\underline{k}}| \cos(\underline{k}\cdot\underline{r} - \phi_{\underline{k}})$$

The wavenumber $\underline{k}(k_l, k_m, k_n)$ (number of wavelengths per unit distance) is related to l, m, n in equation (2.18), by (e.g. Kolb & Turner (1990), p.325):

$$k_x = \frac{2\pi l}{L}, \quad k_y = \frac{2\pi m}{L}, \quad k_z = \frac{2\pi n}{L} \quad (2.19)$$

and the wavelength of a perturbation is related to the wavenumber by $\lambda = \frac{2\pi}{k}$. So the wavelength λ in 3^D is:

$$\begin{cases} \lambda_x = \frac{2\pi}{k_x} = \frac{2\pi}{2\pi l} L = \frac{L}{l} \\ \lambda_y = \frac{2\pi}{k_y} = \frac{2\pi}{2\pi m} L = \frac{L}{m} \\ \lambda_z = \frac{2\pi}{k_z} = \frac{2\pi}{2\pi n} L = \frac{L}{n} \end{cases} \quad \text{for } l, m, n \in (-\infty, \infty) \quad (2.20)$$

Because in practice it is very difficult to have a sum over $(-\infty, \infty)$ in eq. (2.18) we choose limited number of frequencies. This number is characterized by a minimum wavelength λ_{\min} , and a maximum which is the distance of the volume we consider. If we assume that $a=L/\lambda_{\min}$ than the wavelengths are given by:

$$\lambda_1 = \frac{L}{1}, \quad \lambda_2 = \frac{L}{2}, \quad \dots, \quad \lambda_a = \frac{L}{a}$$

with $l, m, n = 1, 2, \dots, a$. The corresponding wavenumbers are

$$k_1 = \frac{2\pi}{L}, \quad k_2 = \frac{4\pi}{L}, \quad \dots, \quad k_a = \frac{2\pi a}{L}$$

Using the theory of this chapter we set up a programme which, in the beginning, generates random functions. The selection of the frequencies in the programme is based on the method described in the last section. The programme reads the size of the side of the cube, 'limit', we wish to consider, and the minimum wavelength, 'incstep'. Then it divides the 'limit' by the 'incstep' giving the number of frequencies, 'numfreq', we are going to use. The highest frequency corresponds to 'incstep' and the lowest to length 'limit'. The value 'incstep' must be smaller than the 'meansep' which represents the correlation length. Starting with this way and applying the theory of the last section we generate realizations for the function $\delta(\underline{x})$. A general idea of how it looks like is given in the fig. 2.6-2.9.

Using density contrast so generated we are in a position to make direct calculation of the angular correlation function.

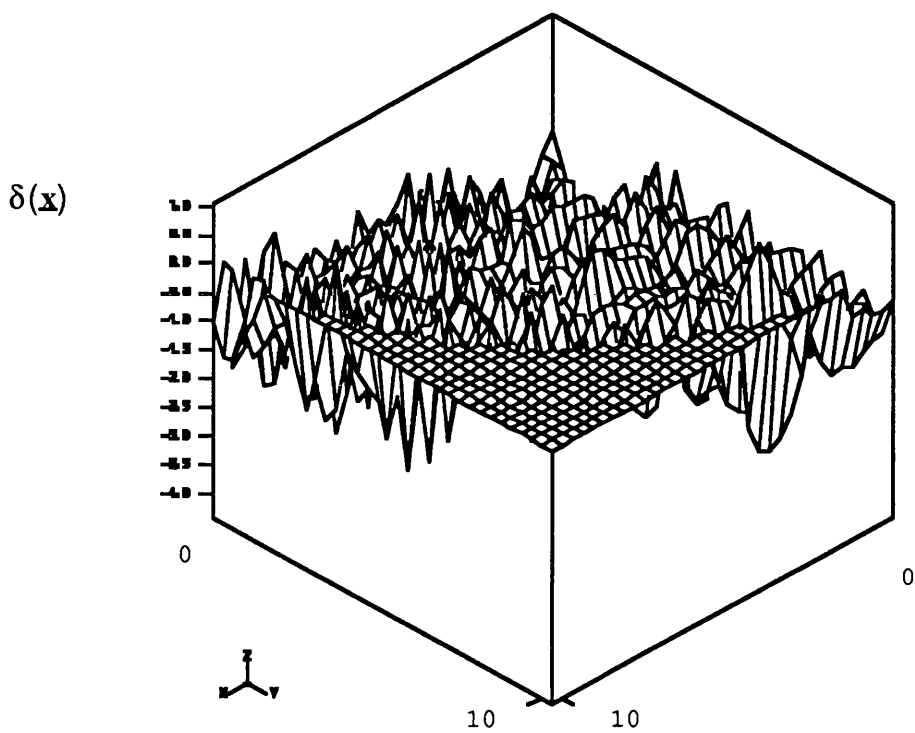


Fig. 2.6 : Density function corresponding to the S.C.F. $(r/r_0)^{-\gamma}$
for min. wavelength = 2, L=20, R=10, Correlation Len.=2.5

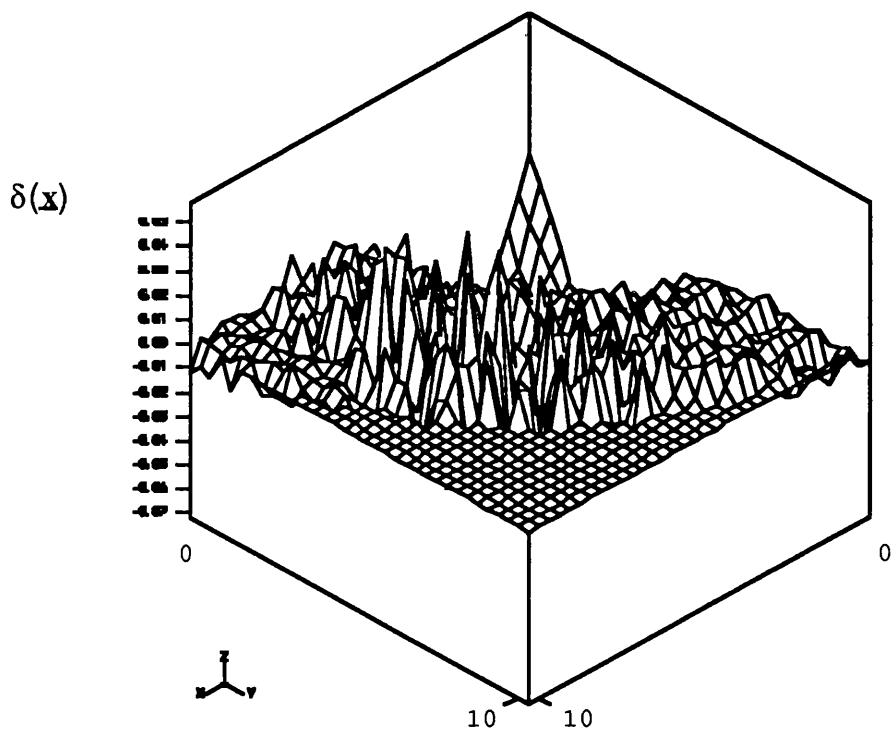


Fig. 2.7: Density function corresponding to the s.c.f. $\exp(- (r / r_0)^2)$ for min. wavelength=2, $L=20$, $R=10$ & Correl. Length=2.5

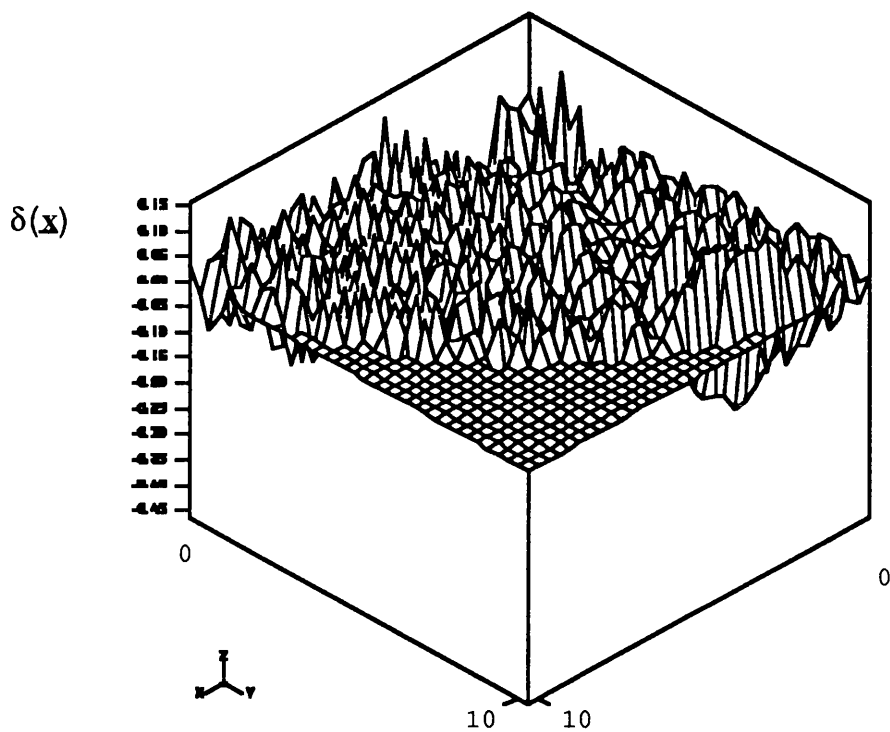


Fig. 2.8 : Density function corresponding to the S.C.F. $\exp(-r/r_0)$
for min. wavelength=2, L=20, R=10 & Correlation Length=2.5

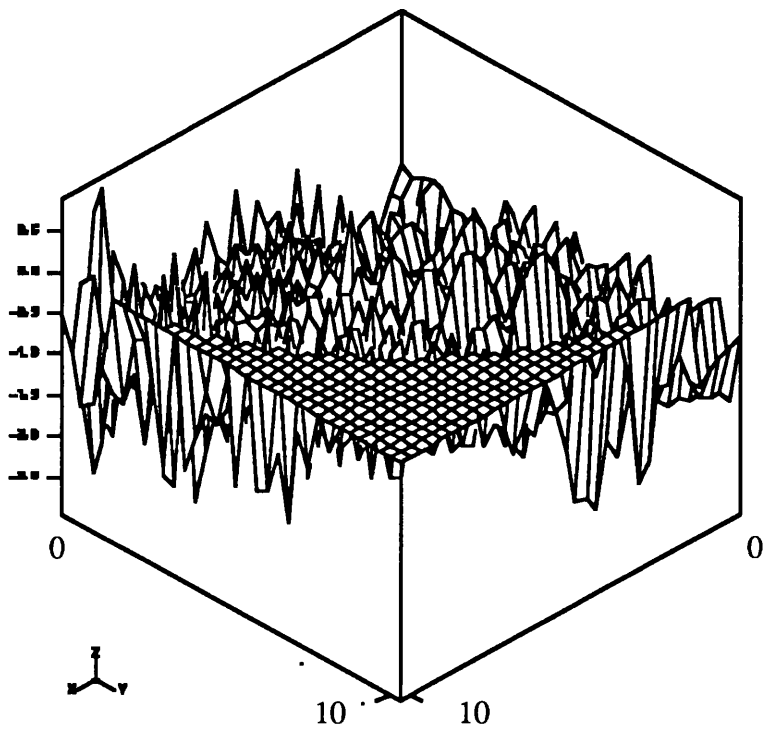


Fig. 2.9 : Density function corresponding to the S.C.F. $((r+r_0)/r_0)^{-\gamma}$
for min. wavelength = 2, L=20, R=10, Correlation Len.=2.5

CHAPTER 3**CORRELATION FUNCTIONS**

In this chapter we apply the theory presented in the previous one, to the description of the distribution and clustering of galaxies. We generate random functions using four different forms of correlation functions in three dimensions. We define the spatial and angular correlation functions and a new form for spatial correlation function is suggested. At the end we give a short review about fractals, and discuss the form that the spatial correlation function takes according to this theory.

3.1 Spatial Correlation Function (s.c.f.)

The problem of the spatial distribution of galaxies can be placed in the framework of random functions. Although this approach was adapted by Limber (1953), the usual approach has been to talk of probabilities of finding galaxies, regarding the galaxies as points, rather than the mass density as a random function. But, as we can see below, the two approaches are equivalent.

Let us take an element volume dV and points which are distributed according to the Poisson distribution. The density, n , of Poisson points, equals the expected number of points per unit volume and is independent of position. If the volume dV is very

small then the probability of finding one object in this volume dV (which represents the s.c.f.) is given by:

$$dP = P(1) = e^{-ndV} ndV \cong (1 - ndV) ndV \cong ndV$$

The mean number of objects within a finite volume V is given by

$$\langle N \rangle = nV$$

The two point s.c.f., $\xi(r)$, is defined by considering the joint probability of finding a point in volume dV_1 and a second point in volume dV_2 separated by a distance r

$$P(1,2) = n^2 [1 + \xi(r)] dV_1 dV_2 \quad (3.1)$$

It follows from this definition that the probability that a galaxy is found in dV_2 , given that a galaxy exists in dV_1 is given by

$$P(2/1) = \frac{P(1,2)}{P(1)} \quad \text{or} \quad P(2/1) = n[1 + \xi(r)] dV_2 \quad (3.2)$$

Furthermore, if dV_1 and dV_2 are taken to be infinitesimal, so that probability of more than one galaxy in dV_1 or dV_2 is negligible, we must have

$$\langle dn_1 dn_2 \rangle = n^2 [1 + \xi(r)] dV_1 dV_2 \quad (3.3)$$

If, on the other hand, we assume that matter is described by a continuous density function $\rho(\underline{x})$, we can say that the number of objects for one realization in dV_1 and dV_2 is given by

$$\left. \begin{array}{l} dn_1 = \rho(x_1)dV_1 \\ dn_2 = \rho(x_2)dV_2 \end{array} \right\} \Rightarrow \left\{ \begin{array}{l} \langle dn_1 \rangle = \rho_0 dV_1 \\ \langle dn_2 \rangle = \rho_0 dV_2 \end{array} \right. \quad (3.4)$$

Hence

$$dn_1 dn_2 = \rho(x_1)\rho(x_2)dV_1 dV_2$$

Taking the average over the ensemble of functions we have

$$\langle dn_1 dn_2 \rangle = dP = \langle \rho(\underline{x}_1)\rho(\underline{x}_2) \rangle dV_1 dV_2 \quad (3.5)$$

Now by definition

$$\langle [\rho(\underline{x}) - \langle \rho \rangle][\rho(\underline{x}+\underline{r}) - \langle \rho \rangle] \rangle = \sigma^2 R(\underline{r}) \Rightarrow$$

$$\langle \rho(\underline{x})\rho(\underline{x}+\underline{r}) \rangle = \sigma^2 R(\underline{r}) + \langle \rho \rangle^2$$

Noting from (3.4) $\langle \rho \rangle = n$ and comparing eq. (3.5) with eq. (3.2), we have

$$\sigma^2 R(\underline{r}) + \langle \rho \rangle^2 = \langle \rho \rangle^2 [1 + \xi(\underline{r})]$$

$$\text{or } \sigma^2 R = \xi(\underline{r}) \langle \rho \rangle^2 \quad \therefore \quad \xi(\underline{r}) = \frac{\sigma^2 R}{n^2} \quad (3.6)$$

Thus Limber's approach is equivalent with Peebles' approach.

If objects were distributed in uniformly random or Poisson manner the joint probability of finding any two objects at any two points would be independent of this separation: $\xi(r)=0$. The fact that the objects are not Poisson distributed results in a non zero value of ξ and the variation of this function with separation r then tells us something about the strength of pairwise clustering on various scales.

3.2 Observed S.C.F.

A description of how we can derive the s.c.f. from surveys is given by Bahcall (1988), (but we can find it in many papers concerned with the analysis of catalogues, like Eder et al. (1989), Huchra et al. (1990) etc.) for the case of cluster-cluster correlation function, but could be applied to the measurement of the degree of clustering of other objects. This method suggested by Bahcall & Soneira (1983) and sometimes is called, for example, BS or BS83. First we need to generate a set of 1000 catalogues with 104 clusters randomly distributed within the angular boundaries, including the same selection function. Then we take two frequency distributions of cluster pairs $F(r)$ and $F^R(r)$. The former corresponds to the observed sample and the latter to the average comes from the ensemble. Then the s.c.f. is

$$\xi_{\infty}(r) = \frac{F(r)}{F^R(r)} - 1$$

The s.c.f. for clusters is due to physical clustering of rich clusters of galaxies that extends to large scales. Bahcall came to this result based on three tests: (i) study of surveys of different depths

and comparing them, (ii) using the evaluated by redshift correlation of the clusters and (iii) comparing the a.c.f. of different regions of the sky.

Generally it is claimed that the s.c.f. can be fitted, say a power law, viz.

$$\xi(r) = (r_0/r)^\gamma \quad (3.7)$$

The form (3.7) has been confirmed by a number of authors as they estimated it from observational catalogues. They investigated different subsamples of the catalogues, to different distances, regions and/or richnesses, applied different techniques and/or corrections (Bahcall, 1988). It is rather unlikely that the correlations are a result of catalogue biases or omissions. Although the data are consistent with a power law form for the correlation function with exponent $\gamma \cong 1.8$ at small separations, the power law is not established for galaxy clusters.

Summarizing the results for different 'scales' (galaxies, clusters, superclusters) we have

$$\text{s.c.f. for galaxies} \quad \xi_g(r) \cong 20r^{-1.8} \quad , r \leq 20 \text{ h}^{-1}\text{Mpc}$$

$$\text{s.c.f for cluster} \quad \xi_c(r) \cong \begin{cases} 360r^{-1.8} = \left(\frac{r}{26}\right)^{-1.8}, R \geq 1 \\ 1080r^{-1.8} = \left(\frac{r}{48}\right)^{-1.8}, R \geq 2 \end{cases} , r \leq 100 \text{ h}^{-1}\text{Mpc}$$

$$\text{s.c.f. for superclusters} \quad \xi_s(r) \cong 1500r^{-1.8} = \left(\frac{r}{58}\right)^{-1.8}$$

As we can see the cluster s.c.f. has the same shape and slope as those of galaxy s.c.f., but it is considerably stronger, by a factor of ~ 18 , than the s.c.f. of galaxies. The supercluster correlation

strength is stronger than that of the cluster correlations by a factor of approximately 4. The increase of correlation strength with richness implies that rich, luminous systems are more strongly clustered, at a given separation, than other systems (Bahcall, 1988).

Additional information can be obtained using the higher-order s.c.f., such as the spatial triplet correlation function (or three point correlation function), which is usually denoted by ζ . This is such that

$$dP = n[1 + \xi(r_{12}) + \xi(r_{23}) + \xi(r_{31}) + \zeta(r_{12}, r_{23}, r_{31})] dV_1 dV_2 dV_3$$

is the joint probability of finding objects in the three element volumes dV_1, dV_2, dV_3 , separated by the distances r_{12}, r_{23} , and r_{31} . It must be a symmetric function of these arguments. The middle three terms on the right hand side accounts for the clustering in triples from uncorrelated pairs, where the last term ζ accounts for purely triple clustering and is referred to as the 'irreducible' triplet s.c.f. (Fall, 1979).

3.3 Spectrum of Power Law

Now we work out the power spectrum $f(\underline{k})$, assuming that the correlation function $R(\underline{r})$ is known, say

$$R(\underline{r}) = Ar^{-\gamma} \tag{3.8}$$

then from (2.9a) is

$$f(\underline{k}) = f(k) = \int \int \int_{\underline{k}, \underline{r} = rk \cos \theta} Ar^{-\gamma} e^{-i\mathbf{k} \cdot \mathbf{r}} dx dy dz \Bigg\}$$

$$f(\mathbf{k}) = \iiint A r^{-\gamma} e^{-i\mathbf{k}\mathbf{r} \cdot \cos \theta} dx dy dz$$

We convert the cartesian to spherical coordinates

$$x = r \sin \theta \cos \phi, y = r \sin \theta \sin \phi, z = r \cos \theta \quad \& \quad \frac{D(x, y, z)}{D(r, \theta, \phi)}$$

So

$$\begin{aligned} f(\mathbf{k}) &= A \int_0^{\infty} \int_0^{2\pi} \int_0^{\pi} r^{2-\gamma} e^{irk(-\cos\theta)} (\sin \theta d\theta) d\phi dr \\ &= \frac{2\pi A}{k} \int_0^{\infty} r^{(2-\gamma)-1} \sin kr dr \\ &= \frac{2\pi A}{k^{3-\gamma}} \Gamma(2-\gamma) \sin\left(\frac{2-\gamma}{2}\pi\right) \end{aligned} \quad (3.9)$$

And that is because the Fourier sine transform of function say $f(t)$:

$$F_s(k) = \left(\frac{2}{\pi}\right)^{1/2} \int_0^{\infty} f(t) \sin r k dr$$

for t^{a-1} , ($0 < a < 1$) is

$$F_s(k) = \sqrt{\frac{2}{\pi}} k^{-a} \Gamma(a) \sin\left(\frac{1}{2}\pi a\right)$$

As we can see, the power spectrum is isotropic, depend only upon $k=|\underline{k}|$

3.4 Other Correlation Functions and Their Spectra

Along with the 'typical' s.c.f. we study and two other forms. The Gaussian (Peebles, 1980)

$$(i) \quad R_1(r) = Ae^{-\left(\frac{r}{r_0}\right)^2} \quad (3.10)$$

and

$$(ii) \quad R_2(r) = Ae^{-\left(\frac{r}{r_0}\right)} \quad (3.11)$$

using the theory developed in the previous section we work out the spectra $f_1(k)$ and $f_2(k)$ as follow:

$$\begin{aligned} (i) \quad f_1(k) &= A \iiint e^{-\left(\frac{r}{r_0}\right)^2} e^{i\mathbf{k}\cdot\mathbf{r}} dx dy dz \\ &= \frac{2A}{k} \iint \sin kre^{-\left(\frac{r}{r_0}\right)^2} r dr d\varphi = \frac{4\pi A}{k} \int \sin kre^{-\left(\frac{r}{r_0}\right)^2} r dr \\ &= \frac{4\pi r_0^3}{2^{3/2} e^{\frac{1}{4}k^2 r_0^2}} \end{aligned} \quad (3.12)$$

$$\begin{aligned} (ii) \quad f_2(k) &= A \iiint e^{-\left(\frac{r}{r_0}\right)} e^{i\mathbf{k}\cdot\mathbf{r}} dx dy dz \\ &= \frac{4\pi A}{k} \int \sin kre^{-\left(\frac{r}{r_0}\right)} r dr \end{aligned}$$

and because

$$\int xe^{-ax} \sin kx dx = \frac{2ak}{(a^2 + k^2)^2}, \quad \text{Re } a > 0, k > 0$$

we have

$$f_2(k) = A \frac{4\pi}{k} \frac{\frac{2}{r_0}k}{\left(\frac{1}{r_0^2} + k^2\right)^2} = A \frac{8\pi}{r_0 \left(\frac{1}{r_0^2} + k^2\right)^2} \quad (3.13)$$

In both these case $f(\underline{k})$ is in fact only a function of $|\underline{k}|$

3.5 Alternative S.C.F.

The forms usually used in literature are based on the power law (3.8). Of course this is the law fits the data, but when we have to apply it in stochastic processes a difficulty arises. We encounter the problem that the s.c.f. tends to infinity as $r \rightarrow 0$ and according to the theorem given in section 2.1.4, we need to have correlation function which is continuous at 0 to generate a continuous r.f. In order for the function to fulfil this requirement, we suggest the following s.c.f.

$$R(r) = \frac{\langle \delta\rho(x+r)\delta\rho(x) \rangle}{\sigma^2} = \left(\frac{r+r_0}{r_0}\right)^{-\gamma} \quad (3.14)$$

where the r_0 is the characteristic length. $R(r)$ is now finite at $r=0$. We studied this s.c.f. along the 'classical ones'. The power spectrum is derived in Appendix A.

3.6 Angular Correlation Function (a.c.f.)

3.6.1 Estimated from the Generated Distribution of Galaxies

We can define the a.c.f., $w(\theta)$, with a similar way as we did for the s.c.f. If $dP(\theta)$ is the joint probability of finding two points in a two dimensional sample separated by an angle θ and within the solid angles $d\Omega_1$ and $d\Omega_2$, than

$$dP(\theta) = n^2 [1 + w(\theta)] d\Omega_1 d\Omega_2$$

where n is the surface number density in the sample (e.g. Infante (1989), Peebles (1980)). The two point a.c.f. describes, as a function of angular separation, the net projected pair clustering of objects on the sky above that expected from a random distribution (Bahcall, 1988).

The angular covariance function w is the result of an average over an ensemble of positions in the direction n_1 and n_2

$$\langle h(\underline{n}_1) h(\underline{n}_2) \rangle = w(\theta)$$

where $\cos\theta = \underline{n}_1 \cdot \underline{n}_2$. The number of objects (which could be galaxies or clusters according to the scale we use) within the cell defined by $d\Omega$ \underline{n} is obtained by integrating the density function along lines of 'sight'

$$\langle N \rangle = d\Omega \int_0^R \rho(r, \theta, \phi) r^2 dr \quad (3.15)$$

where R is the limiting (maximum) distance out to which a particular (typical) galaxy can be detected (observed). We assume that eq. 3.15 is for the idealised case where all galaxies out to the distance R may be detected. Taking the Riemman sum for the function ρr^2 over $[1, M]$, corresponding to the integral (3.15), we have

$$\langle N_{\underline{n}} \rangle \equiv \Delta\Omega\Delta r \sum_{i=1}^M \rho(r_i, n) r_i^2 \quad (3.16)$$

The quantities $\Delta\Omega$, \underline{n} and Δr are not very important in the computation because they cancel out when we estimate $w(\theta)$. Starting with the definition for a correlation function we can find the expression which allows the estimation of $w(\theta)$

$$\begin{aligned} w(\theta) &= \frac{\langle (n_0 - \langle n \rangle)(n_\theta - \langle n \rangle) \rangle}{\langle (n_0 - \langle n \rangle)^2 \rangle} \\ &= \frac{\langle n_0 n_\theta - n_0 \langle n \rangle - n_\theta \langle n \rangle + \langle n \rangle^2 \rangle}{\langle (n_0 - \langle n \rangle)^2 \rangle} \\ &= \frac{\langle n_0 n_\theta \rangle - \langle n \rangle^2}{\langle (n_0 - \langle n \rangle)^2 \rangle} = \frac{\langle n_0 n_\theta \rangle - \langle n \rangle^2}{\langle n_0^2 \rangle - \langle n \rangle^2} \end{aligned} \quad (3.17)$$

where $\langle n \rangle$ is the average number of objects.

3.6.2 Analytic Expression for the a.c.f. and Small Angle Approximation

Above we described how we can estimate the a.c.f. from the number of points, generated by the function $\rho(\underline{x})$. We were interested in the correlation of the number of the points along the lines of sight, in different directions. As we said the a.c.f. is the joint probability of finding two objects in element solid angles $\delta\Omega_1$ and $\delta\Omega_2$ are separated by angle θ . Thus we may write an analytic expression for the a.c.f. in terms of the s.c.f. viz

$$w(\theta) = \frac{\int_0^R \int_0^R \xi(r_{12}) r_1^2 r_2^2 dr_1 dr_2}{\int_0^R \int_0^R \xi'(r_{12}) r_1^2 r_2^2 dr_1 dr_2} \quad (3.18)$$

where is ξ' the s.c.f. for $\theta=0$ and r_{12} is given by writing

$$r_{12}^2 = |\mathbf{r}_1 - \mathbf{r}_2|^2 = r_1^2 + r_2^2 - 2r_1 r_2 \cos \theta \quad (3.19)$$

Significant contribution will only come from the integrand when $\theta \cong 0$ and $r_1 \cong r_2$. Peebles (1980) gives the a.c.f. at small angle approximation to have the form $w(\theta) = A\theta^{-\delta}$ where $\delta \cong 0.8$, fitting the Zwicky and Lick galaxy catalogues.

3.7 A.C.F. Estimation

In order to estimate the a.c.f. from a survey we take a list of the objects in terms of their angular position. As we know the a.c.f. gives the probability, dP , to find an object in solid angle $d\Omega_2$ at separation θ from a random placed object in solid angle $d\Omega_1$. which means that the probability that an object $1 \in d\Omega_1$, given an object $2 \in d\Omega_2$, is

$$P(2 / 1) = \frac{P(1, 2)}{P(2)} = N[1 + w(\theta)]d\Omega_1$$

where N is the ensemble average number of objects per steradian. Based on this definition Hauser and Peebles (1973) described the estimation of a.c.f. They point out the problem we might have evaluating the a.c.f. in the " large-scale gradients" from galactic

obscuration. A way to avoid this is to divide the sample in different zones, according to their latitude. Then they take the objects in turn in the zone and counts the number of objects at angular distance (in successive intervals) $0^{\circ}.2$. After averaged over all objects in the zone we divide by the solid angle of (the angular ring) and by N (and of course subtracting 1). This process is repeated for every member of the sample.

A simpler description arises if we assume we have $N(\theta)$ pairs of objects separated by angular distance θ and $N^R(\theta)$ number of pairs obtained by the randomly distributed number of objects. Then the a.c.f is (e.g. Haynes & Giovanelli, 1988)

$$w(\theta) = \frac{N(\theta)}{N^R(\theta)} - 1$$

The a.c.f. for each morphological types of galaxies is slightly different. They have their own characteristic slope, on the power law, as Davis & Geller (1975) estimated.

Peebles (1973) using the Limber's equation (Limber, 1953), which gives the a.c.f. in terms of the s.c.f. (a form for small approximation), derived a scale relation in terms of the characteristic depth D^*

$$w(\theta) = \frac{w(\theta D^*)}{D^*}$$

This relation means that on spatial scale θD^* , the apparent strength of clustering decreases inversely with the sample depth D^* , because the number of uncorrelated intervening galaxies along the line of sight is proportional to D^* (Michael Fall, 1979).

3.8 Fractals

3.8.1 Definitions & Properties

Discussing and stating the different forms of s.c.f., we saw that it takes a variety of forms according to scale and objects it describes. Despite this 'step change' property, we can see a 'continuity' in its behaviour as the size of the described structures increases. This automatically raises the question of whether the connection of these functions is possible. The dependence of the amplitude of the observed s.c.f. from the sample size was firstly pointed out by Einasto et al. (1986). Crucial for the different amplitude of the spatial correlation functions is the correlation length r_0 , for which Calzetti et al. (1988) claim that 'it is inappropriate, as is usually made in the literature, to attach a physical meaning'. The link between different scales is possible if we accept the model of the fractal structure of the Universe; at least in a limited distance. Fractal is a term adopted by Mandelbrot (1982) describing 'strange' geometrical patterns which actually represent different self-similar structures over certain scale ranges. We assume that the hierarchical structure is the same for every observer (i.e. observer-homogeneous). A combination of both (self-similar and observer-homogeneous distribution) means that all the probability functions describing a set of points which are, on average, invariant if we change the reference frame (Mandelbrot (1982), Giavalisco et al. (1990))

In order to describe the fractal dimension we use the fig. (3.7) (e.g. Calzetti et al. (1987a)). This tetrahedron is constructed if we develop the bigger tetrahedron (shown on the corner) homogeneously, which means we can divide each size by the scale,

say 3. So we take four new tetrahedron equivalent to the original. We carry on with the same method as many times as we like. We can apply by same method in reverse to extend to larger scales. If we denote with k the hierarchical order, R_k the size of the tetrahedron and N_k the number of points in hierarchical order $<k$, we have

$$\frac{N_k}{N_{k-1}} = N \quad \text{and} \quad \frac{R_k}{R_{k-1}} = R$$

where R is a scale parameter. Denoting with D the fractal (or effective) dimension, we can define it as

$$D = \frac{\log N}{\log R}$$

Of course studying the distribution of galaxies we must consider the number N as the average count of galaxies taking every time different galaxy as centre. In the example of fig. 3.7, $D=1.2618$ (Giavalisco et al., 1990) which is the dimension related to the slope of s.c.f. through the equation: $D=3-\gamma \approx 1.2$ (Szalay & Schramm, 1985). If within certain scale range, D is constant, then we have self-similar set of points; but generally D can be considered as a function of R (Wen Zheng et al., 1988). The dimension D varies between 0 and 3. In Euclidian space the dimension D_E is always an integer. But D need not be an integer and the two dimensions need not coincide; they only satisfy the Szpilrajn inequality $D \geq D_E$ (Mandelbrot, 1982). Mandelbrot referring to the application of fractal dimension in Astronomy (and especially Cosmology) says: '... the Universe appears to involve a sequence of several different

effective dimensions. Starting with scales of the order of Earth's radius, one first encounters the dimension 3 (due to solid bodies with sharp edges). Then the dimension jumps to 0 (matter being viewed as a collection of isolated points). Next is the range of interest, ruled by some nontrivial dimension satisfying $0 < D < 3$. If scaling clustering continues ad infinitum, so does the applicability of this last value of D . If, on the contrary, there is a finite cut-off, a fourth range is added on top, in which points lose their identity and one has a uniform fluid, meaning that the dimension again equals 3. On the other hand, the most naive idea is to view the galaxies as distributed near uniformly throughout the Universe. Under this untenable assumption, one has the sequence $D=3$, then $D=0$, and again $D=3$. The general theory of relativity asserts that in the absence of matter, the local geometry of space tends to the local flat and Euclidean, with the presence of matter making it locally Riemannian. Here we could speak of globally flat Universe of dimension 3 with local $D < 3$ '.

3.8.2 Global Density

If we try to evaluate the large scale average density, f , of the matter in the Universe will see that as the volume becomes larger and larger the density tends to very small values (fig. 3.8) from the equation

$$\rho = \frac{m(R)}{\frac{4}{3}\pi R^3}$$

where the m is a function of the radius R . According to de Vaucouleurs (1970), Mandelbrot (1982), $m \propto R^D$ i.e $\rho \propto R^{D-3}$ with $D-3$ constant. This relation seems to have similarities with the fractal dimension and indicates that the problem can be overcome

assuming a scale dependent property. After a particular scale the distribution of the matter becomes homogeneous with a constant average density.

3.8.3 Cut-off

A quite successful way to connect the distribution of galaxies with the fractals, is to represent the filamentary distributions as trees (Einasto 1990). The 'size' of the trees is defined by the scale length we choose to determine the upper limit of the self-similar structures. At larger scales we have the forest which consists of randomly distributed trees. the upper limit is called cut-off and gives the range in which the fractal dimension extends. A probable value is 51 Mpc, but deeper samples are necessary in order to investigate the asymptotic behaviour of the correlation amplitudes, getting information as how homogeneity is actually reached in the Universe (Giavalisco et al., 1990). New models come up (Ruffini et. al., 1989) to suggest galaxy formation process with galaxies distributed in a fractal mode.

3.9.4 Fractal S.C.F.

A good deal of the fractals and the form the s.c.f. takes, assuming a self-similar model, is given in special issue of the 'Vistas in Astronomy' under the title 'Fractals in Astronomy' in 1990.

That the amplitude of the s.c.f. depends on the sample size was firstly noticed by Einasto et. al. (1986). If the sample radius is R_s and D the fractal dimension, the coefficient of the eq. (3.8) becomes

$$A = \left(1 - \frac{\gamma}{3}\right) R_s^\gamma \quad (3.20)$$

and because $A = r_0^\gamma$, 3.20 gives $r_0 = \left(1 - \frac{\gamma}{3}\right)^{1/\gamma} R_s$. The exponent γ is connected with D , with the eq.

$$\gamma = 3 - D \quad (3.21)$$

The (3.20) is actually valid till the upper cut-off, beyond which the distribution becomes homogeneous and the average number density is constant.

In order to prove (Calzetti et al., 1988) the eq. (3.20) we start off defining the volume density, n_v , and differential density, n_d , as

$$n_v(r) = \frac{N(r)}{V(r)}$$

and

$$n_d(r) = \frac{1}{4\pi r^2} \frac{dN(r)}{dr}$$

where $N(r)$ is the number of objects contained in a volume $V = \frac{4\pi}{3} r^3$.

The $N(r)$ is also given as $N(r) = Fr^D$ in the continuous limit for

$F = \frac{N_k}{r_k^D}$. So we have

$$\left. \begin{aligned} \frac{dP}{dV} = n_d(r) = \langle n \rangle [1 + \xi(r)] \Rightarrow \xi(r) = \frac{n_d(r)}{\langle n \rangle} - 1 \\ \langle n \rangle = n_v(R_s) \end{aligned} \right\} \Rightarrow$$

$$\xi(r) = \frac{n_d(r)}{n_v(R_s)} - 1 = \frac{\left(\frac{DF}{4\pi}\right)r^{D-3}}{\left(\frac{3F}{4\pi}\right)R_s^{D-3}} - 1 \Rightarrow$$

$$\xi(r) = \left[\left(\frac{3-\gamma}{3} \right) R_s^\gamma \right] r^{-\gamma} - 1 \quad (3.22)$$

fulfilling the normalization condition

$$\int_0^R \xi(r) r^2 dr = 0$$

The fractal a.c.f. obtained from catalogues for different depths R_s is found to be (e.g. Calzetti et al. 1990)

$$w(\theta) = B_0 \theta^{-\beta}$$

where $B_0 \propto R_s^{-\beta}$ and $\gamma = \beta + 1$

In fig. (3.1) we give a schematic description of the way the programme generates a sample. This sample consists of a series of realizations along the axes L . The distance between the vertical lines (which signifies the beginning of the new realization) is greater than the mean separation (= 'meansep' + 2) to avoid strongly correlated parts to overlap. The radii are R units long and rotating form an angle θ from the vertical lines. The figures 3.2-3.5 give the a.c.f. from the so generated sample. Every figure consists of two graphs corresponding to the same correlation length, but different radius (10 and 15). The radius, R , can be Mpc or any other suitable units of distance. The fig. 3.6 gives the a.c.f. in small angle approximation, as explained in sec. 3.6.2, derived with the analytical form 3.18. This expression works only for s.c.f without

singularity (of integral). A problem appears to the denominator for the form $(r_{12}/r_0)^{-\gamma}$ where the r_{12}^{-1} tends to infinity as r_1 and $r_2 \rightarrow 0$. Even if we assume that the lower limit in the integrals (eq. 3.18) is very close to zero, say $\epsilon \rightarrow 0$, the denominator becomes very large with the consequence that the a.c.f. takes very small values. That means it is much steeper (unnaturally) than the other ones. In the case of small angle approximation, we took the graphs of the a.c.f. corresponding to the s.c. functions: $\exp(-(r/r_0)^2)$, $\exp(r/r_0)$, $(r+r_0/r_0)^{-\gamma}$.

There is a theorem in calculus (e.g. Tomas & Finney, 1979), stating that: \forall function $f(x)$, that is continuous on a closed bounded ($|f(x)| \leq M, \forall x \in [a, b]$ for constant M) interval $[a, b]$, is Riemann integrable there. But not only the continuous functions are integrable. It is possible to have 'piecewise continuous' which means that the interval $[a, b]$ can be divided in a finite number of nonoverlapping open subintervals (a_i, a_{i+1}) over which the function is continuous. In this case the 'total' integral is the sum of the integral over the parts of the function in the subintervals (a_i, a_{i+1}) . We must be careful when we take the equations 3.15 & 3.16, for the density function, corresponding to $(r/r_0)^{-\gamma}$. It is very important the number of discontinuities not to be infinite or known, as required from the above theory, to integrate over $[0, R]$. The reason the a.c.f., coming from the power law $(r/r_0)^{-\gamma}$, is similar with that one coming from the 3.14 form is that, integrating the density function, we smear out all the discontinuities because of the contribution of positive and negative values.

When we expand a function in Fourier series, this must have two presumptions (i) to be in the interval $[a, b]$, with at most a finite number of maxima and minima and (ii) to have a finite number of

discontinuities in the $[a,b]$. Theoretically the sum 2.13 must be defined from $(-\infty, \infty)$. But in practice this is impossible. So we need to make an approximation imposing a cut-off on the number of frequencies. In our case this depends upon the volume L^3 and the minimum wavelength. An other question arises, from the presumption in order to expand a function in a Fourier series, is whether the density function $\rho(x_i)$ is continuous for the s.c.f. 3.8. If it actually has a large number of discontinuities, we cannot expand it in Fourier series.

The dispersion in the a.c.f. plots can be explained if we assume that the values corresponding to a particular $w(\theta)$ is a sample of size n say w_1, w_2, \dots, w_n . The distribution of the sample w_1, w_2, \dots, w_n is defined to be the joint distribution of w_1, w_2, \dots, w_n . So if we let w_1, w_2, \dots, w_n be a random sample from a density function $f(x)$ which

has mean μ and finite variance σ^2 and let $\bar{w} = \frac{1}{n} \sum_{i=1}^n w_i$. Then

$\langle \bar{w} \rangle = \mu_w = \mu$ & $\text{var}(\bar{w}) = \sigma_w^2 = \frac{1}{n} \sigma^2$. If we have an infinite number of values of the random variable w_i , we can approximate 'exactly' the expected value $\langle w \rangle$. In our situation we integrate over a limited number of generated random functions. The problem is whether we make any reliable inferences about $\langle w \rangle$ by a finite number of values of w (a random sample of size n , say). The reliability of the inferences can be measured in terms of probability. For example we want to see how large a sample must be taken in order that the probability will be at last .95 that the sample mean \bar{w}_n will lie within .05 of the population mean (i.e. $P(-\epsilon < \bar{w}_n - \mu < \epsilon) \geq 1 - \delta$).

Say for $\sigma^2 = 1$, $\epsilon = .05$ and $\delta = 0.05$ then $n > \frac{\sigma^2}{\delta \epsilon^2} = 8000$!!.

Although this value is extreme, indicates that better results can be achieved averaging over more realizations. An other point, that may

cause concern, is the complicated power spectrum derived by the form 3.14.

The forms 3.8 & 3.14 appear to have similar behaviour. For $R=10$ they decrease sharply until about 7° and then tend to zero. For $R=15$ they drop off until 5° , then oscillate about zero. The form 3.10, falls off more slowly than the above ones. For the 3.11 the nature of the line becomes obscured as a lot of noise is present. But it is clear that for $>8^\circ$ it is close to zero. For $R=15$ both exponential laws give quite similar a.c.f.s, approaching zero slightly faster than those with $R=10$. Comparing the fig. 3.6 with the fig. 3.2-3.4, for the other forms, we can see clearly that the a.c.f., in small angle approximation is much stronger at very small angles than those coming from the simulation (especially for the exponential law s.c.f.).

In the figures 3.2-3.5 for the case $R=15$, we can identify two characteristics: (i) the a.c.f. falls off much faster than the corresponding from $R=10$, which can be explained by the fact that the contribution of the closer galaxies is much more significant than those further, and (ii) the errors are smaller because we average over more realizations.

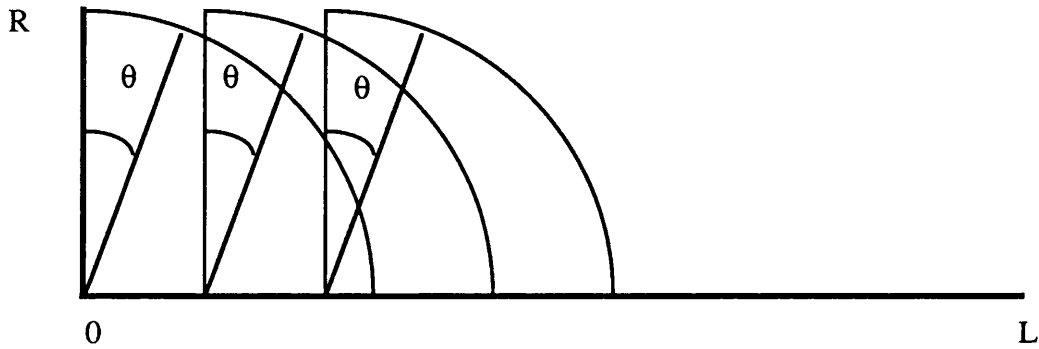


Fig. 3.1 :Schematic representation of the way the different realizations generated by the programme. The resultant values arise from the average over all the cases.

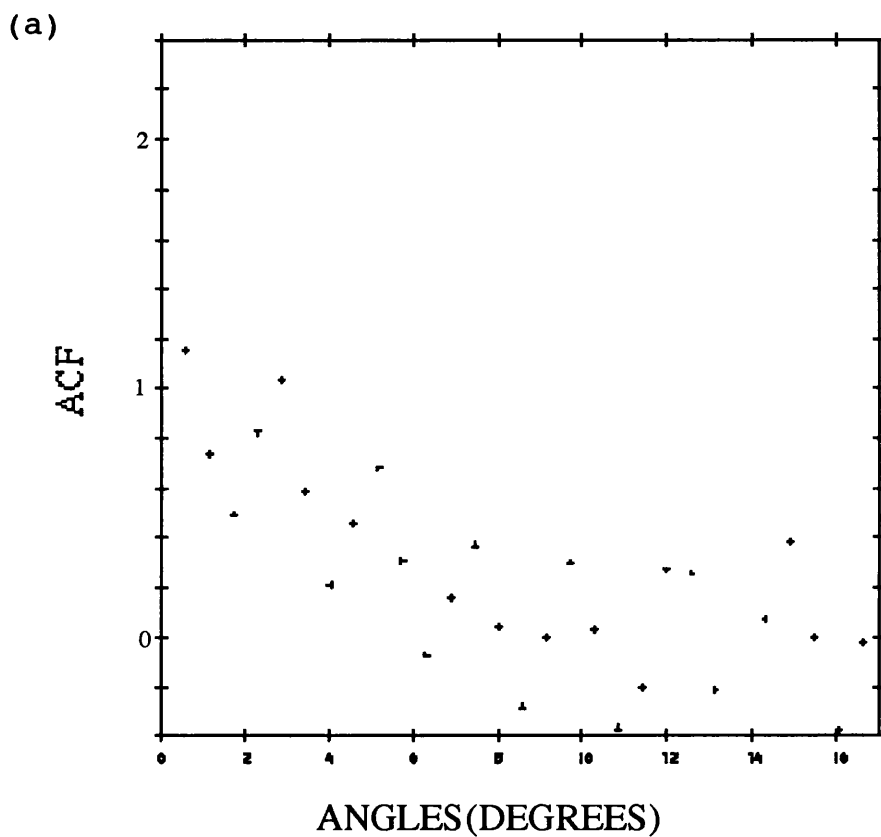
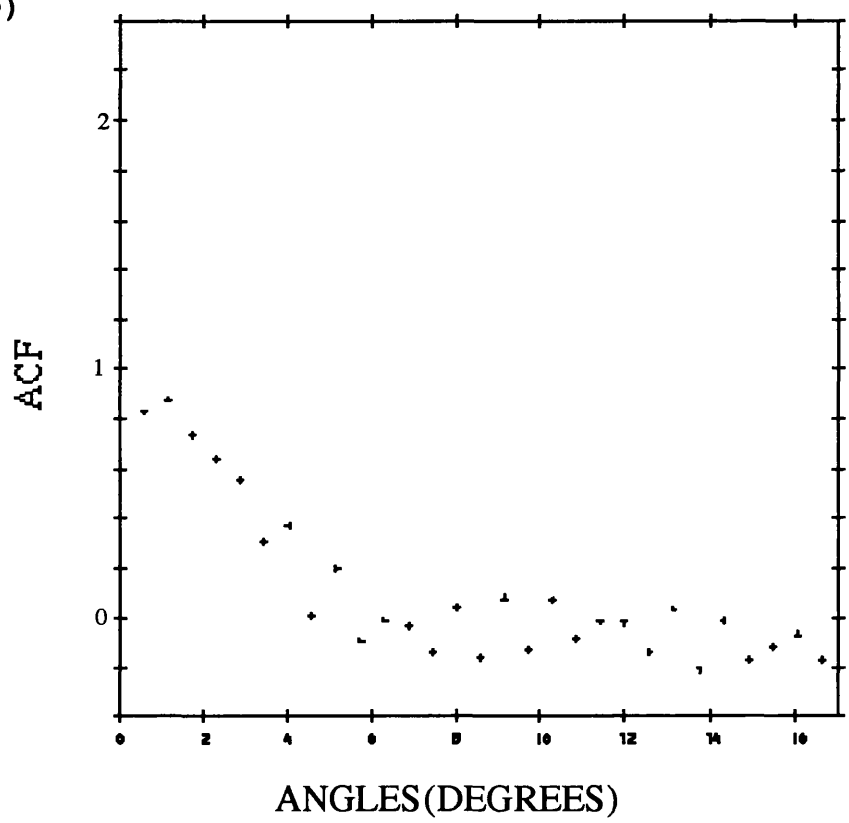


Fig. 3.2 : A.C.F. derived by the S.C.F. $(r / r_0)^{-\gamma}$
 for min. wavelength = 2 and
 (a) Limit = 20, Radius = 10, Correlation Length = 2.5
 (b) Limit = 30, Radius = 15, Correlation Length = 2.5

(b)



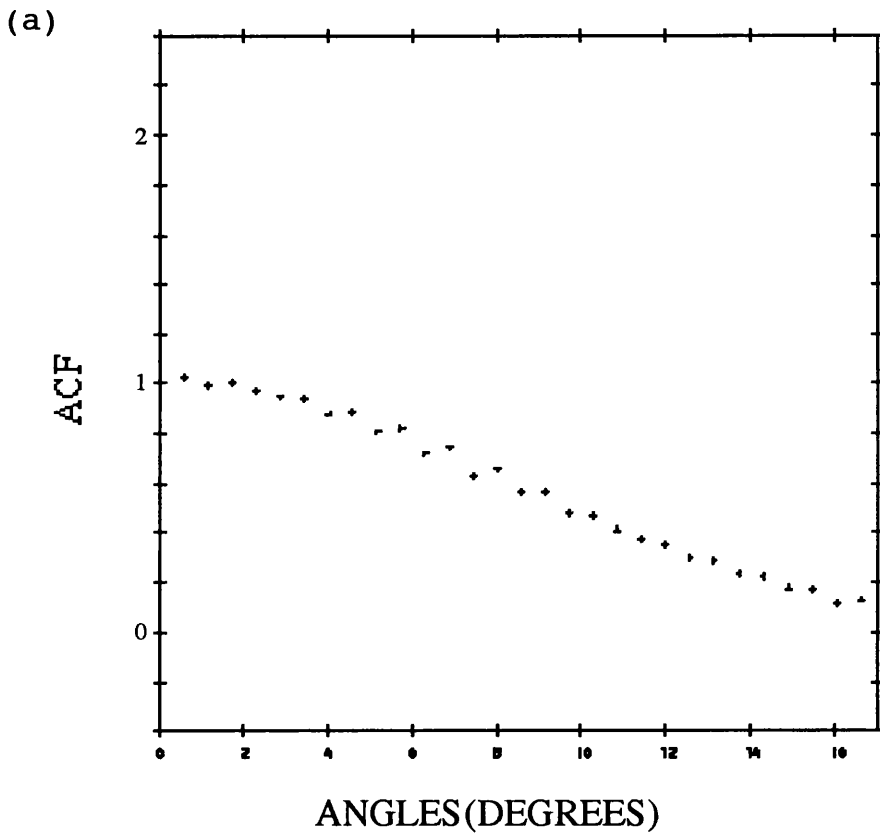


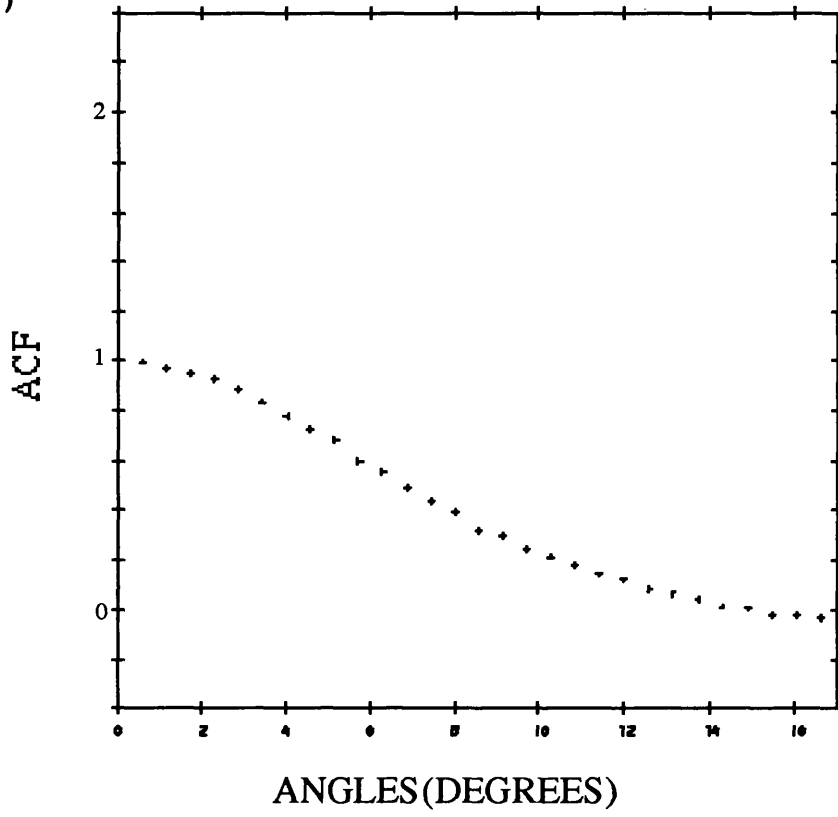
Fig. 3.3 : A.C.F. derived by S.C.F. $\exp(- (r / r_0)^2)$ for min.

wavelength = 2 and

(a) Limit = 20, Radius = 10, Correlation Length = 2.5

(b) Limit = 30, Radius = 15, Correlation Length = 2.5

(b)



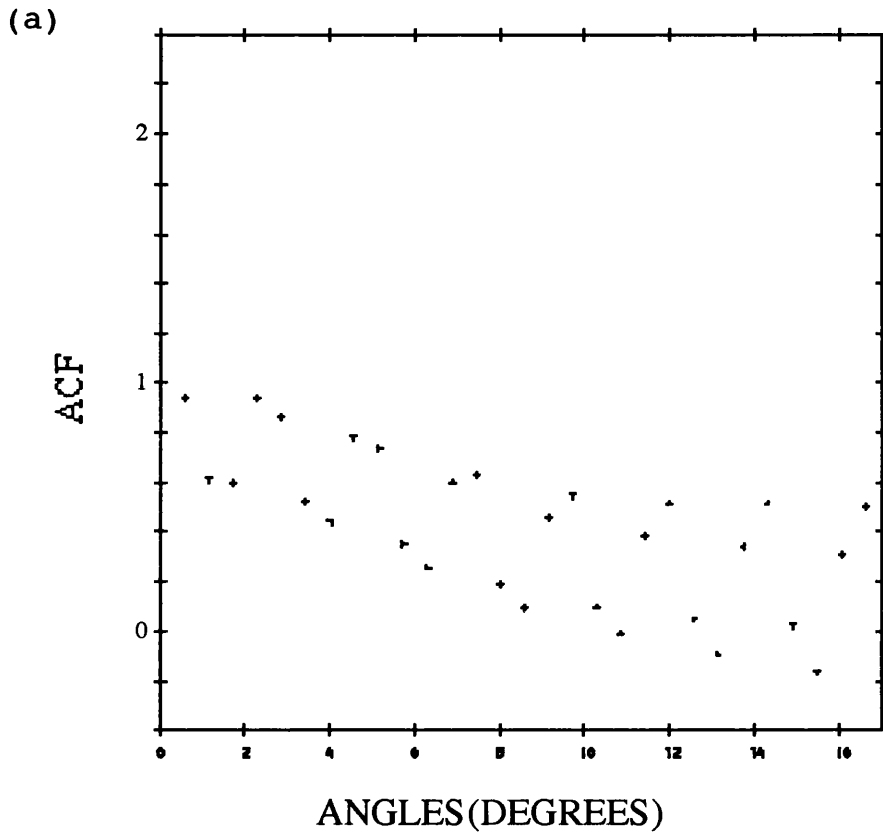


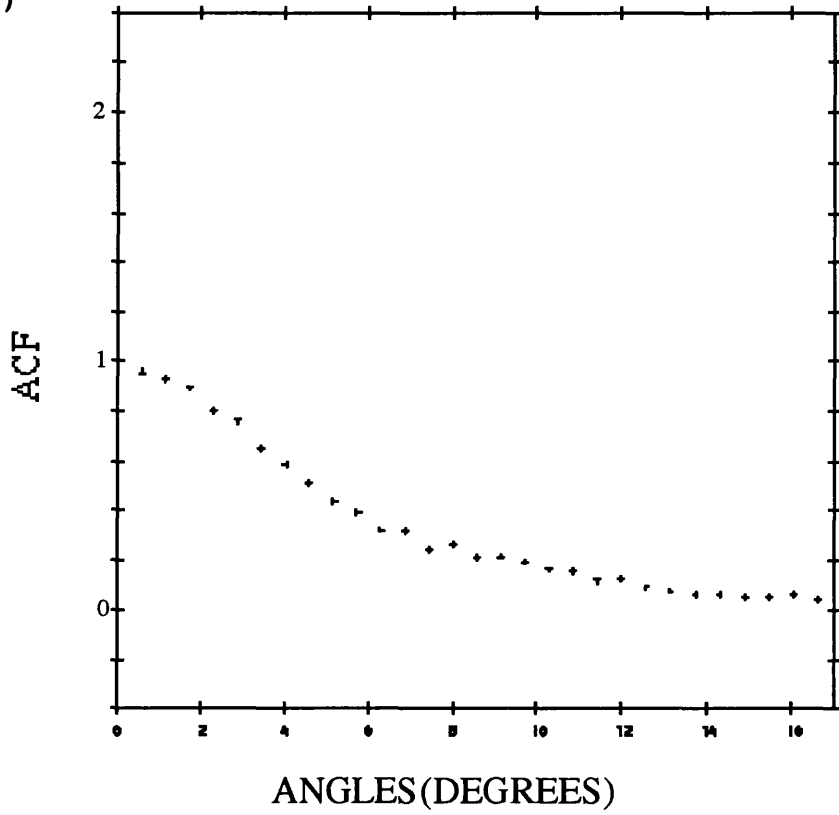
Fig. 3.4 : A.C.F. derived by the S.C.F. $\exp(-r/r_0)$ for min.

wavelength = 2 and

(a) Limit = 20, Radius = 10, Correlation Length = 2.5

(b) Limit = 30, Radius = 15, Correlation Length = 2.5

(b)



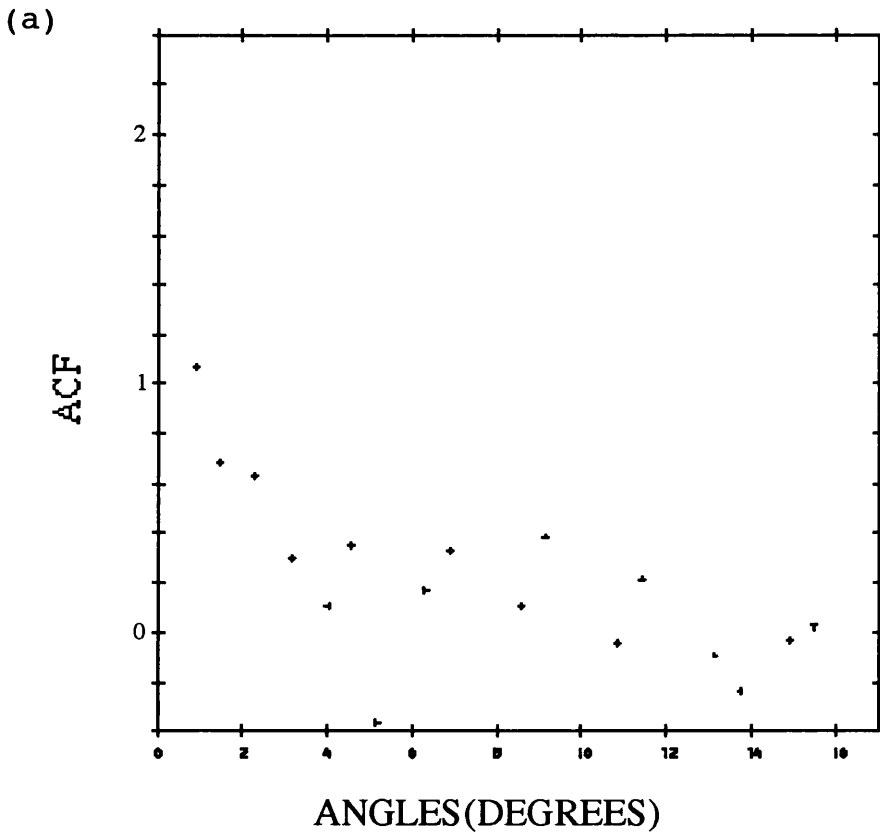


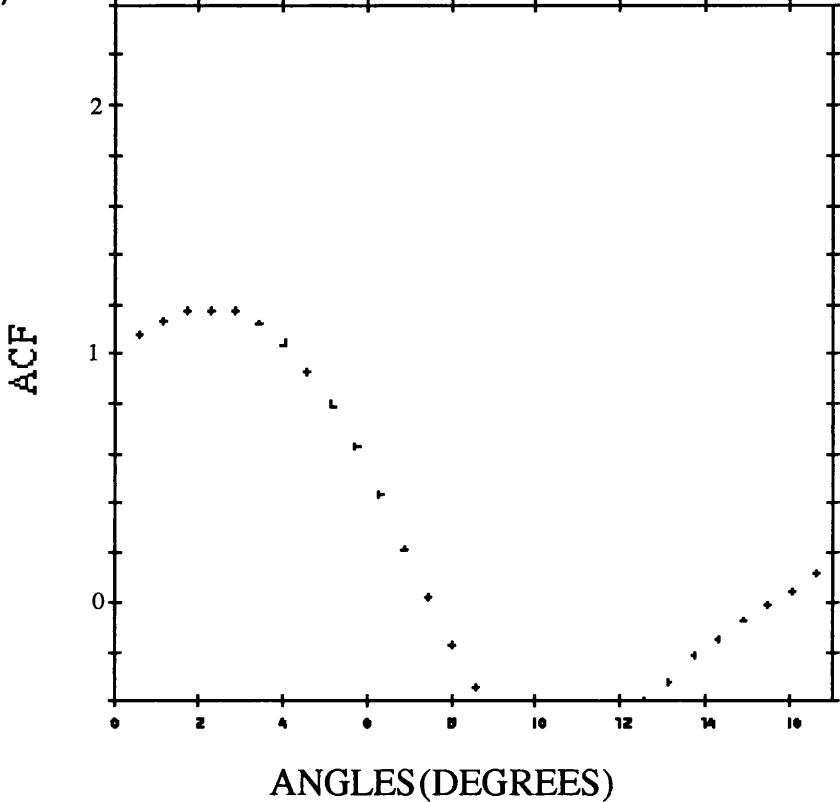
Fig. 3.5: A.C.F. derived by the S.C.F. $((r + r_0) / r_0)^{-g}$ for

min. wavelength = 2 and

(a) Limit = 20, Radius = 10, Correlation Length = 2.5

(b) Limit = 30, Radius = 15, Correlation Length = 2.5

(b)



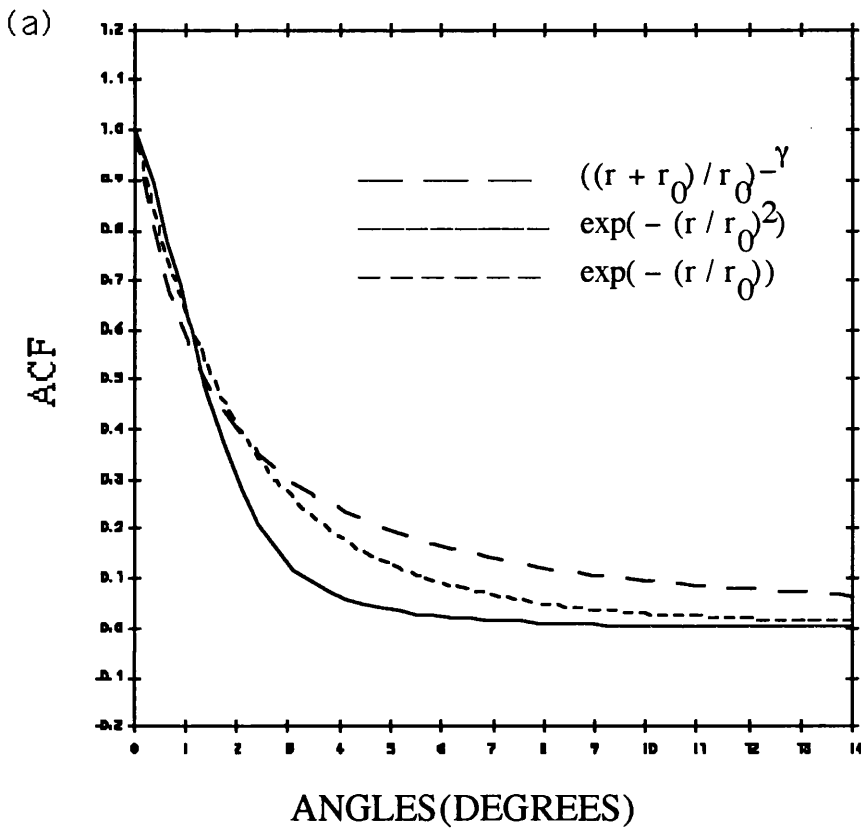
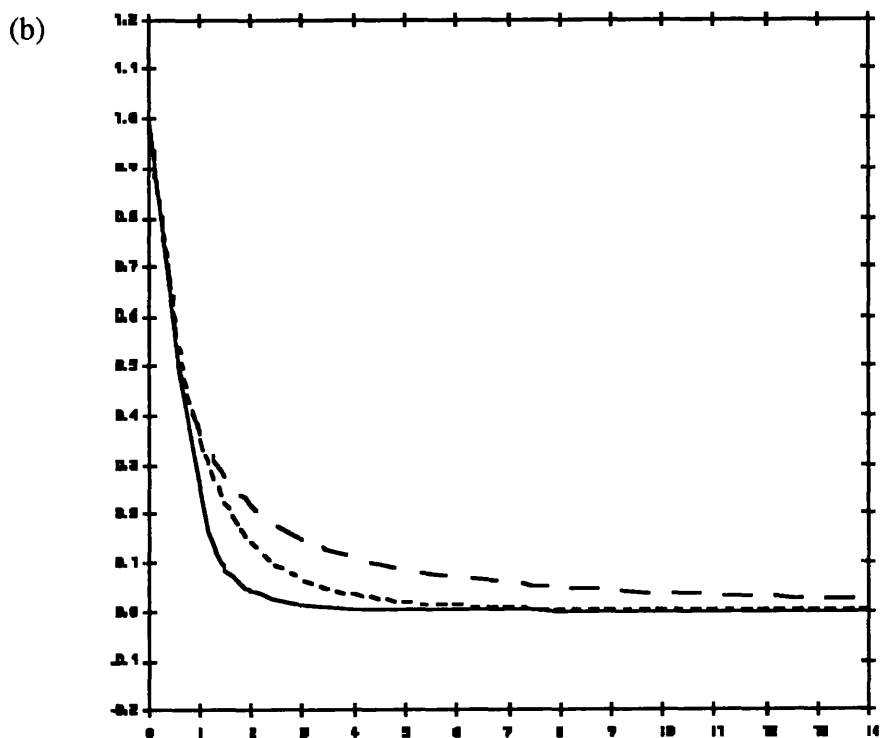


Fig. 3.6: A.C.F. as derived by analytical expression in small angle approximation, for (a) $R=10$ and (b) $R=15$



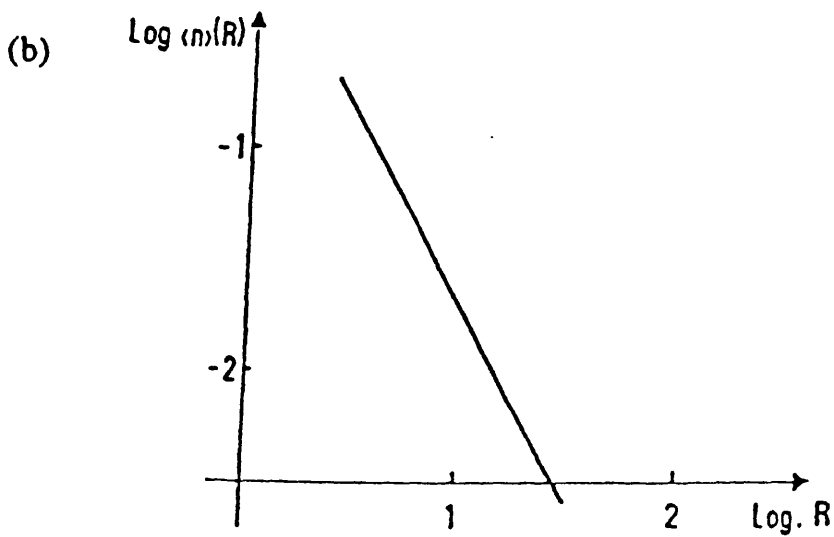
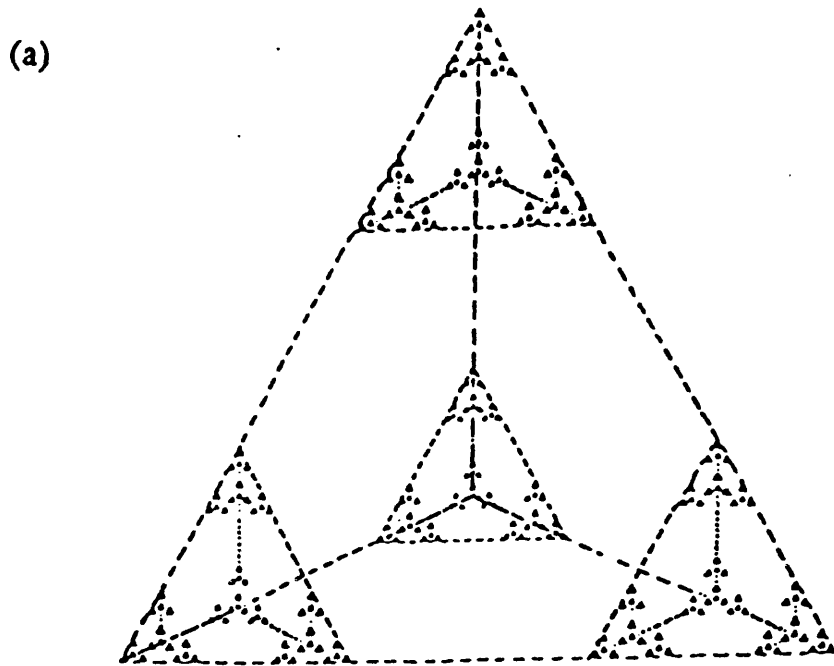


Fig. 3.7: (a) Generated fractal distribution of points in space for $D = \log 4 / \log 3 = 1.2618\dots$ and (b) the corresponding average volume density (Giavalisco et al., 1990)

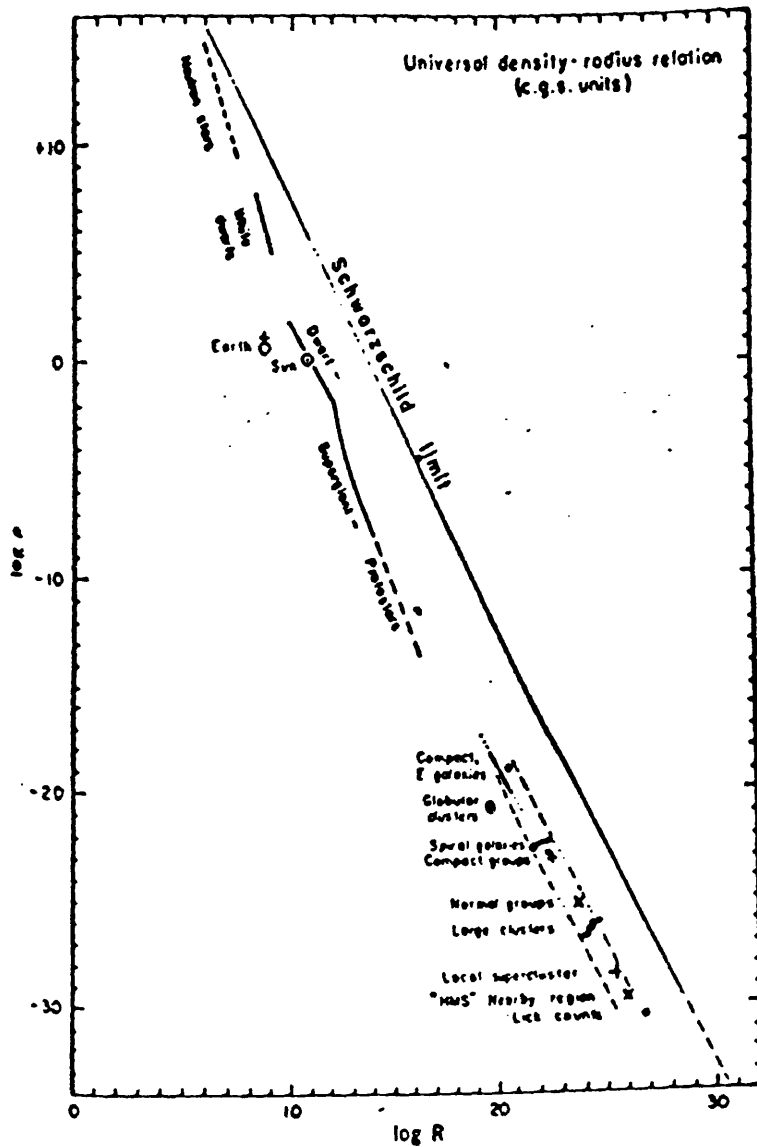


Fig. 38: Density (gr/cm^3) versus radius (cm) of spherical volumes. The thin dashed lines derived by the virial theorem for stellar and galaxy clusters (de Vaucouleurs, 1970)

CHAPTER 4

LUMINOSITY FUNCTION

In the previous chapters we showed how we can generate continuous random functions (which represent the distribution of galaxies), using spectral analysis for different forms of s.c.f. At the end of the last chapter we evaluated the a.c.f. coming from the generated point. In this chapter we extend the developed theory, studying how the luminosity function and selection effects will affect the a.c.f. We assume that the density and magnitude are statistically independent

4.1 Definitions

4.1.1 Morphology-density Relationship

Let $n(M, \underline{x})dM dV$ denote the number of galaxies in volume dV at \underline{x} that have absolute magnitude between M and $M+dM$. If we assume that the magnitudes are not correlated with spatial locations then we may write

$$n(M, \underline{x})dM dV = \Phi(M)\rho(\underline{x}) dM dV$$

with

$$\int_{-\infty}^{\infty} \Phi(M) dM = 1 \tag{4.1}$$

where $\phi(M)$ is a probability distribution called the *luminosity function*. It gives the fraction of galaxies per unit magnitude having absolute magnitudes in the interval $(M, M+dM)$. The last equation which is the integral over all magnitudes, normalizes the luminosity function to unity. The probability that a galaxy with absolute magnitude in the range $(M, M+dM)$ in an element volume dV is then given by

$$dP = \phi(M) \rho(\underline{x}) dM dV$$

and the joint probability of finding two galaxies with different magnitudes M_1, M_2 and placed in different volumes dV_1 and dV_2 is correspondly

$$dP = \phi(M_1) \phi(M_2) \rho(x_1) \rho(x_2) dV_1 dV_2 dM_1 dM_2$$

Taking the average over all the realizations for objects, which are found at distance r_{12} apart, we have

$$dP = n^2 [\phi(M_1) \phi(M_2) + \xi(r_{12}) \phi(M_1) \phi(M_2)] dV_1 dM_1 dV_2 dM_2$$

If the galaxies were uncorrelated in position and magnitude then $\xi = 0$.

We considered the luminosity function, $\phi(M)$, to be independent on the density, $\rho(\underline{x})$. This assumption is not consistent with observations. In the last two decades, it has been well proven that the population of galaxies in groups and clusters, is composed mostly of spirals in low density field and largely of SO and elliptical

galaxies in the rich clusters. The first hint, that galaxies were segregated by types, depending upon their location, was made by Hubble & Humason (1931). More recently, the phenomenon was studied extensively and although there is no fixed number for the composition, we can get an idea using the quantities given by Dressler (1980): 80% of field galaxies are spirals and 15% of cluster galaxies are spirals out in the periphery of clusters. This result defines a relationship between galaxy density and galaxy type, which can be converted either with the galaxy formation (and evolution) or by subsequent environmental processes. The universality of this principle is supported, also, by the redshift surveys and data on rich clusters. There are three morphology-density relation of particular interest (Postman & Geller, 1984): for densities less than ~ 5 galaxies/Mpc³ the population fractions are independent of density; at a density ~ 600 galaxies/Mpc³, the fraction of SO galaxies becomes greater than the fraction of spiral galaxies; for densities greater than ~ 3000 galaxies/Mpc³ the elliptical fraction rises steeply.

A few models: Generally speaking, we can say that the relationship between morphology and density is strong. An 'objection' was made by Bhavsar (1981) who argued that there are some inconsistencies between the morphology-density relationship for groups and clusters, but Postman & Geller (1984) believe that the results of de Souza et al. (1982), that the composition of groups and clusters of galaxies is more or less the same, are more reliable as Bhavsar did not use redshift information.

Some of the mechanisms, which could explain the observations in an environmental approach are the galaxy-galaxy collision, the ram pressure stripping and gas evaporation.

Another process is called the sweeping mechanism and depends strongly on the density of the intergalactic medium. The high density is the responsible for the removal of gas from spirals and formation of SO galaxies. If these process was true we could expect to see many more SO galaxies in the dense regions and quite a few in low density areas and clusters of high concentration should be depleted of spirals. But the population gradients of the data is not exactly like that. There are significant numbers of SO galaxies present in even lower density environments of loose groups. There is another point which can not be explained by this theory. The fact that the bulges and bulge/disk ratios of SO galaxies are larger than those of spirals galaxies in all density regimes.

An alternative hypothesis to the above suggestion is the formation of the disk component of galaxies. In an long time scale, an increase in local density may slow or even halt the growth of the disk components. So in very high density regions we have a large number of elliptical galaxies and in low densities a prevalence of spirals (Dressler, 1980). The disk components may have a longer formation time which could be comparable to the age of the Universe. So, if the galaxies formed from density enhancements, which were independent from those which grew to give the clusters, there is no relation between local galaxy density and morphological type; because, assuming that the formation of the disk is a slow process, it could have been interrupted as local density increased (e.g. Gunn & Grott (1972), Gott (1977)).

4.1.2 Schechter's Luminosity Function

Different analytic expressions for the luminosity function have been suggested (e.g.. see Zwicky (1957), Kiang (1961), Abell (1962, 1965) etc.) and most recently by Schechter (1976). The

 Schechter's luminosity function can be used for galaxies and clusters of galaxies as well. If $\phi(L)dL$ denotes number of galaxies per unit volume in the luminosity interval $(L, L+dL)$ then the luminosity function is:

$$\phi(L)dL = c^* \left(\frac{L}{L^*}\right)^a e^{-\left(\frac{L}{L^*}\right)} d\left(\frac{L}{L^*}\right) \quad (4.2)$$

where c^* is the number per unit volume, L^* is a 'characteristic luminosity' that is the point in which the slope of luminosity function changes in the $(\log\phi, \log L)$ -plane and a gives the slope of the luminosity function in the same plane when $L \ll L^*$. All the above parameters are determined by the data and they are roughly the following

$$a = -\frac{5}{4} \quad c^* = 0.0277 \quad M^* = -19.46$$

(or for most recent determination of the parameters see e.g. Efstathiou et al. (1988) (for CfA, DARS and KOSS surveys) and de Lapparent et al. (1989)). An advantage of eq. (4.2) is that it allows us to adjust the 'faint-end' slope according to the data, changing the parameter a . A form which is not very often used is the *integrated* (or *cumulative*) luminosity function, $\Phi(M)$, (Yahil, 1988)

$$\Phi(L) = C \left(\frac{L}{L^*}\right)^{-a} \left(1 + \frac{L}{\beta L^*}\right)^{-\beta}$$

where $a=0.55 \pm 0.08$, $\beta=1.92 \pm 0.16$, $L^*=(3.6 \pm 0.9)10^9 h^{-2} L_0$ and $C=5.59 \cdot 10^{-3} h^3 \text{ Mpc}^{-3}$. The corresponding differential luminosity function is

$$\phi(L) = \frac{d\Phi(L)}{dL} = - \left(\frac{\alpha}{L} + \frac{\beta}{\beta L^* + L} \right) \Phi(L)$$

For other definitions see also e.g. Yahil (1988), Sandage et al. (1979). The luminosity functions, stated above, are mainly labeled as *universal* functions, because are general functions for field galaxies and clusters of galaxies. Kaiser and Lahav (1988), referring to the universal luminosity function say that is highly idealized and almost certainly unrealistic. So, if we want to be more precise, we should make a distinction between the luminosity functions for galaxies of specified Hubble type.

4.1.3 Change of Variables

We know that the luminosity, L , is connected with the flux, F , through the equation

$$F = \frac{L}{4\pi R^2}$$

where R is the distance of the objects under consideration. Say we have two galaxies at distance R_1 and R_2 and luminosities L_1 and L_2 . Then the fluxes are

$$F_1 = \frac{L_1}{4\pi R_1^2} \quad \text{and} \quad F_2 = \frac{L_2}{4\pi R_2^2} \quad (4.3)$$

and

$$\log(F_1/F_2) = -(m_1 - m_2) \log 2.5 \Rightarrow$$

$$m_1 - m_2 = -2.5 \log \left[\frac{L_1 \left(\frac{R_2}{R_1} \right)^2}{L_2} \right]$$

$$\Rightarrow \frac{L}{L^*} = 10^{(M^* - M)/2.5} \quad (4.4)$$

Since the study of the LF is more convenient as a function of M , we change the variable from L to M . Φ is the p.d.f. of random variable L and the variable L is a function of M . We can derive the p.d.f., $\Phi(M)$, from $\phi(L)$ by changing the variables, according to the rule

$$\Phi(M)dM = \phi(L)dL \Rightarrow \Phi(M) = \left| \frac{dL}{dM} \right| \phi(L) \quad (4.5)$$

From eq. (4.4) we have $\left| \frac{dL}{dM} \right| = 25 \frac{1}{L}$, which combined with eq (4.5) is

$$\Phi(M) = \phi(L) \frac{L}{2.5}$$

and using the eq (4.2) and (4.5)

$$\Phi(M) = \frac{\phi^*}{2.5} \left[10^{\frac{(M^* - M)}{2.5}} \right]^{\alpha + 1} e^{-10^{\frac{(M^* - M)}{2.5}}} \quad (4.6)$$

and because

$$M = m - 5 \log r - 25 \quad (\text{with } r \text{ in Mpc}) \quad (4.7)$$

$$\Phi(M) = \frac{\phi^*}{2.5} \left[10^{(M^* - m + 5 \log r + 25) / 2.5} \right]^{\alpha + 1} e^{-10^{(M^* - m + 5 \log r + 25) / 2.5}} \quad (4.8)$$

Noticing that the samples of galaxies are magnitude limited, we can clearly see that it is pointless to take the integral as that in eq. (4.1) with upper limit infinity.

4.2 Selection Effects

In the previous chapter, we have described how we can generate a random function to get a 'complete sample of objects'. In practice the situation is a bit different. In the observation the samples are affected by phenomena like the galactic absorption, the limiting magnitude and uncertainties in magnitude estimates near the limiting magnitude (Peebles & Hauser, 1974). One of the main causes of statistical bias of a sample is the Malmquist bias. This problem occurs because the telescopes are unable to detect faint galaxies in long distance and confirmed by Malmquist (1920) studying the distribution of stars. In our simulation we impose a cut-off in the distance R which causes the magnitude to be limited. This phenomenon is quite important because using magnitude bigger than the limiting m_0 , we include galaxies which are not observable and the resultant a.c.f. becomes stronger. A way to avoid this is to use a function, called selection function. $S(r,M)$ expresses the probability that an object at distance r and with magnitude M is included in the catalogue. As an approximation we could write

$$S(m - m_0) = \begin{cases} 1 & \text{for } m \leq m_0 \\ 0 & \text{for } m > m_0 \end{cases}$$

i.e. galaxies below a limiting magnitude m_0 are visible, but galaxies above this limiting magnitude are unobservable. Let us define the

function, s , as an integral over the luminosity function and selection function as

$$s(r) = \int_{-\infty}^{\infty} S(r, M) \Phi(M) dM \quad (4.9)$$

where $\Phi(M)$ is the luminosity function. The integral gives the probability that a galaxy, at distance r , is actually observed. We can replace the equation (4.9) by another one which has a cut-off at a magnitude M_L that depends upon the sample. The value M_L can change according to our ability to go 'deeper' in the sky.

A further complication arises if the luminosity function depends on environment, particularly if it is a function of density (Yahil, 1988). If we want to split the luminosity function into others that describe the specific Hubble type, we should apply the same restriction for the magnitude cut-off, we did for the general luminosity function.

In the definition of the LF we used the absolute magnitude M^* as a typical value. If we assume that a galaxy of absolute magnitude M^* is at distance R (Mpc) then its apparent magnitude is $m_L (=M^*+5\log R+25)$

Now we can go back to the section 3.7 and especially in eq. (3.15) to see how the number of galaxies will be affected if we include the selection effects and the luminosity function as they are combined in the eq. (4.9). Integrating over M and r we get the number of objects within the solid angle $d\Omega$ in direction \underline{n} including the luminosity function as

$$\langle N \rangle = d\Omega \int_0^{\infty} \int_{-\infty}^{M_L} \rho(r, \theta, \varphi) S(r, M) \Phi(M) r^2 dr dM \quad (4.10)$$

Substituting the 4.10 to the 3.15 we can derive a.c.f., as shown in the figures 4.1-4.4

In this chapter, we studied how the consequences of the luminosity function on the generated sample. The luminosity function denotes the probability of selecting a galaxy of magnitude, m , for observation. When a catalogue is constructed, there is another distribution for the selected galaxies independent of the selection probability. This probability is called selection function and indicates if a galaxy of a certain magnitude will be included in the sample or not. Imposing the selection effects in the generated number of objects, we actually subtract a number of points, which correspond to magnitudes above a particular apparent magnitude $m_L (=10)$. Introducing the luminosity function and selection effects causes, the closer points to be less correlated and the a.c.f. to be higher than that obtained for the complete sample. This is obvious from the figures 4.1-4.4, where the Schechter luminosity function is included to study the effects on the a.c.f.

On keeping the mean absolute magnitude constant and increasing the distance, the effects of the luminosity functions are stronger. Limited computer memory did not permit us to examine these effects to very large distance.

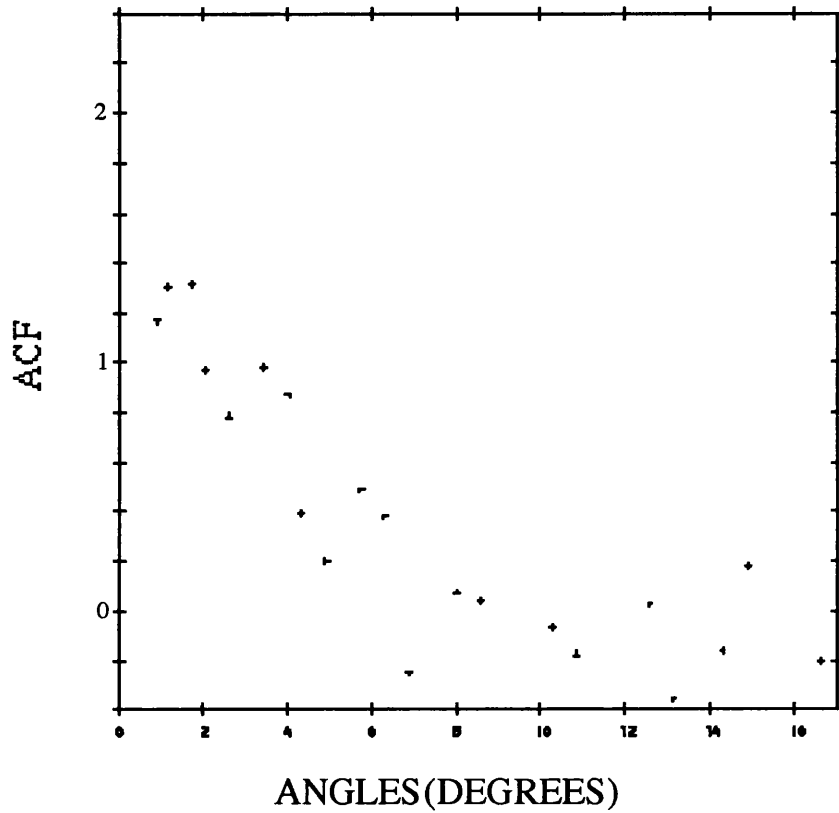


Fig. 4.1 : A.C.F. including the luminosity function and the selection effects.

It corresponds to the S.C.F. $A_{r_0}^{-\gamma}$ with min. wavel. = 2,
 $L=20$, $R=10$, Correlation length=2.5 and $m_L = 10$

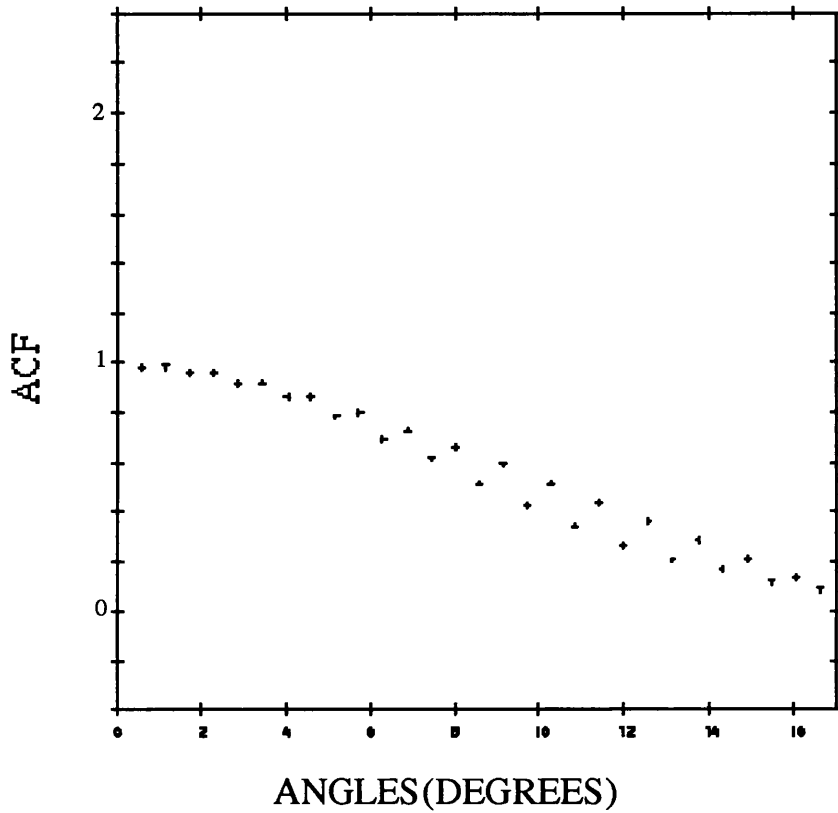


Fig. 4.2 : A.C.F. including the luminosity function and the selection effects

It corresponds to the S.C.F. $\exp(- (r / r_0)^2)$ with

min. wavelength = 2, $L=20$, $R=10$, Correlation Length = 2.5
and $m_L = 10$

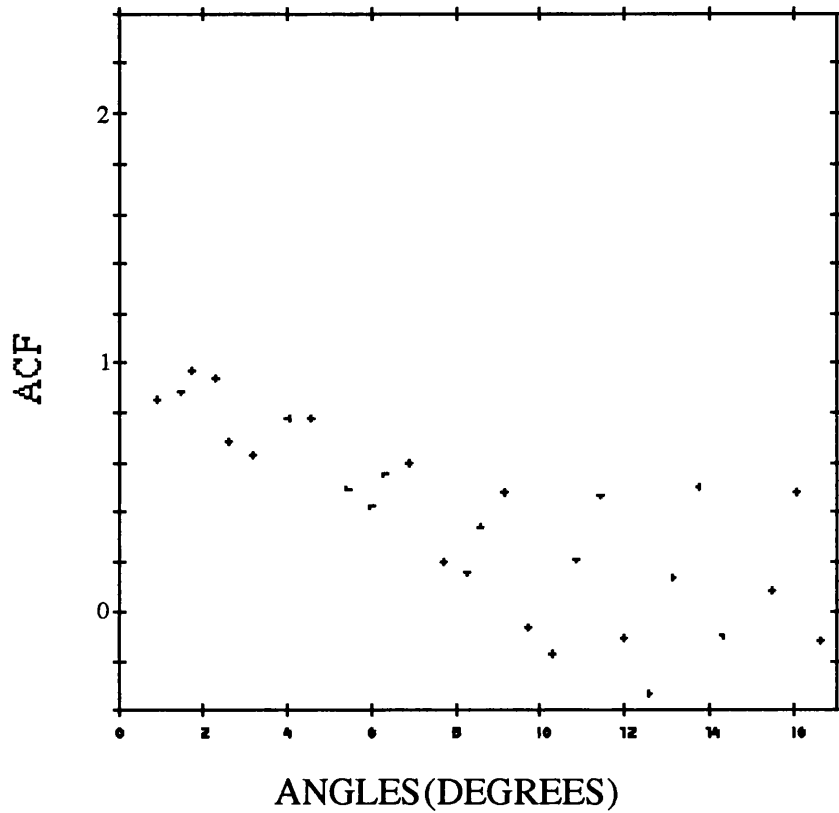


Fig. 4.3 : A.C.F. including the luminosity function and the selection effects.

It corresponds to the S.C.F. $\exp(-r/r_0)$ with
 min. wavelength = 2, $L=20$, $R=10$, Correlation Length = 2.5
 and $m_L = 10$

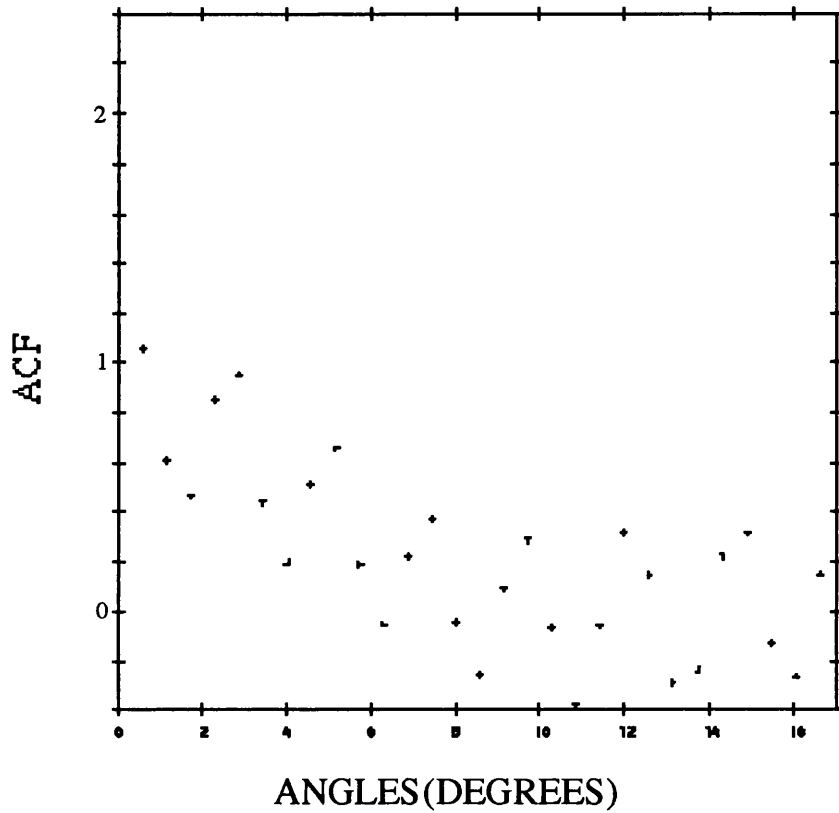


Fig. 4.4 : A.C.F. including the luminosity function and the selection effects.

It corresponds to the S.C.F. $((r + r_0) / r_0)^{-\gamma}$ with
 min. wavelength = 2, L=20, R=10, Correlation Length = 2.5 and
 $m_L = 10$

CHAPTER 5**DISCUSSION**

In this thesis we applied the theory of stochastic processes to the description of the distribution of galaxies. In our approach the number density of galaxies is given by a realization of a random function. The average quantities, such as the mean density and the correlation function, are obtained by averaging over the ensemble of realizations. Of course, there is only one Universe, and so such a procedure is impossible in practice. However average quantities can be obtained by taking the space average, provided a large enough region is taken, and assuming, of course, the density to be stationary. There are several advantages in presenting the distribution of galaxies as a random function. If we assume that the matter density can be described by a random function, then it is natural to suppose the number density of galaxies be connected to this random function. Furthermore, the manner in which the inhomogeneities evolve is naturally described by the linearised perturbation equations, at least insofar as linear theory holds.

A random function is essentially defined by all its moments, or n -point functions. In practice only the two-point function, the correlation function, is determined for galaxies and clusters of galaxies, and this does seem a natural definition of clustering. It is however only one of many possible descriptions, as we briefly described in chapter 1.

We generated a typical density distribution of galaxies by using spectral analysis. The essential idea here is to represent the random function by a Fourier series. The amplitude of each fourier component from the square root of the FT of the a.c.f. is determined by the fourier transform of the correlation function, or power spectrum and including random phase factors in the cosine term. Any random function generated in this way, using a countable number of frequencies, must be periodic. However the function so generated can only be taken as an approximate realization of the random function in a restricted region, $(L/2)$, as we discussed in chapter 2.

There does however seem to be some difficulty in the description of point processes where the correlation function is present. Peebles' definition of the correlation function is essentially empirical and depends on counting the number of galaxies within a shell at any radius from a given galaxy. In practice, Peebles' definition yields the same results as our approach, which is similar to Limber's, and regards the distribution of galaxies to be described by a random function.

In the nonlinear stage, the phases of the Fourier transform cease to be statistically independent and so both power spectrum and c.f., strictly speaking, do not completely describe the statistical distribution. For different phases we have different spatial distributions and so the s.c.f. does not contain full statistical information.

As we pointed out and illustrated in chapter 2, for realizations of a random function to be almost everywhere continuous imposes constraints on the correlation function. In particular it must take the value 1 at $r=0$. The power law form that is assumed by Peebles cannot give rise to a continuous density

distribution, as it is singular at the origin. The effects of this obscurity can be seen clearly in 1^D random processes we generated. But although the s.c.f. 3.14 fulfil the theorem and the 1^D realization satisfies the expected, these discontinuities are not clear in the 3^D graph, probably, because of the average taken over many realizations and the application of interpolation in order to obtain the graph.

Although this difficulty arose from the Peebles' power law for the generation of random functions, its relationship with a possible fractal like structure of the distribution of galaxies seems to me an open but important question, due to the discontinuous nature of fractals as referred to in sec. 3.8.1

We are particularly interested in the relationship between the spatial and angular correlation function and we applied our analysis to four different forms of s.c.f. One approach is to directly calculate the angular correlation function from the analytic expression 3.18. Another is to generate a density field using spectral analysis, and estimate the angular correlation function by averaging over a number of cones (eq. 3.17). According to the natural definition, the Peebles' power law spatial correlation function should give rise to the singular angular correlation function because of the singularity at $r=0$. The effect of carrying out the spectral analysis with a cut-off in higher frequencies (see eq. 2.13, where n represents the highest frequency corresponding to the minimum wavelength we choose) provides a physically meaningful angular correlation function. For those spatial correlation functions that give rise to continuous realizations of the density function, both methods give comparable results. The advantage in using spectral analysis is that it is easily generalised to incorporate more complicated effects etc.

When we integrate, in eq. 3.15, to get the number of points in one direction, we impose a cut-off at distance of R . In doing this we actually include a selection function. In order to be more precise we can say that the eq. 3.17 may be written as

$$w(\theta) = \frac{\langle \int_0^\infty \int_0^\infty [\rho(r_1) - \rho_0][\rho(r_2) - \rho_0] S(r_1) S(r_2) r_1^2 r_2^2 dr_1 dr_2 \rangle}{\langle [\int_0^\infty (\rho(r_1) - \rho_0) S(r_1) r_1^2 dr_1]^2 \rangle}$$

In the analytic expression of the s.c.f. 3.18, we can see that the direct derivation of the a.c.f. for the form $A r_{12}^{-\gamma}$ is impossible, because of the singularity at $r_{12}=0$.

Our work is mainly concerned with the use of generated random fields to calculate the a.c.f. Although, as we explained, it is possible to approach the problem using analytical forms, the random fields generation can be justified by the following: (i) spectral analysis does give a means of arriving at an a.c.f., since $\rho(\underline{x})$ so generated is continuous (by virtue of high frequency cut-off), (ii) it would allow one to generalise the Monte Carlo type simulation of more realistic selection and bias effects, (iii) comparison of analytic form for $w(\theta)$ and numerical form give indication of the effectiveness of spectral analysis.

An attractive area for further work, would be the application of stochastic theory to fractals. Generally, we can generate a fractal set in two ways (Castagnoly et al., 1990): (i) deterministic algorithm and (ii) stochastic processes; characterized by some probability distribution with second moment proportional to the same scaling exponent. There is a difference between deterministic and stochastic fractal (Calzetti et al., 1988). In the former, one defines the number of clusters, $\langle N_c \rangle$, as the fraction of mean number of galaxies, $\langle N_g \rangle$, divided by the number of galaxies,

N_c , which form clusters (i.e. $\langle N_c \rangle = \langle N_g \rangle / N$). But in the stochastic case, we include a factor s which gives the fraction of galaxies forming clusters and is sample independent (i.e. $\langle N_c \rangle = s \langle N_g \rangle / N$). In the same sense we can generate multifractal set, by using different scaling exponents. An important task, which needs to be studied, is the lower cut-off imposed by existence of galaxies, and upper cut-off, derived from the cosmological principle (e.g. Calzetti et al., 1988).

It is well known that the luminosity functions differ in shape for different types and different environmental densities as well (so we could say that $\phi(M) = \sum_i \phi_i(M) f_i$ where f_i is the fraction of the galaxies of morphological type i and luminosity function $\phi_i(M)$). In our analysis we used the Schechter's luminosity function as a first approach to our problem. Later work could include more specific functions to cover as many cases as possible.

In order to calculate the correlation functions, we need to measure the galaxy distance. Usually, most distances are estimated using the Hubble law, $v=Hr$, with v to be the radial velocity of a galaxy, and r the distance. The problem with this method is that errors arise, due to the peculiar velocities of the galaxies. It would be interesting to study how the bias of distance estimator (an extensive analysis of distance estimators is given, for example, in 'Errors, Bias and Uncertainties in Astronomy', 1990, edited by Carlos Jaschek & Fionn Murtagh) enter the estimation of a.c.f. from s.c.f., using the method developed in this thesis.

The 'mapping' of the density structures based on statistical methods, is an 'open area' for further elaboration. The information of the 3^D surveys give us the capability to compare the results of large numerical simulations based on a variety of theories (i.e. HDM,

CDM) and particular sets of initial conditions. New statistical techniques (i.e. 'jack-knife' and 'bootstrap' statistical tests, Ling et. al. (1986)) have started to be used as complementary measures of clustering patterns. The study of these tests along with the correlation functions will probably be proved useful.

Without being considered a "structuralist", I should like to examine some possible viewpoints. It concerns the resemblance between the fundamental ideas, throughout history, for the creation of the cosmos. Is it a coincidence that the same patterns are used today as in the ancient mythologies? 'Everything' started from 'nothing' and chaos eventually became order. We can distinguish the same way of thinking in, for instance, Anaximander, where the matter is unformed (apeiron) in the beginning, and in the theory of the big bang of modern cosmology. If this is not a coincidence, we must ask ourselves whether what we assume today is a reality, or simply a consequence of the experience and logic of the human brain. Today's models and assumptions may or may not be true. If they are true we need evidences in order to prove them. If they are not true we may seek the evidences within our limited sphere of knowledge/experience. But, if that evidences lies outwith our recognition, how are we to recognise it?

APPENDIX A

In this appendix we work out the power spectrum of the spatial correlation function $((r+a)/r_0)^{-\gamma}$. Of course, we could have assumed from the beginning that $\gamma=2$, significantly simplifying the situation, but we considered that it was more useful to derive the general case, than to be restricted to an expression for one particular value.

$$\int \int \int \left(\frac{r+a}{r_0}\right)^{-\gamma} e^{-ikr} \sin \theta d\theta d\phi dr = \frac{4\pi r_0^\gamma}{k} \int_0^\infty \frac{r}{(r+a)^\gamma} \sin kr dr \tag{A.1}$$

Using the transformation $u=r+a \Rightarrow r=u-a \Rightarrow dr=du$ we have

$$\begin{aligned} & \int_a^\infty \frac{(u-a)}{u^\gamma} \sin k(u-a) du \\ &= \int_a^\infty \frac{u}{u^\gamma} [\sin ku \cos ka - \sin ka \cos ku] du \\ & - a \int_a^\infty \frac{1}{u^\gamma} [\sin ku \cos ka - \sin ka \cos ku] du \\ &= \cos ka \frac{k^{-(1-\gamma)}}{k} \int_{ka}^\infty (ku)^{1-\gamma} \sin kud(ku) - \sin ka \frac{k^{-(1-\gamma)}}{k} \int_{ka}^\infty (ku)^{1-\gamma} \cos kud(ku) \\ & - a \cos ka \frac{k^\gamma}{k} \int_{ka}^\infty (ku)^{-\gamma} \sin kud(ku) + a \sin ka \frac{k^\gamma}{k} \int_{ka}^\infty (ku)^{-\gamma} \cos kud(ku) \\ & \text{for } ku=y = k^{\gamma-2} \cos ka \int_{ka}^\infty (ku)^{1-\gamma} \sin kud(ku) - k^{\gamma-2} \sin ka \int_{ka}^\infty (ku)^{1-\gamma} \cos kud(ku) \\ & - k^{\gamma-1} a \cos ka \int_{ka}^\infty (ku)^{-\gamma} \sin kud(ku) + k^{\gamma-1} a \sin ka \int_{ka}^\infty (ku)^{-\gamma} \cos kud(ku) \tag{A.2} \end{aligned}$$

The two general forms we need for the last integrals are:

$$\int_y^\infty x^{\mu-1} \cos x dx = \frac{1}{2} \left\{ e^{-\frac{\pi}{2}i\mu} \Gamma(\mu, iy) + e^{\frac{\pi}{2}i\mu} \Gamma(\mu, -iy) \right\} \tag{A.3}$$

for $\text{Re}\mu < 1$ (Gradshteyn/Ryzhik, p421)

$$\int_y^\infty x^{\mu-1} \sin x dx = \frac{1}{2} \left\{ e^{-\frac{\pi}{2}i\mu} \Gamma(\mu, iy) - e^{\frac{\pi}{2}i\mu} \Gamma(\mu, -iy) \right\} \tag{A.4}$$

for $\text{Re}\mu > -1$ (Gradshteyn/Ryzhik, p420)

where $\Gamma(a, x) = \int_x^\infty e^{-t} t^{a-1} dt$ (Gradshteyn/Ryzhik, p940) is the incomplete Gamma Function. But because in our case the limit x becomes complex we will connect the incomplete Gamma Function with the function $\gamma^*(a, x)$ which is developed as a series

$$\gamma^*(a, x) = e^{-x} \sum_{n=0}^\infty \frac{x^n}{\Gamma(a+n+1)} \tag{A.5}$$

(Abramowitz & Stegun, p262)

and

$$\Gamma(a, x) = \Gamma(a) - \gamma(a, x) \tag{Abramowitz & Stegun, p260}$$

with

$$\gamma^*(a, x) = \frac{x^{-a}}{\Gamma(a)} \gamma(a, x) \tag{Abramowitz & Stegun, p260}$$

So

$$\Gamma(\mu, iy) = \Gamma(\mu) - \gamma(\mu, iy) = \Gamma(\mu) - \gamma^*(\mu, iy) \Gamma(\mu) (iy)^\mu = \Gamma(\mu) [1 - (iy)^\mu \gamma^*(\mu, iy)]$$

$$\begin{aligned} \Gamma(\mu, -iy) &= \Gamma(\mu) - \gamma(\mu, -iy) = \Gamma(\mu) - \gamma^*(\mu, -iy) \Gamma(\mu) (-iy)^\mu \\ &= \Gamma(\mu) [1 - (-iy)^\mu \gamma^*(\mu, -iy)] \end{aligned}$$

It is more convenient to express the iy and $-iy$ as an exponential form

$$(iy)^\mu = y^\mu i^\mu = y^\mu e^{i\frac{\pi}{2}\mu} \quad \text{and} \quad (-iy)^\mu = y^\mu (-i)^\mu = y^\mu e^{-i\frac{\pi}{2}\mu}$$

Substituting to the equation (A.3) we have

$$\begin{aligned}
 \int_y^{\infty} x^{\mu-1} \cos x dx &= \frac{1}{2} \{ e^{-\frac{\pi}{2}i\mu} \Gamma(\mu) - e^{-\frac{\pi}{2}i\mu} \Gamma(\mu) \gamma^*(\mu, iy) (iy)^\mu + \\
 &\quad + e^{\frac{\pi}{2}i\mu} \Gamma(\mu) - e^{\frac{\pi}{2}i\mu} \Gamma(\mu) \gamma^*(\mu, -iy) (-iy)^\mu \} \\
 &= \frac{1}{2} \{ \Gamma(\mu) [e^{-\frac{\pi}{2}i\mu} + e^{\frac{\pi}{2}i\mu}] - e^{-\frac{\pi}{2}i\mu} e^{\frac{\pi}{2}i\mu} y^\mu \Gamma(\mu) \gamma^*(\mu, iy) \\
 &\quad - e^{-\frac{\pi}{2}i\mu} e^{\frac{\pi}{2}i\mu} y^\mu \Gamma(\mu) \gamma^*(\mu, -iy) \} \\
 &= \frac{1}{2} \{ \Gamma(\mu) 2 \cos \frac{\pi}{2} \mu - y^\mu \Gamma(\mu) \gamma^*(\mu, iy) - y^\mu \Gamma(\mu) \gamma^*(\mu, -iy) \} \\
 &= \frac{1}{2} \{ \Gamma(\mu) 2 \cos \frac{\pi}{2} \mu - y^\mu \Gamma(\mu) [\gamma^*(\mu, iy) + \gamma^*(\mu, -iy)] \} \quad (A.6)
 \end{aligned}$$

Working similarly for the equation (A.4) we get

$$\begin{aligned}
 \int_y^{\infty} x^{\mu-1} \sin x dx &= \frac{i}{2} \{ e^{-\frac{\pi}{2}i\mu} \Gamma(\mu, iy) - e^{\frac{\pi}{2}i\mu} \Gamma(\mu, -iy) \} \\
 &= \frac{i}{2} \{ e^{-\frac{\pi}{2}i\mu} \Gamma(\mu) - e^{-\frac{\pi}{2}i\mu} \Gamma(\mu) \gamma^*(\mu, iy) (iy)^\mu \\
 &\quad - e^{\frac{\pi}{2}i\mu} \Gamma(\mu) + e^{\frac{\pi}{2}i\mu} \Gamma(\mu) \gamma^*(\mu, -iy) (-iy)^\mu \} \\
 &= \frac{i}{2} \{ \Gamma(\mu) [e^{-\frac{\pi}{2}i\mu} - e^{\frac{\pi}{2}i\mu}] - e^{-\frac{\pi}{2}i\mu} e^{\frac{\pi}{2}i\mu} y^\mu \Gamma(\mu) \gamma^*(\mu, iy) \\
 &\quad + e^{-\frac{\pi}{2}i\mu} e^{\frac{\pi}{2}i\mu} y^\mu \Gamma(\mu) \gamma^*(\mu, -iy) \} \\
 &= \frac{i}{2} \{ -\Gamma(\mu) 2i \sin \frac{\pi}{2} \mu - y^\mu \Gamma(\mu) \gamma^*(\mu, iy) + y^\mu \Gamma(\mu) \gamma^*(\mu, -iy) \} \\
 &= \frac{i}{2} \{ \Gamma(\mu) 2i \sin \frac{\pi}{2} \mu - y^\mu \Gamma(\mu) [\gamma^*(\mu, iy) - \gamma^*(\mu, -iy)] \} \quad (A.7)
 \end{aligned}$$

Now the problem is to work out the quantities

$$K = \gamma^*(\mu, iy) - \gamma^*(\mu, -iy) \qquad L = \gamma^*(\mu, iy) + \gamma^*(\mu, -iy)$$

Using the equation (A.5) we have

$$\begin{aligned}
 K &= e^{-iy} \sum_{n=0}^{\infty} \frac{(iy)^n}{\Gamma(\mu + n + 1)} - e^{iy} \sum_{n=0}^{\infty} \frac{(-iy)^n}{\Gamma(\mu + n + 1)} \\
 &= e^{-iy} \sum_{n=0}^{\infty} \frac{y^n (\cos \frac{\pi}{2}n + i \sin \frac{\pi}{2}n)}{\Gamma(\mu + n + 1)} - e^{iy} \sum_{n=0}^{\infty} \frac{y^n (\cos \frac{\pi}{2}n - i \sin \frac{\pi}{2}n)}{\Gamma(\mu + n + 1)} \\
 &= 2i [\cos y \sum_{n=0}^{\infty} \frac{y^n \sin \frac{\pi}{2}n}{\Gamma(\mu + n + 1)} - \sin y \sum_{n=0}^{\infty} \frac{y^n \cos \frac{\pi}{2}n}{\Gamma(\mu + n + 1)}] \\
 L &= e^{-iy} \sum_{n=0}^{\infty} \frac{(iy)^n}{\Gamma(\mu + n + 1)} + e^{iy} \sum_{n=0}^{\infty} \frac{(-iy)^n}{\Gamma(\mu + n + 1)} \\
 &= e^{-iy} \sum_{n=0}^{\infty} \frac{y^n (\cos \frac{\pi}{2}n + i \sin \frac{\pi}{2}n)}{\Gamma(\mu + n + 1)} + e^{iy} \sum_{n=0}^{\infty} \frac{y^n (\cos \frac{\pi}{2}n - i \sin \frac{\pi}{2}n)}{\Gamma(\mu + n + 1)} \\
 &= 2 [\cos y \sum_{n=0}^{\infty} \frac{y^n \sin \frac{\pi}{2}n}{\Gamma(\mu + n + 1)} + \sin y \sum_{n=0}^{\infty} \frac{y^n \cos \frac{\pi}{2}n}{\Gamma(\mu + n + 1)}]
 \end{aligned}$$

Substituting the equations K and L to the (A.6) & (A.7) we have

$$\begin{aligned}
 (A.6) &= \frac{1}{2} \{ \Gamma(\mu) 2 \cos \frac{\pi}{2}\mu - y^\mu \Gamma(\mu) \\
 &\quad [2 \cos y \sum_{n=0}^{\infty} \frac{y^n \cos \frac{\pi}{2}n}{\Gamma(\mu + n + 1)} + 2 \sin y \sum_{n=0}^{\infty} \frac{y^n \sin \frac{\pi}{2}n}{\Gamma(\mu + n + 1)}] \}
 \end{aligned}$$

$$\begin{aligned}
 (A.7) &= \frac{i}{2} \{ -\Gamma(\mu) 2i \sin \frac{\pi}{2}\mu - y^\mu \Gamma(\mu) 2i \\
 &\quad [\cos y \sum_{n=0}^{\infty} \frac{y^n \sin \frac{\pi}{2}n}{\Gamma(\mu + n + 1)} - \sin y \sum_{n=0}^{\infty} \frac{y^n \cos \frac{\pi}{2}n}{\Gamma(\mu + n + 1)}] \\
 &= \Gamma(\mu) \sin \frac{\pi}{2}\mu + y^\mu \Gamma(\mu) [\cos y \sum_{n=0}^{\infty} \frac{y^n \sin \frac{\pi}{2}n}{\Gamma(\mu + n + 1)} - \sin y \sum_{n=0}^{\infty} \frac{y^n \cos \frac{\pi}{2}n}{\Gamma(\mu + n + 1)}]
 \end{aligned}$$

Now we use these results to get an analytic form for the integral. We adjust the last part of equation (A.2) to be equivalent to the general forms (A.3) and (A.4)

$$\begin{aligned}
 (A.2) &= k^{\gamma-2} \cos ka \int_{ka}^{\infty} (ku)^{(2-\gamma)-1} \sin kud(ku) \\
 &\quad - k^{\gamma-2} \sin ka \int_{ka}^{\infty} (ku)^{(2-\gamma)-1} \cos kud(ku) \\
 &= k^{\gamma-1} a \cos ka \int_{ka}^{\infty} (ku)^{(1-\gamma)-1} \sin kud(ku) + k^{\gamma-1} a \sin ka \int_{ka}^{\infty} (ku)^{(1-\gamma)-1} \cos kud(ku) \\
 &= k^{\mu} \cos ka \left\{ \Gamma(-\mu) \sin \frac{\pi}{2}(-\mu) + (ka)^{\mu} \Gamma(-\mu) \right. \\
 &\quad \left. \left[\cos(ka) \sum_{n=0}^{\infty} \frac{(ka)^n \sin \frac{\pi}{2}n}{\Gamma(-\mu+n+1)} - \sin(ka) \sum_{n=0}^{\infty} \frac{(ka)^n \cos \frac{\pi}{2}n}{\Gamma(-\mu+n+1)} \right] \right\} \\
 &\quad - k^{\mu} \sin ka \left\{ \Gamma(-\mu) \cos \frac{\pi}{2}(-\mu) - (ka)^{\mu} \Gamma(-\mu) \right. \\
 &\quad \left. \left[\cos(ka) \sum_{n=0}^{\infty} \frac{(ka)^n \cos \frac{\pi}{2}n}{\Gamma(-\mu+n+1)} + \sin(ka) \sum_{n=0}^{\infty} \frac{(ka)^n \sin \frac{\pi}{2}n}{\Gamma(-\mu+n+1)} \right] \right\} \\
 &= k^{-\nu} a \cos ka \left\{ \Gamma(\nu) \sin \frac{\pi}{2}\nu + (ka)^{\nu} \Gamma(\nu) \right. \\
 &\quad \left. \left[\cos(ka) \sum_{n=0}^{\infty} \frac{(ka)^n \sin \frac{\pi}{2}n}{\Gamma(\nu+n+1)} - \sin(ka) \sum_{n=0}^{\infty} \frac{(ka)^n \cos \frac{\pi}{2}n}{\Gamma(\nu+n+1)} \right] \right\} \\
 &\quad + k^{-\nu} \sin ka \left\{ \Gamma(\nu) \cos \frac{\pi}{2}\nu - (ka)^{\nu} \Gamma(\nu) \right. \\
 &\quad \left. \left[\cos(ka) \sum_{n=0}^{\infty} \frac{(ka)^n \cos \frac{\pi}{2}n}{\Gamma(\nu+n+1)} + \sin(ka) \sum_{n=0}^{\infty} \frac{(ka)^n \sin \frac{\pi}{2}n}{\Gamma(\nu+n+1)} \right] \right\}
 \end{aligned}$$

where $\mu = 2 - \gamma$ and $\nu = 1 - \gamma$

APPENDIX B

- description of the programme
- flow chart
- programme

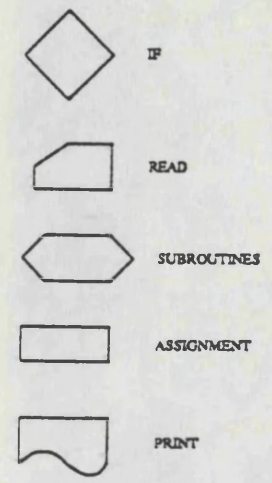
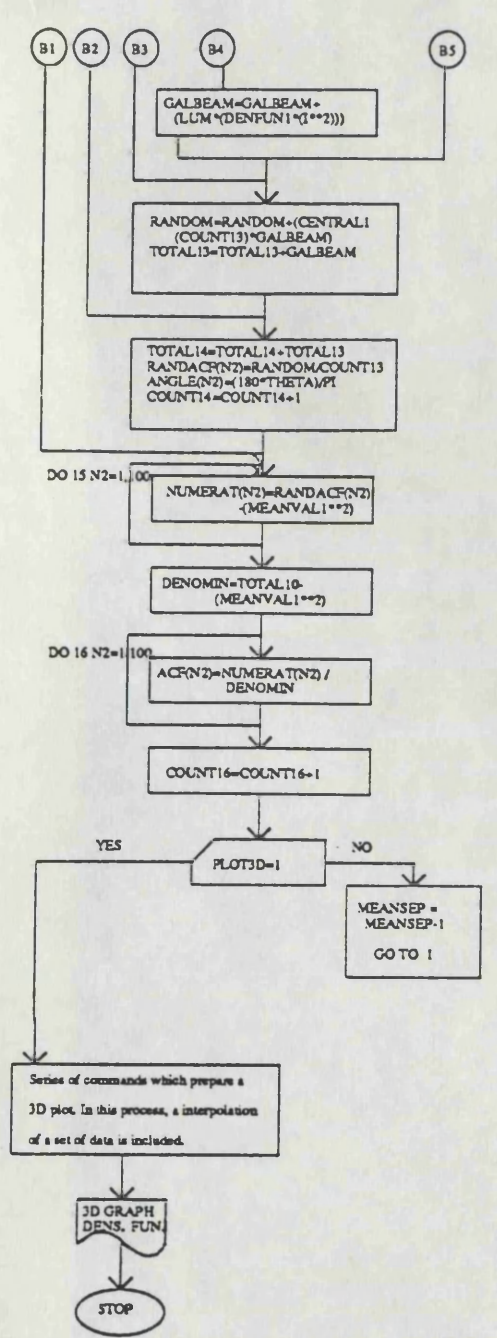
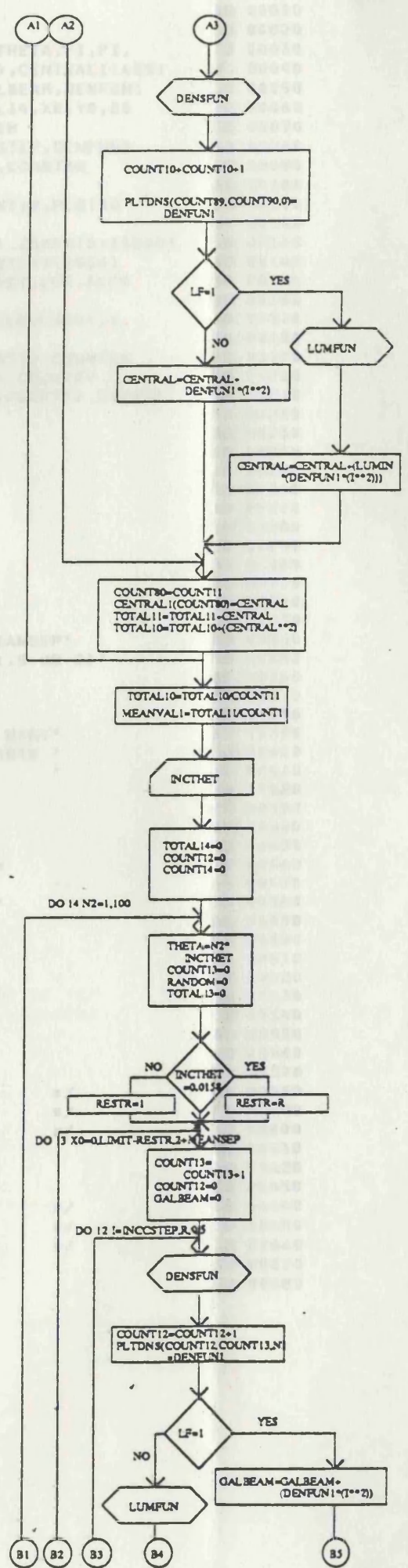
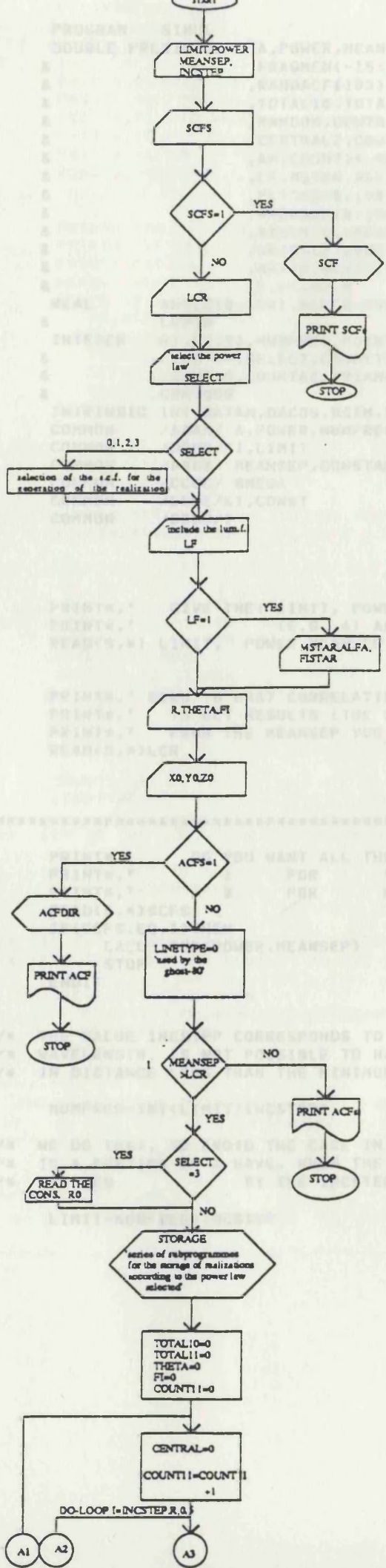
DESCRIPTION

After calculating the number of frequencies (as described in sec. 2.3), the program asks the user to input which one of the forms (3.8), (3.10), (3.11) & (3.14) he wants to use in order to work out the power spectrum. There are five subroutines connected with the main program which carries out the above. The first includes a triple loop which represents the components of the array 'fragmen'. This 3^D array is evaluated by the square root of the power spectrum. The particular subroutine called, depends on our choice of the correlation function. There are four different 'functions' which take the frequency, k , and return a value $|\delta_k|^2$. The density function, $\delta(x)$, is obtained on the basis of the 'fragmen'. On calling the subroutine 'product' we have a triple loop which gives the sum of the equation (2.18). A 'nagroutine' returns a pseudo-random number for the phase angle, ϕ_k , taken from a uniform distribution $\sim U(0, 2\pi)$. Here we use a special 'nagroutine' which sets the basic generator to a non-repeatable initial value, in order to avoid taking exactly the same realization, every time we run the program. At the end of this process, the subroutine 'denfun' returns the ratio $\delta\rho/\rho$. As we can see in these graphs there is an evaluated area which covers a quarter circle with origin on the axes (in the background). The area outside this region is flat, as the program gives it zero value. This occurred because we tried to take a 3^D graph corresponding to the average of the realizations we generated, which have 'circular' form as shown in fig. (3.1).

At this point a problem arose. The coordinates we use are polar and in order to get a plot we need cartisians. In theory this is easy to solve, but using the computer, the storage, of the converted values into two arrays, is very difficult. This was overcome by interpolation. We must be careful with regards to the direct interpretation of the plots of the $\delta(x)$. Although, the increasing step of angle θ is small, for large values of radius, R , the distance between the initially calculated values becomes larger which means a less accurate approximation than that for points close to origin.

The a.c.f. is evaluated in the main program and the theory of the chapter 3 is used. Firstly we choose an increment step for the mean separation, 'meansep'. After taking realizations across the length L with step 'meansep+2', we integrate along the line of sight and average over all the realizations. There are two ways to generate a random function: (i) developing points along the one line and averaging over it, and (ii) developing random processes parallel to one another and then averaging. We applied the former. More details are given in the 'flow-chart', where all the process is clear. The programme also gives the s.c. functions, a.c.f. in small angle approximation and includes the selection effects.

The programme is written in Fortran 77 on the IBM 3090 Computer run by the Glasgow University Computing Service, using the VM/SP HPO (Virtual Machine/System Product-High Performance Option) operating system and particular the component VM/CMS (Conversational Monitor System).




```

PROGRAM SIMUL
DOUBLE PRECISION A,POWER,MEANSEP,SUM,LIMIT,R,THETA,FI,PI,
& FRAGMEN(-15:15,-15:15,-15:15),CENTRAL1(400)
& ,RANDACF(100),NUMERAT(100),GALBEAM,DENFUN1
& ,TOTAL10,TOTAL11,TOTAL13,TOTAL14,X0,Y0,Z0
& ,RANDOM,CENTRAL,MEANVAL,DENOMIN
& ,CENTRAL2,COUNT11,INCTHET,INCSTEP,DENFUN2
& ,AM,COUNT14,MEANVAL1,MEANVAL2,CONSTAN
& ,LF,MSTAR,ALFA,FISTAR,MLIMIT
& ,PLTDNS(0:100,0:20,0:100),COUNT10,PLOT3D
& ,AVERAGE(0:150,0:150)
& ,XAXES(0:15000),YAXES(0:15000),ZAXES(0:15000)
& ,GRADS(2,2000),INTERX(2000),INTERY(2000)
& ,MAXIM,MINIM,SCFS,RESTR,K1,CONST,LCR,ACFS
& ,F,W1,W2,M
REAL ANGLE(0:100),ACF(0:100),PLT3D(90,90),CLEVLS(5),I,
& LUMIN
INTEGER R1,R2,R3,NUMFREQ,POINTS,THETA1,N2,COUNT12,COUNT16
& ,LINETYP,SELECT,COUNT13,COUNT18,COUNT19,COUNT89
& ,COUNT90,COUNT80,TRIANG(50000),COUNT20,COUNT70,COUNT71
& ,CONTOUR
INTRINSIC INT,DATAN,DACOS,DSIN,DCOS,DMAX1,DMIN1
COMMON /AAAA/ A,POWER,NUMFREQ
COMMON /DDDD/PI,LIMIT
COMMON /BBBB/ MEANSEP,CONSTAN
COMMON /CCCC/ OMEGA
COMMON /EEEE/K1,CONST
COMMON /DDDD/I
C
C
PRINT*,' GIVE THE: LIMIT, POWER(E.G. -1.8), MEANSEP'
PRINT*,' (E.G. 4) AND INCSTEP(E.G. 1.5 OR 2)'
READ(5,*) LIMIT, POWER,MEANSEP,INCSTEP
C
C
PRINT*,' DOWN TO WHAT CORRELATION LENGTH DO YOU WANT'
PRINT*,' TO GET RESULTS (THE STEP IS 1 AND STARTS '
PRINT*,' FROM THE MEANSEP YOU GAVE ABOVE '
READ(5,*)LCR
C
C
C
C*****
C
PRINT*,' DO YOU WANT ALL THE SCF TOGETHER? '
PRINT*,' 1 FOR YES'
PRINT*,' 0 FOR NO '
READ(5,*)SCFS
IF(SCFS.EQ.1)THEN
CALL SCF(POWER,MEANSEP)
STOP
ENDIF
C
C
C/* THE VALUE INCSTEP CORRESPONDS TO THE MINIMUM */
C/* WAVELENGTH. IS NOT POSSIBLE TO HAVE AN OBJECT */
C/* IN DISTANCE LESS THAN THE MINIMUM WAVELENGTH */
C
NUMFREQ=INT(LIMIT/INCSTEP)
C
C/* WE DO THAT, TO AVOID THE CASE IN WHICH THERE */
C/* IS A PORTION OF A WAVE, WHEN THE LIMIT IS NOT */
C/* DIVIDED BY THE INCSTEP */
C
LIMIT=NUMFREQ*INCSTEP

```

```

3D 00010
3D 00030
3D 00040
3D 00050
3D 00060
3D 00070
3D 00080
3D 00090
3D 00100
3D 00110
3D 00120
3D 00130
3D 00140
3D 00150
3D 00160
3D 00170
3D 00180
3D 00190
3D 00200
3D 00210
3D 00220
3D 00230
3D 00240
3D 00250
3D 00260
3D 00270
3D 00280
3D 00290
3D 00300
3D 00310
3D 00320
3D 00330
3D 00340
3D 00350
3D 00360
3D 00370
3D 00380
3D 00390
3D 00400
3D 00410
3D 00420
3D 00430
3D 00440
3D 00450
3D 00460
3D 00470
3D 00480
3D 00490
3D 00500
3D 00510
3D 00520
3D 00530
3D 00540
3D 00550
3D 00560
3D 00570
3D 00580
3D 00590
3D 00600
3D 00610
3D 00620
3D 00630
3D 00640
3D 00650
3D 00660
3D 00670
3D 00680

```

```

      PI=4*DATAN(1.D0)
C
C/* CHOOSE THE POWER LAW */
C
      PRINT*,'CHOOSE THE POWER LAW'
      PRINT*,'0 FOR A*R**(-GAMMA)'
      PRINT*,'1 FOR A*EXP**(-(R/R0)**2)'
      PRINT*,'2 FOR EXP**(-R/R0)'
      PRINT*,'3 FOR (R/(R+R0))**(-GAMMA)'
      READ(5,*)SELECT
C
C
      PRINT*,'DO YOU WANT THE LF TO BE INCLUDED?'
      PRINT*,'IF YES TYPE 1'
      PRINT*,'IF NO " 0'
      READ(5,*)LF
      IF(LF.EQ.1)THEN
        PRINT*,'GIVE THE VALUES OF'
        PRINT*,'MSTAR WHICH IS USUALY USED, IS|-19.46'
        PRINT*,'ALFA " " " " IS|-5/4 OR -1.02'
        PRINT*,'FISTAR " " " " IS|0.0277'
        READ(5,*)MSTAR,ALFA,FISTAR
      ENDIF
C
C
      PRINT*,' THE BEAM WHICH WILL BE CONS.'
      PRINT*,'GIVE R,THETA,FI'
      READ(5,*)R,THETA,FI
      PRINT*,'TELL ME THE INITIAL POINT PLEASE'
      READ(5,*)X0,Y0,Z0
C
C
      PRINT*,' DO YOU WANT THE ACFS DIRECTLY?''
      PRINT*,' 1 FOR YES'
      PRINT*,' 0 FOR NO'
      READ(5,*)ACFS
      IF(ACFS.EQ.1)THEN
        CALL ACFDIR(R)
        STOP
      ENDIF
C
C
      COUNT16=1
      LINETYP=0
C
C/* LCR IS THE LIMIT FOR THE CORRELATION LENGTHS */
C
      1 IF(MEANSEP.GT.LCR)THEN
        A=1/(MEANSEP**POWER)
C
C
C/* IF THE SUGGESTED POWER LAW HAS BEEN CHOSEN, THE R0 IS */
C/* THE CONSTANT AND USUALY IS THE SAME AS THE COR. LENGTH*/
C
      IF(SELECT.EQ.3)THEN
        PRINT*,' GIVE THE CONSTANT R0'
        READ(5,*)CONST
      ENDIF
C
C-----
C THE GENERATION OF RANDOM FIELDS FOR THE ESTIMATION
C OF A.C.F. BEGINS
C-----
C
C
C/* DENSITY FUNCTION */
C

```

```

3D 00690
3D 00700
3D 00710
3D 00720
3D 00730
3D 00740
3D 00750
3D 00760
3D 00770
3D 00780
3D 00790
3D 00800
3D 00810
3D 00820
3D 00830
3D 00840
3D 00850
3D 00860
3D 00870
3D 00880
3D 00890
3D 00900
3D 00910
3D 00920
3D 00930
3D 00940
3D 00950
3D 00960
3D 00970
3D 00980
3D 00990
3D 01000
3D 01010
3D 01020
3D 01030
3D 01040
3D 01050
3D 01060
3D 01070
3D 01080
3D 01090
3D 01100
3D 01110
3D 01120
3D 01130
3D 01140
3D 01150
3D 01160
3D 01170
3D 01180
3D 01190
3D 01200
3D 01210
3D 01220
3D 01230
3D 01240
3D 01250
3D 01260
3D 01270
3D 01280
3D 01290
3D 01300
3D 01310
3D 01320
3D 01330
3D 01340
3D 01350
3D 01360

```

```

C          TOTAL10=0.DO          3D 01370
          TOTAL11=0.DO          3D 01380
C          THETA=0.DO           3D 01390
          FI=0                   3D 01400
          COUNT11=0.DO          3D 01410
C          3D 01420
C          3D 01430
C/* DIFFERENT INITIAL POINTS ALONG THE X AXES SO THAT TO * 3D 01440
C/* HAVE MANY REALIZATIONS * 3D 01450
C/* I GIVE STEP 2+MEANSEP TO AVOID PART OF ONE SAMPLE TO * 3D 01460
C/* OVERLAP OTHER ONE * 3D 01470
C          3D 01480
          DO 11 X0=0,LIMIT/2,MEANSEP+2 3D 01490
C          3D 01500
C/* STORAGE OF ONE REALIZATION * 3D 01510
C          3D 01520
          CALL STORAGE(FRAGMEN,SELECT) 3D 01530
C          3D 01540
          CENTRAL=0.DO          3D 01550
          COUNT11=COUNT11+1    3D 01560
          DO 10 I=0,R,0.2       3D 01570
            CALL DENSFUN(FRAGMEN,DENFUN1,I,THETA,FI,X0,Y0,Z0) 3D 01580
            COUNT10=COUNT10+1  3D 01590
C          3D 01600
C/* THE 3D ARRAY IS USED IN ORDER TO PLOT THE (DENSITY * 3D 01610
C/* FUNCTION/MEAN DENSITY) IN THREE DIMENSION * 3D 01620
C          3D 01630
          COUNT89=1*COUNT10    3D 01640
          COUNT90=1*COUNT11    3D 01650
          PLTDNS(COUNT89,COUNT90,0)=DENFUN1 3D 01660
C          3D 01670
C/* WITH THIS IF WE CONTROL WHETHER OR NOT WE'LL INCLUDE * 3D 01680
C/* THE LUMINOSITY FUNCTION.IF YES WE MULTIPLY THE LUMIN * 3D 01690
C/* BY THE DENSITY. THE VALUE OF LUMIN COMES FROM THE SU-* 3D 01700
C/* BROUTINE LUMFUN * 3D 01710
C          3D 01720
          IF(LF.EQ.1)THEN       3D 01730
C          3D 01740
          CALL DOIAJF(LUMFUN,1,I ,0.0E0,1.0E-01,LUMIN, 3D 01750
C          & ABSERR,W,1000,IW,250 ,1) 3D 01760
          3D 01770
          CALL LUMFUN(_UMIN,R)  3D 01770
          CENTRAL=CENTRAL+(LUMIN *(DENFUN1*(I**2))) 3D 01780
          ELSE                   3D 01790
          LUMIN=0.               3D 01800
          CENTRAL=CENTRAL+(DENFUN1*(I**2)) 3D 01810
          ENDIF                 3D 01820
C          3D 01830
10      CONTINUE               3D 01840
C          3D 01850
          COUNT80=COUNT11      3D 01860
          CENTRAL1(COUNT80)=CENTRAL 3D 01870
          TOTAL11=TOTAL11+CENTRAL 3D 01880
C          3D 01890
C/* THE AVERAGE OF {TOTAL10/COUNT11} IS USED FOR THE * 3D 01900
C/* DENOMINATOR FOR THE EVALUATION OF ACF * 3D 01910
C          3D 01920
          TOTAL10=TOTAL10+(CENTRAL**2) 3D 01930
11      CONTINUE               3D 01940
C          3D 01950
          TOTAL10=TOTAL10/COUNT11 3D 01960
C          3D 01970
C          3D 01980
C/* THE MEANVAL1 GIVES THE MEAN NUMBER OF OBJECTS * 3D 01990
C/* IN COS(0) DIRECTION. * 3D 02000
C          3D 02010
          MEANVAL1=TOTAL11/COUNT11 3D 02020
C          3D 02030
C/* NOW I TAKE DIFFERENT ANGLES. THE INC(REMENT) FOR * 3D 02040

```

```

C/* ANGLE AND POINTS ON THE BEAM ARE GIVEN */ 3D 02050
C 3D 02060
PRINT*, 'WHAT IS THE INCTHETA?' 3D 02070
PRINT*, 'FOR 90 DEGREES GIVE 0.055 OR 0.01 OTHERWISE ' 3D 02080
READ(5,*)INCTHET 3D 02090
3D 02100
3D 02110
3D 02120
K=0.DO 3D 02130
TOTAL14=0.DO 3D 02140
COUNT12=0 3D 02150
COUNT14=1.DO 3D 02160
C ANGLE(0)=0.001 3D 02170
DO 14 N2=1,30 3D 02180
THETA=DIFTHETA + (N2*INCTHET) 3D 02190
COUNT13=0 3D 02200
RANDOM=0.DO 3D 02210
TOTAL13=0.DO 3D 02220
C 3D 02230
C/* THE SAME WORK AS ABOVE BUT WITH DIFFERENT ANGLES */ 3D 02240
C 3D 02250
DO 13 X0=0,LIMIT/2,MEANSEP+2 3D 02260
C 3D 02270
C/* STORAGE OF ONE REALIZATION */ 3D 02280
C 3D 02290
CALL STORAGE(FRAGMEN,SELECT) 3D 02300
C 3D 02310
COUNT13=COUNT13+1 3D 02320
COUNT12=0 3D 02330
GALBEAM=0.DO 3D 02340
DO 12 I=0 ,R,0.2 3D 02350
CALL DENSFUN(FRAGMEN,DENFUN1,I,THETA,FI,X0,Y0,Z0) 3D 02360
PRINT*,DENFUN1 3D 02370
C 3D 02380
C/* THE 3D ARRAY IS USED IN ORDER TO PLOT THE (DENSITY */ 3D 02390
C/* FUNCTION/MEAN DENSITY) IN THREE DIMENSION */ 3D 02400
C 3D 02410
COUNT12=COUNT12+1 3D 02420
PLTDNS(COUNT12,COUNT13,N2)=DENFUN1 3D 02430
C 3D 02440
C/* WITH THIS IF WE CONTROL WHETHER OR NOT WE'LL INCLUDE */ 3D 02450
C/* THE LUMINOSITY FUNCTION. IF YES WE MULTIPLY THE LUMIN */ 3D 02460
C/* BY THE DENSITY. THE VALUE OF LUMIN COMES FROM THE SU- */ 3D 02470
C/* BROUINE LUMFUN */ 3D 02480
C 3D 02490
IF(LF.EQ.1)THEN 3D 02500
CALL DO1AJF(LUMFUN,1,MLIMIT,0.0E0,1.0E-03,LUMIN, 3D 02510
& ABSERR,W,1000,IW,250,1) 3D 02520
CALL LUMFUN(LUMIN,R) 3D 02530
GALBEAM=GALBEAM+(LUMIN *(DENFUN1*(I**2))) 3D 02540
ELSE 3D 02550
GALBEAM=GALBEAM+(DENFUN1*(I**2)) 3D 02560
ENDIF 3D 02570
12 CONTINUE 3D 02580
RANDOM=RANDOM+(CENTRAL1(COUNT13)*GALBEAM) 3D 02590
TOTAL13=TOTAL13+GALBEAM 3D 02600
13 CONTINUE 3D 02610
TOTAL14=TOTAL14+TOTAL13 3D 02620
RANDACF(N2)=RANDOM/COUNT13 3D 02630
3D 02640
C 3D 02650
ANGLE(N2)=(180*THETA)/PI 3D 02660
COUNT14=COUNT14+1 3D 02670
14 CONTINUE 3D 02680
C 3D 02690
C 3D 02700
C** 3D 02710
MEANVAL2=TOTAL14/(COUNT13*(N2)) 3D 02720

```

```

MEANVAL=(MEANVAL1+MEANVAL2)/2
C
C/* THE NUMERATOR IS GIVEN BY */
C/* E([NUMBER OF OBJECTS IN ANGLE 0]*[NUM. OF OBJECTS */
C/* IN OTHER DIRECTIONS])-(MEAN NUM. OF OBJECTS)**2 */
C
C
DO 15 N2=1,30
NUMERAT(N2)=RANDACF(N2)-(MEANVAL**2)
C
15 CONTINUE
C
C/* THE DENOMIN(ATOR) IS GIVEN BY */
C/* <{[NUM. OF OBJECTS IN COS(0) DIRECTION]- */
C/* [MEAN NUM. OF OBJECTS]**2> OR */
C/* <(NUMBER OF OBJECTS IN COS(0) DIRECTION)**2> */
C/* -<MEAN NUMBER OF OBJECTS>**2 */
C
C
DENOMIN=TOTAL10-(MEANVAL**2)
DENOMIN=TOTAL10-(MEANVAL1**2)
C
C/* HERE IS THE FINAL ANGULAR CORRELATION FUNCT. */
C
C
OPEN(10,FILE='GRAPH2')
C
ACF(0)=1
DO 16 N2=1,30
ACF(N2)=(NUMERAT(N2)/DENOMIN)
16 CONTINUE
COUNT16=COUNT16+1
C
DO 889 N2 = 0,30
ANGLE(N2) = (N2 * INCTHET * 180) / PI
889 CONTINUE
C-----
C SO WE WORKED OUT THE A.C.F.
C-----
C
C NOW
C INTERPOLATION-PLOTTING-CONTOURS
C FOLLOW
C-----
C
C/* NOW WE HAVE THE CHOICE TO GET A 3D PLOTTING OF THE */
C/* DENSITY FUNCTION / MEAN DENSITY THROUGH THE SUBROU */
C/* TINE PLOT */
C
PRINT*,'DO YOU WANT A 3D PLOTTING OF THE (DENSITY FUNCTION/MEAN
&DENSITY) '
PRINT*,'IF YES TYPE 1 '
PRINT*,'IF NO " 0 '
READ(5,*)PLOT3D
IF(PLOT3D.EQ.1)THEN
C
COUNT20=0
ICNTPNT=0
DO 20 I=0,30
THETA=I*INCTHET
COUNT19=0
DO 19 B=INCSTEP,R,0.2

```

```

3D 0273
3D 0274
3D 0275
3D 0276
3D 0277
3D 0278
3D 0279
3D 0280
3D 0281
3D 0282
3D 0283
3D 0284
3D 0285
3D 0286
3D 0287
3D 0288
3D 0289
3D 0290
3D 0291
3D 0292
3D 0293
3D 0294
3D 0295
3D 0296
3D 0297
3D 0298
3D 0299
3D 0300
3D 0301
3D 0302
3D 0303
3D 0304
3D 0305
3D 0306
3D 0307
3D 0308
3D 0309
3D 0310
3D 0311
3D 0312
3D 0313
3D 0314
3D 0315
3D 0316
3D 0317
3D 0318
3D 0319
3D 0320
3D 0321
3D 0322
3D 0323
3D 0324
3D 0325
3D 0326
3D 0327
3D 0328
3D 0329
3D 0330
3D 0331
3D 0332
3D 0333
3D 0334
3D 0335
3D 0336
3D 0337
3D 0338
3D 0339
3D 0340

```

```

COUNT20=COUNT20+1
COUNT19=COUNT19+1
COUNT18=0
D=0.D0
IF(INCTHET.EQ.0.0158)THEN
  RESTR=R
ELSE
  RESTR=1.D0
ENDIF
DO 18 C=0,LIMIT/2,MEANSEP+2
  COUNT18=COUNT18+1
  D=D+PLTDNS(COUNT19,COUNT18,I)
18 CONTINUE
  AVERAGE(COUNT19,I)=D/COUNT18

C

C/* AT THIS POINT WE NEED TO DO INTERPOLATION BECAUSE WE */
C/* HAVE POLAR COORD. AND IT IS NOT POSSIBLE TO STORE */
C/* THEM WITH SUCH WAY, SO THAT TO BE USED BY THE GHOST- */
C/* 80 FOR 3D PLOTTING */
C
C/* FIRST WE CONVERT THE POLAR TO CARERT. COORD. AND WE */
C/* STORE THE RESULTS TO THE ARRAYS XAXES, YAXES, ZAXES */
C/* THE ZAXES ARRAY CONTAINES THE AVERAGE OF THE REALI- */
C/* ZATIONS FOR EACH POINT */
C
XAXES(COUNT20)=B*DSIN(THETA)
YAXES(COUNT20)=B*DCOS(THETA)
ZAXES(COUNT20)=AVERAGE(COUNT19,I)

IF(ZAXES(COUNT20).GT.1)THEN
  ICNTPNT=ICNTPNT+1
END IF
19 CONTINUE
20 CONTINUE

C
C/* E01SAF GENERATES A TWO-DIMENSIONAL SURFACE */
C/* INTERPOLATING A SET OF SCATTERED DATA POINTS */
C
CALL E01SAF(COUNT20,XAXES,YAXES,ZAXES,TRIANG,GRADS,0)

COUNT70=0
DO 26 W1=0,R,0.3
  COUNT70=COUNT70+1
  COUNT71=0
  DO 25 W2=0,R,0.3
    COUNT71=COUNT71+1
    IF((W1**2)+(W2**2).LT.R**2)THEN
C
C/* E01SBF EVALUATES AT A GIVEN POINT THE TWO-DIMENSIONAL*/
C/* INTERPOLANT FUNCTION COMPUTED BY THE NAG FORTRAN */
C/* LIBRARY ROUTINE E01SAF */
C
CALL E01SBF(COUNT20,XAXES,YAXES,ZAXES,TRIANG,
& GRADS,W1,W2,F,0)
C
C/* THE -1 COMES FROM THE EQUATION DENSFUN=1+DELTA. */
C/* WE WANT TO PLOT THE DELTA FUNCTION */
C
PLT3D(COUNT70,COUNT71)=F-1
ELSE
PLT3D(COUNT70,COUNT71)=0

```

	ENDIF	3D 04090
25	CONTINUE	3D 04100
26	CONTINUE	3D 04110
C		3D 04120
C		3D 04130
	CALL PAPER(1)	3D 04140
	CALL SURDIR(2)	3D 04150
C	CALL PSPACE(0.,0.1,0.,0.1)	3D 04160
	CALL SURAXE(2,0.,0.,0.3,0.3)	3D 04170
	PRINT*,' DO YOU WANT CONTOURS?'	3D 04180
	PRINT*,' 1 FOR YES'	3D 04190
	PRINT*,' 0 FOR NO '	3D 04200
	READ(5,*)CONTOUR	3D 04210
	IF(CONTOUR.EQ.1)THEN	3D 04220
		3D 04230
	MAXIM=0	3D 04240
	MINIM=3	3D 04250
	DO 29 I=1,COUNT20	3D 04260
	MAXIM=DMAX1(MAXIM,ZAXES(I))	3D 04270
	MINIM=DMIN1(MINIM,ZAXES(I))	3D 04280
29	CONTINUE	3D 04290
		3D 04300
C	CLEVL(1)=0.2	3D 04310
C	CLEVL(2)=0.5	3D 04320
C	CLEVL(3)=0.75	3D 04330
C	DO 30 I=2,3	3D 04340
C	CLEVL(I)=CLEVL(I-1)+((MAXIM-0)/2)	3D 04350
C30	CONTINUE	3D 04360
	CALL BORDER	3D 04370
	CALL BROKEN(20,10,20,10)	3D 04380
	PRINT*,COUNT70,COUNT71	3D 04390
	CALL CONTRA(PLT3D,1,COUNT70,90,1,COUNT71,COUNT71	3D 04400
&	,CLEVL,1,3)	3D 04410
	CALL FULL	3D 04420
C	CALL CONTRA(PLT3D,1,COUNT70,90,1,COUNT71,COUNT71	3D 04430
C	& CLEVL,3,3)	3D 04440
	ELSE	3D 04450
	CALL SURPLT(PLT3D,1 ,COUNT70,90,1,COUNT71,COUNT71	3D 04460
&)	3D 04470
	ENDIF	3D 04480
	CALL GREND	3D 04490
	CALL FRAME	3D 04500
	STOP	3D 04510
	ENDIF	3D 04520
		3D 04530
C	-----	3D 04540
	CALL PAPER(1)	3D 04550
	CALL BROKEN(LINETYP,LINETYP,LINETYP,LINETYP)	3D 04560
	LINETYP=LINETYP+4	3D 04570
	CALL MAP(0.,17.,-0.4,2.4)	3D 04580
	CALL SCALES	3D 04590
	CALL BORDER	3D 04600
	CALL PTPLOT(ANGLE,ACF,1,30)	3D 04610
C		3D 04620
	MEANSEP=MEANSEP-1	3D 04630
	GOTO 1	3D 04640
	ELSE	3D 04650
C	CALL PCSCEN(5.,-0.3,'ANGLE (DEGREES)')	3D 04660
	CALL CTRORI(90.0)	3D 04670
C	CALL PCSCEN(-2.,.6 , 'ACF')	3D 04680
	CALL FRAME	3D 04690
	CALL GREND	3D 04700
C		3D 04710
	ENDIF	3D 04720
		3D 04730
	STOP	3D 04740
	END	3D 04750
C		3D 04760

```

C////////////////////////////////////
C SUBROUTINES & FUNCTIONS /
C /
C////////////////////////////////////
C
C*****
C THIS SUB GIVES THE ACF DIRECTLY. THAT MEANS WE DO NOT **
C NEED TO GENERATE A RANDOM PROCESS. IT IS CALLED SMALL **
C ANGLE APPROXIMATION **
C **
C*****
C
SUBROUTINE ACFDIR(R)
REAL THETA(100),I1,I2,R,I12
& ,MEANSEP,ACF1(100),ACF2(100),ACF3(100)
& ,I1DEN,I1NUM,I2DEN,I2NUM,I3DEN,I3NUM
DOUBLE PRECISION MSTAR,ALFA,FISTAR,MLIMIT,LUMIN1,LUMIN2,RI1,RI2
& ,E
COUNT=0
MEANSEP=2.5
I1DEN=0.
I2DEN=0.
I3DEN=0.
MSTAR=-19.46
ALFA=-1.25
FISTAR=0.0277
E=0.00
MLIMIT=20
DO 6 RI1=0,R,0.5
C CALL LUMFUN(MSTAR,ALFA,FISTAR,MLIMIT,RI1,0.00
C & ,0.00,E,LUMIN1)
C DO 5 RI2=0,R,0.5
C CALL LUMFUN(MSTAR,ALFA,FISTAR,MLIMIT,RI2,0.00
C & ,0.00,E,LUMIN2)
I12=(RI1-RI2)**2
I1=(RI1**2)
I2=(RI2**2)
IF((I12/MEANSEP)**2.GT.60.0)THEN
I1DEN=I1DEN+(I1*I2/EXP(60.0))
I2DEN=I2DEN+(I1*I2/EXP(60.0))
ELSE
I1DEN=I1DEN+(EXP(-(I12/MEANSEP)**2)*I1*I2)
I2DEN=I2DEN+(EXP(-I12/MEANSEP)*I1*I2)
ENDIF
I3DEN=I3DEN+((((I12+MEANSEP)/MEANSEP)**(-1.8))*I1*I2)
5 CONTINUE
6 CONTINUE
DO 10 RADIANS=0,0.6,0.01
COUNT=COUNT+1
THETA(COUNT)=(RADIANS*180)/3.1415
I1NUM=0.
I2NUM=0.
I3NUM=0.
DO 9 RI1=0,R,0.5
C CALL LUMFUN(MSTAR,ALFA,FISTAR,MLIMIT,RI1,0.00
C & ,0.00,E,LUMIN1)
C DO 8 RI2=0,R,0.5
C CALL LUMFUN(MSTAR,ALFA,FISTAR,MLIMIT,RI2,0.00
C & ,0.00,E,LUMIN2)
I12=((RI1-RI2)**2)+(RI1*RI2*RADIANS)
I1=(RI1**2)
I2=(RI2**2)

```

```

3D 04770
3D 04780
3D 04790
3D 04800
3D 04810
3D 04820
3D 04830
3D 04840
3D 04850
3D 04860
3D 04870
3D 04880
3D 04890
3D 04900
3D 04910
3D 04920
3D 04930
3D 04940
3D 04950
3D 04960
3D 04970
3D 04980
3D 04990
3D 05000
3D 05010
3D 05020
3D 05030
3D 05040
3D 05050
3D 05060
3D 05070
3D 05080
3D 05090
3D 05100
3D 05110
3D 05120
3D 05130
3D 05140
3D 05150
3D 05160
3D 05170
3D 05180
3D 05190
3D 05200
3D 05210
3D 05220
3D 05230
3D 05240
3D 05250
3D 05260
3D 05270
3D 05280
3D 05290
3D 05300
3D 05310
3D 05320
3D 05330
3D 05340
3D 05350
3D 05360
3D 05370
3D 05380
3D 05390
3D 05400
3D 05410
3D 05420
3D 05430
3D 05440

```



```

      IF((I12/MEANSEP)**2.GT.60.0)THEN
        I1NUM=I1NUM+(I1*I2/EXP(60.))
        I2NUM=I2NUM+(I1*I2/EXP(60.))
      ELSE
        I1NUM=I1NUM+(EXP(-(I12/MEANSEP)**2)*I1*I2)
        I2NUM=I2NUM+(EXP(-I12/MEANSEP)*I1*I2)
      ENDIF
      I3NUM=I3NUM+((((I12+MEANSEP)/MEANSEP)**(-1.8))*I1*I2)
8     CONTINUE
9     CONTINUE
      ACF1(COUNT)=I1NUM/I1DEN
      ACF2(COUNT)=I2NUM/I2DEN
      ACF3(COUNT)=I3NUM/I3DEN
10    CONTINUE
C
C
      CALL PAPER(1)
      CALL MAP(0.,14.,-.2,1.2)
      CALL SCALES
      CALL BORDER
      CALL BROKEN(0,0,0,0)
      CALL CURVEO(THETA,ACF1,1,60)
      CALL BROKEN(10,10,10,10)
      CALL CURVEO(THETA,ACF2,1,60)
      CALL BROKEN(30,30,30,30)
      CALL CURVEO(THETA,ACF3,1,60)
      CALL FRAME
      CALL GREND
C
C
      STOP
      END
C
C
C
C*****
C
C WITH THIS SUBROUTINE WE HAVE THE CHOICE TO GET A
C GRAPH OF ALL THE SCF AT THE SAME TIME
C
C*****
C
      SUBROUTINE SCF(POWER,MEANSEP)
      REAL SCF1(42),SCF2(42),SCF3(42),SCF4(42),
      & POWER,MEANSEP,A,XAXES(42),R
      INTRINSIC EXP
      INTEGER I
C
      A=1/(3 **POWER)
C
      R=0.
      DO 100 I=1,30
        IF(R.NE.0)THEN
          SCF1(I)=A*((1/R)**(-POWER))
        ENDIF
        SCF2(I)=(3 /(R+3 ))**(-POWER)
        SCF3(I)=EXP(-(R/SQRT(2.))**2)/SQRT(2.*3.14)
        SCF4(I)=EXP(-(R/SQRT(2.)))/SQRT(2.*3.14)
        XAXES(I)=R
        R=R+0.5
100    CONTINUE
C
      CALL PAPER(1)
      CALL MAP(0.,20.,0.,1.1)
      CALL SCALES

```

```

3D 05450
3D 05460
3D 05470
3D 05480
3D 05490
3D 05500
3D 05510
3D 05520
3D 05530
3D 05540
3D 05550
3D 05560
3D 05570
3D 05580
3D 05590
3D 05600
3D 05610
3D 05620
3D 05630
3D 05640
3D 05650
3D 05660
3D 05670
3D 05680
3D 05690
3D 05700
3D 05710
3D 05720
3D 05730
3D 05740
3D 05750
3D 05760
3D 05770
3D 05780
3D 05790
3D 05800
3D 05810
3D 05820
3D 05830
3D 05840
3D 05850
3D 05860
3D 05870
3D 05880
3D 05890
3D 05900
3D 05910
3D 05920
3D 05930
3D 05940
3D 05950
3D 05960
3D 05970
3D 05980
3D 05990
3D 06000
3D 06010
3D 06020
3D 06030
3D 06040
3D 06050
3D 06060
3D 06070
3D 06080
3D 06090
3D 06100
3D 06110
3D 06120

```

```

CALL BORDER 3D 06130
CALL BROKEN(0,0,0,0) 3D 06140
CALL CURVEO(XAXES,SCF1,2,30) 3D 06150
CALL BROKEN(10,10,10,10) 3D 06160
CALL CURVEO(XAXES,SCF2,1,30) 3D 06170
CALL BROKEN(20,20,20,20) 3D 06180
CALL CURVEO(XAXES,SCF3,1,30) 3D 06190
CALL BROKEN(30,30,30,30) 3D 06200
CALL CURVEO(XAXES,SCF4,1,30) 3D 06210
CALL FRAME 3D 06220
CALL GREND 3D 06230
C 3D 06240
RETURN 3D 06250
END 3D 06260
C 3D 06270
C 3D 06280
C 3D 06290
C***** 3D 06300
C 3D 06310
C CALLING THIS SUBR. WE CAN STORE ONE REALIZATION * 3D 06320
C OF THE VALUES OF FRAGMEN * 3D 06330
C * 3D 06340
C***** 3D 06350
C 3D 06360
SUBROUTINE STORAGE(FRAGMEN,SELECT) 3D 06370
INTEGER X,L,M,N,SELECT,NUMFREQ 3D 06380
DOUBLE PRECISION SUM,MODULK,VAR,A,FRAGMEN(30,30,30),K1,K2,K3, 3D 06390
& LIMIT,B,PI,POWER,C 3D 06400
COMMON /AAAA/A,POWER,NUMFREQ 3D 06410
COMMON /DDDD/PI,LIMIT 3D 06420
EXTERNAL VARIANC,VARIAN2,VARIAN3,VARIAN4 3D 06430
3D 06440
INTRINSIC DCOS,DSQRT 3D 06450
C 3D 06460
C/* THE WAVENUMBER IS RELATED TO L,M,N BY * 3D 06470
C/* K1=(2*PI*L)/LIMIT,ETC. * 3D 06480
DO 150 L=-NUMFREQ,NUMFREQ 3D 06490
K1=(2*PI*L)/LIMIT 3D 06500
DO 140 M=-NUMFREQ,NUMFREQ 3D 06510
K2=(2*PI*M)/LIMIT 3D 06520
DO 130 N=0,NUMFREQ 3D 06530
K3=(2*PI*N)/LIMIT 3D 06540
C=(K1**2)+(K2**2)+(K3**2) 3D 06550
MODULK=DSQRT(C) 3D 06560
IF(SELECT.EQ.0)THEN 3D 06570
VAR=VARIANC(MODULK) 3D 06580
ELSE IF(SELECT.EQ.1)THEN 3D 06590
VAR=VARIAN2(MODULK) 3D 06600
ELSE IF(SELECT.EQ.2)THEN 3D 06610
VAR=VARIAN3(MODULK) 3D 06620
ELSE IF(SELECT.EQ.3)THEN 3D 06630
VAR=VARIAN4(MODULK) 3D 06640
ENDIF 3D 06650
C FRAGMEN(L ,M ,N )=G05DDF(0,SQRT(VAR)) 3D 06660
FRAGMEN(L,M,N)=SQRT(VAR) 3D 06670
CALL G05CCF 3D 06680
130 CONTINUE 3D 06690
140 CONTINUE 3D 06700
150 CONTINUE 3D 06710
C 3D 06720
C 3D 06730
RETURN 3D 06740
END 3D 06750
C 3D 06760
C 3D 06770
C***** 3D 06780
C * 3D 06790
C THIS FUNCTION IS CALLED BY THE SUBR. STORAGE AND * 3D 06800

```

```

C GIVES THE ENSEMBLE VARIANCE OF THE DENSITY FLUCTUATIONS * 3D 0681
C * 3D 0682
C***** 3D 0683
C 3D 0684
DOUBLE PRECISION FUNCTION VARIANC(K) 3D 0685
DOUBLE PRECISION K,W1,W2,W3,W4,RADIAN,A,POWER,LIMIT,PI 3D 0686
INTEGER NUMFREQ 3D 0687
COMMON /AAAA/A,POWER,NUMFREQ 3D 0688
COMMON /DDDD/PI,LIMIT 3D 0689
INTRINSIC DSIN 3D 0690
C 3D 0691
C 3D 0692
IF(K.EQ.0) THEN 3D 0693
VARIANC = 0 3D 0694
ELSE 3D 0695
W1=(1/((LIMIT/2)**3)) 3D 0696
W2=(A*4*PI)/(K**(2+POWER+1)) 3D 0697
W3=S14AAF((2+POWER),0) 3D 0698
RADIAN=(2+POWER)*(PI/2) 3D 0699
W4=DSIN(RADIAN) 3D 0700
VARIANC= W1*W2*W3*W4 3D 0701
ENDIF 3D 0702
C 3D 0703
C 3D 0704
RETURN 3D 0705
END 3D 0706
C 3D 0707
C 3D 0708
C***** 3D 0709
C * 3D 0710
C THIS FUNCTION IS CALLED BY THE SUBROUTINE STORAGE AND * 3D 0711
C GIVES THE ENSEMBLE VARIANCE OF THE DENSITY FLUCTUATION * 3D 0712
C FOR THE SECOND LAW * 3D 0713
C * 3D 0714
C***** 3D 0715
C 3D 0716
DOUBLE PRECISION FUNCTION VARIAN2(K) 3D 0717
DOUBLE PRECISION A,K,POWER,PI,LIMIT,MEANSEP,CONSTAN,B,W1,W2 3D 0718
INTEGER NUMFREQ 3D 0719
COMMON /AAAA/A,POWER,NUMFREQ 3D 0720
COMMON /DDDD/PI,LIMIT 3D 0721
COMMON /BBBB/MEANSEP,CONSTAN 3D 0722
C 3D 0723
C 3D 0724
B=4*PI*(MEANSEP**3) 3D 0725
W1=(2**(3/2))*((LIMIT/2)**3) 3D 0726
IF(((K*MEANSEP)**2)/4.GT.170)THEN 3D 0727
W2=DEXP(170.D0) 3D 0728
ELSE 3D 0729
W2=DEXP((K*MEANSEP/2)**2) 3D 0730
ENDIF 3D 0731
VARIAN2=B/(W1*W2) 3D 0732
RETURN 3D 0733
END 3D 0734
C 3D 0735
C 3D 0736
C***** 3D 0737
C * 3D 0738
C THIS FUNCTION IS CALLED BY THE SUBROUTINE STORAGE AND * 3D 0739
C GIVES THE ENSEMBLE VARIANCE OF THE DENSITY FLUCTUATION * 3D 0740
C FOR THE THIRD LAW * 3D 0741
C * 3D 0742
C***** 3D 0743
C 3D 0744
DOUBLE PRECISION FUNCTION VARIAN3(K) 3D 0745
DOUBLE PRECISION POWER,A,PI,LIMIT,K,W1,W2,MEANSEP,CONSTAN,W 3D 0746
INTEGER NUMFREQ 3D 0747
COMMON /AAAA/A,POWER,NUMFREQ 3D 0748
COMMON /DDDD/PI,LIMIT 3D 0749

```

```

COMMON /BBBB/MEANSEP,CONSTAN 3D 07490
C 3D 07500
C 3D 07510
W1=(8*PI)/((LIMIT/2)**3) 3D 07520
W2=MEANSEP*((K**2)+((1/MEANSEP)**2)**2) 3D 07530
VARIAN3=W1/W2 3D 07540
RETURN 3D 07550
END 3D 07560
C 3D 07570
C 3D 07580
C***** 3D 07590
C * 3D 07600
C THIS FUNCTION IS CALLED BY THE SUBROUTINE STORAGE AND * 3D 07610
C GIVES THE ENSEMBLE VARIANCE OF THE DENSITY FLUCTUATION * 3D 07620
C FOR THE FORTH LAW * 3D 07630
C * 3D 07640
C***** 3D 07650
C 3D 07660
DOUBLE PRECISION FUNCTION VARIAN4(K) 3D 07670
DOUBLE PRECISION K,A,POWER,CONST,ARG1,ARG2,CONSTAN,MEANSEP 3D 07680
& ,A1,A2,B1,B2,VAR,COEFFIC,PI,LIMIT,K1 3D 07690
REAL M 3D 07700
INTEGER NUMFREQ 3D 07710
COMMON /AAAA/A,POWER,NUMFREQ 3D 07720
COMMON /DDDD/PI,LIMIT 3D 07730
COMMON /BBBB/MEANSEP,CONSTAN 3D 07740
COMMON /EEEE/K1,CONST 3D 07750
C 3D 07760
IF (K.EQ.0) THEN 3D 07770
VARIAN4 = 0 3D 07780
ELSE 3D 07790
COEFFIC=((4*PI*(MEANSEP**(-POWER)))/K)/((LIMIT/2)**3) 3D 07800
M=2+POWER 3D 07810
CALL FIRSTAR(K,M,CONST,ARG1) 3D 07820
CALL SECARG(K,M,CONST,ARG2) 3D 07830
A1=ARG1 3D 07840
A2=ARG2 3D 07850
M=-(1+POWER ) 3D 07860
CALL FIRSTAR(K,M,CONST,ARG1) 3D 07870
CALL SECARG(K,M,CONST,ARG2) 3D 07880
B1=ARG1 3D 07890
B2=ARG2 3D 07900
C 3D 07910
VARIAN4=DABS(COEFFIC*(A1-A2-(CONST*B1)+B2)) 3D 07920
ENDIF 3D 07930
C 3D 07940
RETURN 3D 07950
END 3D 07960
C 3D 07970
C 3D 07980
C***** 3D 07990
C * 3D 08000
C THE NEXT SUBROUTINE IS USED BY THE SUB. VARIAN4 * 3D 08010
C * 3D 08020
C***** 3D 08030
C 3D 08040
SUBROUTINE FIRSTAR(K,M,CONST,ARG1) 3D 08050
DOUBLE PRECISION A1,A2,A3,ARG1,CONST,PI,LIMIT,K,K1,CONST1 3D 08060
REAL M 3D 08070
COMMON /DDDD/PI,LIMIT 3D 08080
COMMON /EEEE/K1,CONST1 3D 08090
EXTERNAL SUM1,SUM2 3D 08100
C 3D 08110
CONST1=CONST 3D 08120
K1=K 3D 08130
A1=(1/(K**M))*DCOS(K*CONST) 3D 08140
A2=S14AAF(-M,0)*DSIN(-(PI/2)*M) 3D 08150
A3=S14AAF(-M,0)*((K*CONST)**M)*(SUM1(M)-SUM2(M)) 3D 08160

```

```

ARG1=A1*(A2+A3)
C
RETURN
END
C
C
C*****
C
C THIS IS CALLED BY THE SUB VARIAN4
C*****
C
SUBROUTINE SECARG(K,M,CONST,ARG2)
DOUBLE PRECISION A1,A2,A3,ARG2,K,CONST,PI,LIMIT,K1,CONST1
REAL M
COMMON /DDDD/PI,LIMIT
COMMON /EEEE/K1,CONST1
EXTERNAL SUM3,SUM4
C
K1=K
CONST1=CONST
A1=(1/(K**M))*DSIN(K*CONST)
A2=S14AAF(-M,0)*DCOS(-(PI/2)*M)
A3=S14AAF(-M,0)*((K*CONST)**M)*(SUM3(M)+SUM4(M))
ARG2=A1*(A2-A3)
C
RETURN
END
C
C
C*****
C
C THE SUM1 IS A FUNCTION WORKING OUT ONE OF THE TWO SUM-
C MATIONS FOR THE EVALUATION OF THE VARIAN4. IT IS CALED
C FROM BOTH THE FIRSTAR AND SECARG
C*****
C
DOUBLE PRECISION FUNCTION SUM1(M)
DOUBLE PRECISION PI,LIMIT,K,CONST,A1,A2
REAL M,I
COMMON /DDDD/PI,LIMIT
COMMON /EEEE/K,CONST
C
A1=DCOS(K*CONST)
A2=0.D0
DO 200 I=0,50
A2=A2+(((K*CONST)**I)*DSIN((PI/2)*I))/S14AAF((-M+I+1),0)
200 CONTINUE
SUM1=A1*A2
RETURN
END
C
C
C*****
C
C THE SAME AS FOR SUM1
C*****
C
DOUBLE PRECISION FUNCTION SUM2(M)
DOUBLE PRECISION PI,LIMIT,K,CONST,A1,A2
REAL M,I
COMMON /DDDD/PI,LIMIT
COMMON /EEEE/K,CONST
C
A1=DSIN(K*CONST)

```

```

3D 08170
3D 08180
3D 08190
3D 08200
3D 08210
3D 08220
3D 08230
3D 08240
3D 08250
3D 08260
3D 08270
3D 08280
3D 08290
3D 08300
3D 08310
3D 08320
3D 08330
3D 08340
3D 08350
3D 08360
3D 08370
3D 08380
3D 08390
3D 08400
3D 08410
3D 08420
3D 08430
3D 08440
3D 08450
3D 08460
3D 08470
3D 08480
3D 08490
3D 08500
3D 08510
3D 08520
3D 08530
3D 08540
3D 08550
3D 08560
3D 08570
3D 08580
3D 08590
3D 08600
3D 08610
3D 08620
3D 08630
3D 08640
3D 08650
3D 08660
3D 08670
3D 08680
3D 08690
3D 08700
3D 08710
3D 08720
3D 08730
3D 08740
3D 08750
3D 08760
3D 08770
3D 08780
3D 08790
3D 08800
3D 08810
3D 08820
3D 08830
3D 08840

```

```

A2=0.D0
DO 201 I=0,50
  A2=A2+((((K*CONST)**I)*DCOS((PI/2)*I))/S14AAF((-M+I+1),0))
201 CONTINUE
  SUM2=A1*A2

  RETURN
  END
C
C
C*****
C
C THE SAME AS FOR SUM1
C
C*****
C
  DOUBLE PRECISION FUNCTION SUM3(M)
  DOUBLE PRECISION PI,LIMIT,K,CONST,A1,A2
  REAL M,I
  COMMON /DDDD/PI,LIMIT
  COMMON /EEEE/K,CONST
C
  A1=DCOS(K*CONST)
  A2=0.D0
  DO 200 I=0,50
    A2=A2+((((K*CONST)**I)*DCOS((PI/2)*I))/S14AAF((-M+I+1),0))
200 CONTINUE
  SUM3=A1*A2
  RETURN
  END
C
C
C*****
C
C THE SAME AS FOR SUM1
C
C*****
C
  DOUBLE PRECISION FUNCTION SUM4(M)
  DOUBLE PRECISION PI,LIMIT,K,CONST,A1,A2
  REAL M,I
  COMMON /DDDD/PI,LIMIT
  COMMON /EEEE/K,CONST
C
  A1=DSIN(K*CONST)
  A2=0.D0
  DO 201 I=0,50
    A2=A2+((((K*CONST)**I)*DSIN((PI/2)*I))/S14AAF((-M+I+1),0))
201 CONTINUE
  SUM4=A1*A2

  RETURN
  END
C
C*****
C
C THIS SUBROUTINE GIVES THE DENSITY FUNCTION
C
C*****
C
  SUBROUTINE DENSFUN(FRAGMEN,DENFUN1,R,THETA,FI,X0,Y0,Z0)
  DOUBLE PRECISION FRAGMEN(30,30,30),X0,Y0,Z0,THETA,FI,TRSUM,X,Y,Z
  & ,DENFUN1,R
  INTRINSIC DCOS,DSIN
C
C
C
C

```

```

3D 08850
3D 08860
3D 08870
3D 08880
3D 08890
3D 08900
3D 08910
3D 08920
3D 08930
3D 08940
3D 08950
3D 08960
3D 08970
3D 08980
3D 08990
3D 09000
3D 09010
3D 09020
3D 09030
3D 09040
3D 09050
3D 09060
3D 09070
3D 09080
3D 09090
3D 09100
3D 09110
3D 09120
3D 09130
3D 09140
3D 09150
3D 09160
3D 09170
3D 09180
3D 09190
3D 09200
3D 09210
3D 09220
3D 09230
3D 09240
3D 09250
3D 09260
3D 09270
3D 09280
3D 09290
3D 09300
3D 09310
3D 09320
3D 09330
3D 09340
3D 09350
3D 09360
3D 09370
3D 09380
3D 09390
3D 09400
3D 09410
3D 09420
3D 09430
3D 09440
3D 09450
3D 09460
3D 09470
3D 09480
3D 09490
3D 09500
3D 09510
3D 09520

```

```

X=R*DSIN(THETA)*DCOS(FI)+X0
Y=R*DSIN(THETA)*DSIN(FI)+Y0
Z=R*DCOS(THETA)+Z0
C
CALL PRODUCT(FRAGMEN,X,Y,Z,TRSUM)
C**WE DO NOT MULTIPLY BY MEANDEN BECAUSE IS C
C**OUT
DENFUN1=TRSUM
RETURN
END
C
C*****
C
C WE EXPRESS THE DENSITY CONTRAST IN A FOURIER IN 3D
C
C*****
C
SUBROUTINE PRODUCT(FRAGMEN,X,Y,Z,SUM)
DOUBLE PRECISION SUM,FRAGMEN(30,30,30),DOTPR,X,Y,Z,K1,K2,K3
& ,PI,POWER,LIMIT,A
REAL PHASE
INTEGER L,M,N,NUMFREQ
COMMON /AAAA/A,POWER,NUMFREQ
COMMON /DDDD/PI,LIMIT
INTRINSIC DCOS,DSIN,DABS
C
C
SUM=0
C-----
C/* TRIPLE SUM
DO 230 L=-NUMFREQ,NUMFREQ
K1=(2*PI*L)/LIMIT
DO 220 M=-NUMFREQ,NUMFREQ
K2=(2*PI*M)/LIMIT
DO 210 N=0,NUMFREQ
K3=(2*PI*N)/LIMIT
C/* DOT PRODUCT
DOTPR=K1*X+K2*Y+K3*Z
C-----
C
PHASE=G05DAF(0.01,6.28)
SUM=SUM+(2*(FRAGMEN(L,M,N))*DCOS(DOTPR-PHASE))
CALL G05CCF
SUM = SUM + (2*FRAGMEN(L,M,N))*DCOS(DOTPR)
210 CONTINUE
220 CONTINUE
230 CONTINUE
C-----
RETURN
END
C
C
C
C
C*****
C
C SUBROUTINE FOR THE STUDY OF THE EFFECTS OF THE
C LUMINOSITY FUNCTION AND SELECTIONS EFFECTS ON THE
C GENERATED RANDOM FUNCTION
C*****
C

```

```

3D 09530
3D 09540
3D 09550
3D 09560
3D 09570
3D 09580
3D 09590
3D 09600
3D 09610
3D 09620
3D 09630
3D 09640
3D 09650
3D 09660
3D 09670
3D 09680
3D 09690
3D 09700
3D 09710
3D 09720
3D 09730
3D 09740
3D 09750
3D 09760
3D 09770
3D 09780
3D 09790
3D 09800
3D 09810
3D 09820
3D 09830
3D 09840
3D 09850
3D 09860
3D 09870
3D 09880
3D 09890
3D 09900
3D 09910
3D 09920
3D 09930
3D 09940
3D 09950
3D 09960
3D 09970
3D 09980
3D 09990
3D 10000
3D 10010
3D 10020
3D 10030
3D 10040
3D 10050
3D 10060
3D 10070
3D 10080
3D 10090
3D 10100
3D 10110
3D 10120
3D 10130
3D 10140
3D 10150
3D 10160
3D 10170
3D 10180
3D 10190
3D 10200

```

C	SUBROUTINE LUMFUN(LUMIN,MLIMIT)	3D 10210
	REAL MSTAR,ALFA,FISTAR,LUMIN,MLIMIT,	3D 10220
	& A,B,C,D,W,Z,M,INTEGR,E,F,G,R,I,LUNFUN,X	3D 10230
	INTRINSIC EXP,LOG	3D 10240
	COMMON /DDDD/I	3D 10250
C		3D 10260
C		3D 10270
	ALFA=-1.25	3D 10280
	MSTAR=-19.46	3D 10290
	LUMIN = 0	3D 10300
	DO 90 X=0.01,MLIMIT,.2	3D 10310
	B=10**(((ALFA+1)/2.5)*(-X+(5*LOG(I))+25))	3D 10320
	C=10**((MSTAR)/2.5)	3D 10330
	D=10**((LOG(I))/2)	3D 10340
	W=10**(-M/2.5)	3D 10350
	Z=10	3D 10360
	LUMIN=LUMIN+(B*EXP(-(C*D*W*Z)))	3D 10370
90	CONTINUE	3D 10380
		3D 10390
	RETURN	3D 10400
	END	3D 10410
		3D 10420

REFERENCES

- Abell, G.O.: 1958, *Ap. J. (Supp.)*, **3**, 211
- _____ : 1962, 'Problems of Extra-Galactic Research', IAU
 Symposium 15, ed G.C. McVittie (New York: Macmillan
 Co.)
- _____ : 1965, *Annu Rev. Astron. Astrophys.*, **3**, p. 1
- Abramovitz Millan, and Stegan Irene: 1965, 'Handbook of
 Mathematical Functions', Dover Publications, INC., New
 York
- Bahcall, Neta: 1988, *Ann. Rev. Astron. Astrophys.*, **26**, 631-86
- Bahcall, N. and Soneira: 1983, *Ap. J.*, **270**, p. 20
- Barrow, J. D., and Tipler, F.J.: 1986, 'The Anthropic Cosmological
 Principal', New York, Clarendon Press
- Barrow, J. D., Bhavsar, S. and Sonoda, D.: 1984, *Mon. Not. R. astr.
 Soc.*, **210**, 19
- _____ : 1985, *Mon. Not. R. astr. Soc.*, **216**, 17
- Bertschinger, E., and Gelb, J. M.: 1991, *Computers in Physics*,
 Mar/Apr, pp. 164-180
- Bhavsar, S.: 1981, *Ap. J.*, **246**, L5-L9
- Bhavsar, S., and Barrow, J.D.: 1983, *Mon. Not. R. astr. Soc.*, **205**, 61
- Bhavsar, S., and Ling, E. N.: 1988, *Ap. J.*, **331**, L63
- Bingelli Bruno, Sandage Allan, Tammann, G.A.: 1988, *Ann.
 Rev. Astron. Astrophys.* **26**, 509-60
- Blackman, R.B., and Tukey, J.W.: 1958, 'The Measurements of the
 Power Spectra', Dover Publications INC., New York

- Bond, J.R.: : 1988, 'Large-Scale Motion in the Universe', (eds VeraC. Rubin and George V. Coyne, S.J.), Princeton University Press
- Borner, Gerhard: 1988, 'Large Scale Structure of the Universe' (edsJean Audouze, Marie-Christine Pelletan and Alex Szalay), pp 63-65
- Brandon, S.G.F.: 1963, 'Creation Legends of the Ancient Near East', Hodder and Stoughton
- Calzetti, D., and Giavalisco, M.: 1990, *Vistas in Astronomy*, **33**, 295- 303
- Calzetti, D., Giavalisco, M., and Ruffini, R.: 1988, *Astron. Astrophys.*,**198**, pp 1-15
- Calzetti, D., Einasto, J., Giavalisco, M., Ruffini, R., and Saar, E.: 1987, *Astrophysics and Space Science*, **137**, pp. 101-106
- Carpenter, E.F.: 1938, *Ap. J.*, **88**, 334
- Castagnoli, C. and Provenzale, A.: 1990, *Vistas in Astronomy*, **33**, pp 323-335
- Chatfield, C.: 1989, 'The Analysis of the Time Series', Chapman and Hall
- Chincarini, G.: 1983, 'Early Evolution of the Universe and its Present Structure' (eds G. O. Abell and G. Chincarini), pp.159-165
- Coles, P., and Barrow, J. D.: 1987, *Mon. Not. R. astr. Soc.*, **228**, 407
- Da Costa, N., Pellegrini, P.S., and Willmer, C.: 1989, *Ap. J.*, **344**, pp 20-23
- Davis, M., and Efstathiou, G.: 1987, 'Large-Scale Motion in the Universe', (eds Vera C. Rubin and George V. Coyne, S.J.), Princeton University Press
- Davis, M. & Geller, M. J.: 1975, *Bull. American Astron. Soc.*, **7**, p. 415
 _____: 1976, *Ap. J.*, **208**, 13

- De Lapparent, V., Geller, M.J., and Huchra, J.P.: 1989, *Ap. J.*, **341**, 1
- De Souza, R.E., Capelato, H.V., Arakaki, L., Logullo, C.: 1982, **263**, pp
..... 557-563
- De Vaucouleurs, G.: 1960, *Ap. J.*, **131**, 585
_____: 1970, *Science*, **167**, N^o 3922, p. 1203
_____: 1971, *PASP*, **83**, 113
- Doroshkevich, A.G., Sunyaen, R.A. & Zeldovich, Ya. B.: 1974,
..... *Confrontation of Cosmology. Theories with Observational*
..... *Data*, 213-225 (ed. M.S. Longair, IAU)
- Dressler Allan: 1980, *Ap. J.*, **236**, 351-365
_____: 1988, *Ap. J.*, **329**, 519
- Duncan Tom: 1981, 'Fields, Waves and Atoms', 2nd Edition, John
..... Murray Ltd.
- Eder, J.A., Schompert, J.M., Dekel, A., and Oemler, A.: 1989, **340**,
..... 29-46
- Efstathiou, G., Ellis, R.S., and Peterson, B.A.: 1988, *Mon. Not. R. astr.*
..... *Soc.*, **232**, 431
- Efstathiou, G., Kaiser, N., Saunders, W., Lawrence, A., Rowan-
..... Robinson, M., Ellis, R., Frenk, C.S.: 1990, *Mon. Not. R. astr.*
..... *Soc.*, **247**, 10
- Einasto, J: 1980, *Nature*, **283**, 47-48
_____: 1990, 2nd I.A.C. Winter School
- Einasto, J., Einasto, M., and Gramann, M.: 1989, *Mon. Not. R. astr. Soc.*,
..... **238**, pp. 155-177
- Einasto, J., Klypin, A.A., Saar E., and Shandarin, S.F.: 1984, *Mon. Not.*
..... *R. astr. Soc.*, **206**, pp. 529-558
_____: 1986, *Mon. Not. R. astr. Soc.*, **219**, pp. 457-478

- Einasto, J., Klypin, A.A., and Shandarin, S.: 1983, 'Early Evolution of the Universe and its Present Structure' (eds G. O. Abell and G. Chincarini), pp. 265-271
- Fall, M.: 1979, *Reviews of Modern Physics*, **51**, No 1
- Giavalisco, M., Calzetti, D., Ruffini, R.: 1990, *Vistas in Astronomy*, **33**, 305-322
- Giovanelli, R., Haynes, M.: 1991, *Annu Rev. Astron. Astrophys.*, **29**, pp. 499-541
- Gott, J.R.: 1977, *Ann. Rev. Astr. Ap.*, **15**, 235
- Gott, J.R., Miller, J., Thuan, T.X., Schneider, S.E., Weinberg, D.H., et al.: 1989, *Ap. J.*, **340**, pp. 625-646
- Gradshteyn, I.S., Ryzhik, I.M.: 1980, 'Tables of Integrales, Series andProducts', Academic Press
- Groth, E. J. & Peebles, P. J. E.: 1977, *Ap. J.*, **217**, 385-403
- Gunn, J.F., and Gott, J.R.: 1972, *Ap. J.*, **176**, 1
- Guth, Alan H., Steinhardt, Paul J.: 1989, 'The New Physics', edited dy Paul Davies, Cambridge University Press
- _____ : 1991, *Scientific American*, Special Issue
- Hauser, M.G. & Peebles, P.J.E.: 1973, *Ap. J.*, **185**, 757-785
- Hawking, S.: 1989, 'The New Physics' (eds Paul Davies), Cambridge University Press
- Haynes, Martha P., and Giovanelli, Riccardo: 1988, 'Large-Scale Motion in the Universe', (eds Vera C. Rubin and George V. Coyne, S.J.), Princeton University Press
- Hinde, A. L., and Miles, R. E.: 1980, *J. Statist. Comput. Simul.*, **10**, 205
- Hoffman, Y., and Shaham, J.: 1983, 'Early Evolution of the Universe and its Present Structure' (eds G. O. Abell and G. Chincarini)

- Hubble and Humason: 1931, *Ap. J.*, **74**, 43
- Huchra, J.P., and Geller, M.J.: 1982, *Ap. J.*, **257**, 423-437
- Huchra, J.P., Henry, J.P., Postman, M., and Geller, M.J.: 1990, *Ap. J.*,
..... **365**, 66-85
- Infante Leopoldo: 1989, *Rev. Mexicana Astron. Astrof.*, **19**, 71-82
- Incke, V., and van der Weygaert, R.: 1991, *Quart. JRAS*, **32**, 85
- James, E.O.: 1969, 'Creation and Cosmology', Leiden, E.J. Brill
- Jones, Bernard J. T., van de Weygart, Rien: 1990, Lecture presented
..... to the XII Autumn School 'The Physical Universe', Lisbon,
..... October 1-5
- Kaiser, N.: 1984, *Ap. J.*, **284**, L9
- Kaiser, N., and Lahav, O.: 1988, 'Large-Scale Motion in the Universe',
..... (eds Vera .C. Rubin and George V. Coyne, S.J.), Princeton
..... University Press
- Kaiser, N., Efstathiou, G., Ellis, R., Frenk, C., Laurence, A., Rowan-
..... Robinson, M., Saunders, W: 1991, *Mon. Not. R. astr. Soc.*,
..... **252**, 1
- Kirshner, R.P., Oemler, A., Schechter, P.L., Sheckman, S.A.: 1987,
..... *Ap.J.*, **314**, p. 493-506
- Kofman, L.A., Linde, A.D., Mukhanon, V.f.: 1988, 'Large Scale
..... Structure of the Universe' (eds Jean Audouze, Marie-
..... Christine Pelletan and Alex Szalay), pp 51-62
- Kolb, E.W., and Turner, M.S.: 1990, 'The Early Universe', Addison-
..... Wesley
- Lifshitz, E. M.: 1946, *J Phys.*, **10**, 116
- Limber, D. Nelson: 1953, *Ap. J.*, **117**, 134
- Ling, E., Frenk, C., and Barrow, J.D.: 1986, *Mon. Not. R. astr. Soc.*,
..... **223**, 21

- Lynden-Bell, D., Fober, S.M., Burstein, D., Davies, R.L., Dressler, A.,
 Terlevich, R.J., and Wegner, G.: 1988, *Ap. J.*, **326**, 19
- Maddox, S., Efstathiou, G., and Loveday, J.: 1988, 'Large-Scale
 Structure of the Universe', (eds J. Audouze, M.-C.
 Pelletan, and A. Szalay), Dordrecht: Kluwer Academic
 Publishers
- Maddox, S., Efstathiou, G., Sutherland, W., Loveday, J.: 1990, *Mon.*
 *Not. R. Astron. Soc.*, **242**, 43
- Malmquist, K.G.: 1920, *Medd. Lund. Astron. Obs.*, **20**
- Mandelbrot Benoit: 1982, 'The Fractal Geometry of Nature', San
 Francisco: Freeman
- _____ : 1990, *New Scientist*, **127**, no 1734
- Martinez, V. J., Jones, J.T.: 1990, *Mon. Not. R. astr. Soc.*, **242**, pp.
 517-521
- Martinez, V. J., Jones, J.T., Dominguez-Tenreiro, R., and van der
 Weygaert, R.: 1990, *Ap. J.*, **357**, 50
- Mataresse, S. Ortolan, A., and Lucchin, F.: 1989, *Phys. Rev.*, D40, 290
- Matsuda, T., and Shina, E.: 1984, *Prog. Theor. Physics*, **71**, 855
- Mood, A., Graybill, F.A., and Boes, D.: 1974, 'Introduction to the
 Theory of Statistics', McGraw-Hill
- Naymann, J., and Scott, E.: 1952, *Ap. J.*, **116**, 144
- Naymann, J., and Scott, E.: 1955, *Astron. J.*, **60**, 33
- Neymann, J., Scott E., and Shane, C. D.: 1954, *Ap. J. (Supp.)*, **1**, 269
- _____ : 1956, *Proc. third Berkeley Symposium Math. Stat.*
 *and Probability*, **3**, 75
- O'Brien, Joan, and Major, Wilfred: 1982, 'In the Beginning: Greation
 Myths from Ancient Mesopotamia, Israel and Greece', The
 American Academy of Religion
- Ostriker, J., and Cowie, L: 1981, *Ap. J.*, **243**, L127

-
- Papoulis Athanasios: 1965, 'Probability, Random Variables and
..... Stochastic Processes', McGraw-Hill Book Company
- Peacock, J. A., and Heavens, A. F.: 1985, *Mon. Not. R. astr. Soc.*, **217**,
..... 805
- Peebles P. J. E.: 1980, 'The Large-Scale Structure of the Universe',
..... Princeton University Press
- _____ : 1973, *Ap. J.*, **185**, 413-440
- _____ : 1974, *Ap. J.*, **189**, L51-L53
- _____ : 1974, *Ap. J. Supp. Series No 253*, 28: 37-50
- _____ : 1975, *Ap. J.*, **196**, 647-652
- Peebles P. J. E & Dicke, R.H.: 1968, *Ap. J.*, **154**, 891
- Peebles P. J. E & Groth, E. J.: 1975, *Ap. J.*, **196**, 1-11
- Peebles P. J. E. & Hauser, M.G.: 1974, *Ap. J. Supp. Series No 253*, 28:
..... 19-36
- Penzias, A.A., & Wilson, R.W.: 1965, *Ap. J.*, **142**, 419
- Postman, M., and Geller, M.J.: 1984, *Ap. J.*, **281**, pp. 95-99
- Ruffini, R., Song, D.J., and Taraglio, S.: 1989, *Astron. Astrophys.*,
..... 190, p.1
- Ripley, B. D.: 1981, *Spatial Statistics*, Wiley: NY
- Roy, A., and Clark, D.: 1982, 'Principles and Practice 2nd edn', Adam
..... Hilger
- Rowan-Robinson, Michael, 1977: 'Cosmology', Oxford University
..... Press
- Rubin, Vera C.: 1988, 'Large-Scale Motion in the Universe', (eds
..... Vera C. Rubin and George V. Coyne, S.J.), Princeton
..... University Press
- Sazhin, M. V.: 1985, *Mon. Not. R. astr. Soc.*, **216**, 25
- Schechter, P: 1976, *Ap. J.*, **203**, 297-306
- Sciama :1975, 'Modern Cosmology', Cambridge University Press

-
- Shandarin, S.F.: 1983, *Sov. Astr. Lett.*, **9**, 104
- Shapley, H: 1930, *Harvard Bull.*, **874**, 9
- _____ : 1933, *Harvard Bull.*, **980**, 9
- _____ : 1934, *Mon. Not. R. astr. Soc.*, **94**, 791
- Shu, F. H.: 1982, 'The Physical Universe, An Introduction to
..... Astronomy', University Science Books
- Silk, Joseph: 1974, *IAU Symposium*, No 63, pp. 195-210
- _____ : 1989, 'The Big Bang', W.H. Freeman and Company
- Sneddon, Ian M.: 1972, 'The Use of Integral Transforms', M^cGraw
..... Hill
- Strauss, Michael A., and Davis, Marc: 1988, 'Large-Scale Motion in
..... the Universe', (eds Vera C. Rubin and George V. Coyne,
..... S.J.), Princeton University Press
- Szalay, A.S., and Schramm, D.N.: 1985, *Nature*, **314**, p. 718
- Tanemura, M., Ogawa, T., Ogita, N.: 1983, *Journal of Computational
..... Physics*, **51**, pp. 191-207
- Thomas, G.B. and Finney, R.L.: 1979, 'Calculus and Analytic
..... Geometry', Addison-Wesley Publishing Company
- Voronoi, G.: 1908, *J. reine angew. Math.*, **134**, 198
- Wen Z., Deng, Z., Liu, Y., Xia, X.: 1988, *Chin. Astron. Astrophys.*, **12**,
..... pp. 269-275
- White, S.D.M.: 1979, *Mon. Not. R. astr. soc.*, **186**, 145
- Xia Xia-yang, Deng Zu-yeng, Dai Hei-jun: 1990, *Chin. Astrn.
..... Astrophys.*, **14/3**, 241-247
- Yaglom, A.M.: 1962, 'An Introduction to the Theory of Stationary
..... Random Variables', Prentice-Hall, INC.
- Yahil, A.: 1988, 'Large-Scale Motion in the Universe', (eds Vera C.
..... Rubin and George V. Coyne, S.J.), Princeton University
..... Press

Yoshioka, S. and Ikeuchi, S.: 1989, *Ap. J.*, **341**, 16

Zeldovich, Ya. P.: 1970, *Astron. Astrophys.*, **5**, 84

_____ : 1972, *Mon. Not. R. Astr. Soc.*, **106**, 1p

Zhi, Fang Li, and Xian, Li Shu: 1989, 'Creation of the Universe',
.....World Scientific

Zwicky, F.: 1933, *Helv. Phys. Acta*, **6**, 110

_____ : 1957, 'Morphological Astronomy', Berlin Springer-
.....Verlag

Zwicky, F., Wield, P., Herzog, e., Karpowitz, M., and Kowal, C.J.: 1961-
.....1968, 'Catalogue of Galaxies and Clusters of Galaxies', 6
.....Volumes, Pasadena, California Inst. Techn.

